Dissertations   Theses and Dissertations

1992

Lithium Transport, Mg2+ Competition, and Phospholipid Composition in Human Erythrocytes: A Multinuclear Magnetic Resonance Study

Aida Abraha
Loyola University Chicago

Recommended Citation

Aida Abraha

Loyola University of Chicago

LITHIUM TRANSPORT, Mg^{2+} COMPETITION, AND PHOSPHOLIPID COMPOSITION IN HUMAN ERYTHROCYTES: A MULTINUCLEAR MAGNETIC RESONANCE STUDY

Using ^6Li and ^7Li NMR, the rate of transport of $^6Li^+$ was faster than $^7Li^+$ by 16.7%. Naturally occurring lithium carbonate consists of 93% ^7Li and 7% ^6Li. Therefore, enriching lithium salts with ^6Li could be one way of circumventing the slow action of lithium uptake. The other possibility is using Li^+ selective ionophores, such as dibenzyl-14-crown-4. Using this ionophore, the Li^+/Na^+ selectivity ratios for RBC suspensions and synthetic PC vesicles were 1.47 ± 0.10 and 2.26 ± 0.07, respectively.

^7Li NMR spin-lattice (T_1) relaxation and ^{31}P NMR chemical shift measurements showed that binding of Li^+ and Mg^{2+} to ATP and ADP was through the phosphate moieties. ^1H and ^{13}C NMR chemical shifts showed that there was no binding of Li^+ and Mg^+ to the base and ribose moieties of the nucleotides. The ^7Li NMR relaxation times of Li^+/Mg^{2+} mixtures of ATP and ADP increased with increasing concentrations of Mg^{2+}, suggesting competition between the two ions for adenine nucleotides.

^{31}P chemical shift anisotropy (CSA) values increased from 51.3 ppm for membrane alone to 69.2 and 83.7 ppm in the presence of 20 mM Mg^{2+} and 200 mM Li^+, respectively. Upon titration with Li^+ and Mg^{2+}, an increase in CSA values, which was caused by motional rigidity of the phosphate groups, was observed indicating binding of these ions to the membrane. ^7Li T_1 relaxation times of 5 mM Li^+ increased from 13.9 s for membrane alone to 19.5 s in the presence of 2 mM Mg^{2+}. This result is indicative of a competitive mechanism between Li^+ and Mg^{2+} for membrane phosphate binding sites.

Na$^+$-Li$^+$ countertransport rates for 10 patients receiving lithium carbonate were significantly lower than 10 matched normals ($p < 0.0025$). Patients' membrane PS content and T$_1$ relaxation times were slightly higher than normals ($p < 0.10$), whereas the PI content was slightly lower for patients than normals ($p < 0.05$). No significant difference was observed between patients and controls in PC, PE, and Sph composition and intracellular Mg^{2+} levels. Na$^+$-Li$^+$ countertransport rates showed positive correlation with PC and PI and negative correlation with PS. These findings suggest that abnormal anionic phospholipid content of RBC membranes of bipolar patients receiving lithium carbonate results in different degrees of Li$^+$ interaction with the RBC membrane and slower rates of Na$^+$-Li$^+$ countertransport.

LITHIUM TRANSPORT, Mg^{2+} COMPETITION, AND PHOSPHOLIPID COMPOSITION IN HUMAN ERYTHROCYTES: A MULTINUCLEAR MAGNETIC RESONANCE STUDY

by

AIDA ABRAHA

A Dissertation Submitted to the Faculty of the Graduate School of

Loyola University of Chicago in Partial Fulfillment

of the Requirements for the Degree of

Doctor of Philosophy

May 1992

Acknowledgement

I would like to thank very much my mentor, Dr. Duarte Mota de Freitas, for all the intellectual advice, emotional support, guidance and encouragement he gave me that enabled me to finish my degree. I thank him for suggesting all the challenging but realistic projects that I was able to accomplish and present at different seminars and conferences.

My deepest thanks to Dr. Patrick Henry and Dr. Bruno Jaselskis for being members of my progress committee and taking the time to read the progress reports and attend the meetings. Thanks very much for all the constructive criticisms and wonderful ideas that helped me with my projects. Special thanks to Dr. Kenneth Olson and Dr. Nega Beru for being members of my dissertation committee.

Thanks to all my lab mates, Mary, Ravi, Lisa, Qinfen, Suilan and Elizabeth for all their help and attention. Special thanks to the Loyola security department for escorting me home during those late night hours.

My greatest appreciation to Dr Walter Dorus, Dr Joel Silberberg, Dr. Walter Wang, Dr G. Borge, and Eileen Elenz, R.N. for the supply of blood samples from bipolar patients and normal controls.

I am very grateful to the IMGIP fellowship program for the support during the first three years of my graduate work without any teaching obligations and for all the financial support they gave me to attend conferences and to buy chemicals. I would like to thank the graduate school, faculty and staff for all the assistance and generosity.

Special thanks to my family and friends that were with me all the way during my good and bad times.

Most of all, thanks to God for giving me the health and courage to seek me through.

A) Refereed Articles:

1) "Measurement of Lithium Transport in RBCs from Psychiatric Patients Receiving Lithium carbonate and Normal Individuals by ^7Li NMR Spectroscopy", D. Mota de Freitas, J. Silberberg, M. Espanol, E. Dorus, A. Abraha, W. Dorus, E. Elenz, and W. Wang, Biol. Psychiatry 28, 415-424 (1990).

2) "Competition Between Li^+ and Mg^{2+} for ATP and ADP in Aqueous Solution: A Multinuclear NMR and Optical Spectroscopy Study", A. Abraha, D. Mota de Freitas, M.M.C.A. Castro, and C.F.G.C. Geraldes, J. Inorg. Biochem. 42, 191-198 (1991).

3) "Nuclear Magnetic Resonance Study of Differences Between ^6Li and ^7Li Ions in Transport Across Human Red Blood Cell Membranes", A. Abraha, E. Dorus, and D. Mota de Freitas, Lithium 2, 118-121 (1991).

4) "Vanadate Interactions With Bovine Copper, Zinc-Superoxide Dismutase as Probed by ^{51}V NMR Spectroscopy", L. Wittenkeller, A. Abraha, R. Ramasamy, D. Mota de Freitas, L. A. Theisen and D. C. Crans, J. Am Chem. Soc. 113, 7872-7881 (1991).

5) "Ionophore Induced Li^+ Transport Across Human Erythrocyte Membranes in the Presence of a Background Na^+ Ions", A. Abraha and D. Mota de Freitas, Lithium (in press).

B) Abstracts:

1) "^7Li NMR Relaxation Studies of Li^+ Storage and Transport in RBC", D. Mota de Freitas, M. Espanol, R. Ramasamy, A. Abraha, and L. Wittenkeller, J. Inorg. Biochem. 36, 187 (1989).

2) "Multinuclear NMR Investigation of the Competition Between Mg^{2+} and Li^+ in Human RBCs", D. Mota de Freitas, R. Ramasamy, and A. Abraha, Mag. Res. 3, 65 (1990).

3) "Elucidation of Transport Mechanisms for Alkali Cations in Human RBCs by Metal NMR", D. Mota de Freitas, A. Abraha, Q. Rong, S. Mo and L. Wittenkeller, J. Inorg. Biochem. 43, 386 (1991).

4) "Competition Between Li^+ and Mg^{2+} for Purine Nucleoside Di- and Triphosphates in Aqueous Solution: A Multinuclear NMR Study", A.Abraha, D. Mota de Freitas, Q. Rong, M.M.C.A. Castro and C.F.G.C. Carlos, J. Inorg. Biochem., 43, 389 (1991).

To Adey and Ababa

TABLE OF CONTENTS

IV   RESULTS

LIST OF TABLES

LIST OF FIGURES

LIST OF ABBREVIATIONS

AA	atomic absorption
ADP	adenosine diphosphate
AIDS	acquired immunodeficiency syndrome
α	alpha phosphate of ATP
AMP	adenosine monophosphate
AT	acquisition time
ATP	adenosine triphosphate
AZT	azidothymidine
β	beta phosphate of ATP
^{13}C	carbon-13 isotope
C211	4,7,13,18-tetraoxa-1,10-diazabicyclo(8.5.5) eicosane
C221	4,7,13,16,21-pentaoxa-1,10-diazabicyclo(8.5.5) tricosane
C222	4,7,13,16,21,24-hexaoxa-1,10-diazabicyclo(8.8.8) hexacosane
14-C-4	14-crown-4
cAMP	cyclic adenosine monophosphate
CPMG	Carl-Purcell-Meiboom-Gill
CSA	chemical shift anisotropy
CSF	cerebrospinal fluid
D_1	delay one
D_2	delay two
1-D	one dimensional
2-D	two dimensional

δ	chemical shift
$\delta_{\alpha\beta}$	chemical shift separation between alpha and beta phosphates of ATP
$\delta_{Pi\alpha}$	chemical shift separation between Pi and alpha phosphates of ATP
DB-14-C-4	6,6-dibenzyl-1,4,8,11-tetraoxacyclotetradecane
DC	diacylglycerol
df	degree of freedom
DIDS	4,4'-diisothiocyanostilbene-2,2'-disulfonic acid
DMPC	1,2-dimyristoyl-*sn*-glycero-3-phosphorylcholine
DMPS	1,2-dimyristoyl-*sn*-glycero-3-phosphorylserine
$Dy(PPP)_2^{-7}$	dysprosium (III) triphosphate
$\Delta\nu_{1/2}$	NMR signal linewidth at half-height
FE	flame emission
γ	gamma phosphate of ATP
G_i	inhibitory G-protein
G_o	G-protein (function unknown)
G_s	stimulatory G-protein
GTP	guanosine triphosphate
hct	hematocrit
HEPES	4-(2 hydroxyethyl)-piperazine-ethanesulfonic acid
5HS7.4	5 mM HEPES, 150 mM NaCl, pH 7.4
5H8	5 mM HEPES, pH 8
5H8-1Mg	5 mM HEPES, 1 mM $MgCl_2$, pH 8
HIV	human immunodeficiency virus
HRAS	Harvey-ras-1 gene

INS	insulin
IP$_3$	inositol-1,4,5-triphosphate
J	spin-spin coupling constant
LD$_{50}$	lethal dosage at 50%
^{6}Li	lithium-6 isotope
^{7}Li	lithium-7 isotope
LUV	large unilamellar vesicles
^{23}Na	sodium-23 isotope
NMR	nuclear magnetic resonance
NT	number of transients
PC	phosphatidylcholine
PE	phosphatidylethanolamine
Pi	orthophosphate (inorganic phosphate)
PI	phosphatidylinositol
PIP$_2$	phosphatidylinositol-4,5-bisphosphate
PL	phospholipid
POPC	1-palmitoyl-2-oleoyl-*sn*-glycero-3-phosphocholine
POPS	1-palmitoyl-2-oleoyl-*sn*-glycero-3-phosphoserine
PPi	pyrophosphate
PS	phosphatidylserine
PW90	ninety degree pulse width
RBC	red blood cell
SD	standard deviation
SR	shift reagent

T_1	spin-lattice relaxation time
T_2	spin-spin relaxation time
TLC	thin layer chromatography
Tris	tris(hydroxymethyl)aminomethane
UV/VIS	ultraviolet-visible spectrophotometer
WBC	white blood cell

CHAPTER I

INTRODUCTION

I.A   History of Lithium

Discovery of lithium salts dates back to the early eighteen hundreds. The word lithium derives from the Greek word "lithion", which means stone or mineral.

Li^+ is of widespread occurrence, being found in most rocks of igneous origin. Approximately 0.006% of the earth crust consists of lithium (1).

Major sources of lithium are: 1) minerals, such as spodumene, amblygonite, lepidolite and petalite, and 2) brines. Lithium is also found scarcely in mineral waters, biological tissues and plant tissues.

Spodium, a lithium-aluminum silicate obtained in the form of raw ore, is crushed and heated to between 1075 - 1110 °C. The chemical reactivity of the lithium-aluminum silicate is thereby enhanced and, when mixed with H_2SO_4 and roasted to 250 °C, it is converted to lithium sulphate which may then be leached out of the ore residue with water (1). The lithium sulphate solution is first purified by processes which precipitate out magnesium and calcium salts and then concentrated. Aluminum impurities are next removed. The Li^+ ion is next precipitated as the relatively insoluble carbonate, extracted and dried (1). After further purification, it is this carbonate form of lithium which is used in the treatment of manic depression (2).

In 1949, an Australian psychiatrist, John Cade, discovered lithium carbonate to be an effective treatment for psychiatric patients (3). Urine from manic depressive, schizophrenic patients, and normal controls was injected into guinea pigs. Urine from the manic depressive patients proved the most toxic, and Cade concluded that the active chemical could be uric acid. Thus, he decided to investigate uric acid toxicity. He started studying lithium urate for it is the most soluble uric acid salt. He used lithium carbonate as a control chemical. Both lithium urate and lithium carbonate made the guinea pigs less timid, calmer, and less responsive to stimulation. Cade first took lithium carbonate himself and when he found it to be without toxic effect, he administered it to psychiatric patients (3). In 1954, Mogens Schou and his colleagues from Denmark were able to establish that lithium was a highly effective therapeutic agent against mania validating Cade's findings (3).

I.B   Chemical, Physical, and Pharmacological Properties of Lithium Salts.

Li^+ is an alkali metal ion which shares many properties with other group IA ions, such as Na^+, K^+, Cs^+, and may resemble some group IIA ions, such as Mg^{2+} and Ca^{2+} as well. Due to its high charge/mass ratio, it has a higher hydration energy than Na^+, K^+ and Cs^+. Some of the properties of alkali metals and alkaline earth metal ions are listed on Table 1. The lithium atom has a silver-white appearance indicative of its metallic nature. Its atomic structure is simple. Naturally occurring lithium salts, including lithium carbonate, contain two stable, non radioactive isotopes of Li^+, ^7Li (92.6%) and ^6Li (7.4%), with Li-6 having one less neutron than Li-7. The nuclei consist of 4 neutrons (Li-7) or 3 neutrons (Li-6) and 3 protons.

Table 1.   Properties of Some Alkali and Alkaline Earth Metals.[a]

Cation	Ionic Radius (Å)	Hydrated Radius (Å)	Coordination #	Charge Density ($10^{20}C$ $Å^{-3}$)	Hydration Energy ($KJ.mol^{-1}$)
Li^+	0.68	3.40	4,6	12.1	515
Na^+	0.95	2.80	6	4.46	406
K^+	1.33	2.32	6,8	1.62	322
Mg^{2+}	0.65	4.67	6	26.8	1940
Ca^{2+}	0.99	3.21	6,8	7.9	1600

[a]Taken from references 4, 5.

Two of the three electrons occur in an inner shell while the third electron occupies an outer shell from which it is readily lost. The easy loss of the second shell electron gives lithium its powerful reducing ability. The metal reacts at room temperature with relatively inert elements, for instance with nitrogen to form nitride. With more readily reactive oxidants the reactions are even more easily achieved (1). It forms a stable hydride on reaction with H_2 and it combines readily with all the halogens and vigorously with mineral acids. Lithium ions pack in body-centered cubic lattices which permit a high degree of electron mobility and thus provide a low electrical resistance (1). One unique physical property of lithium that should be mentioned is its physical ability to dissolve in liquid ammonia to produce a saturated solution possessing the lowest known density of any liquid (1).

Usually the isotopes of an element are handled in the same manner in biochemical processes, but because of their small atomic weights, the mass difference between ^6Li and ^7Li is large, second in magnitude to only hydrogen isotopes in the periodic table (6). ^6Li and ^7Li have different biochemical properties (6-15). An *in vitro* study on human RBCs using AA showed that the quantity of ^6Li which entered the erythrocytes was greater than ^7Li, with a ratio of the concentration of $^6Li/^7Li$ ranging from 5.4 - 8.5% (6). A study with cats done by AA also showed that the average CSF/plasma ratio of Li-6 was higher than Li-7 (7). The inositol metabolism of cerebral cortex in rats was more affected by Li-6 than Li-7 (8). When equimolar concentrations of Li-6 and Li-7 were administered to rats, a higher Li-6 concentration was also observed in the cerebral cortex using AA (8). But when the Li-7 dosage was 150% more than Li-6, the degree of change in inositol metabolism and cerebral cortex lithium concentrations were the same (8). Using magnetic field gradients, the ratio of diffusion rates of Li-6 to Li-7 in aqueous solution was calculated to be 1.003% (9). Due to its higher charge to mass ratio, Li-

6 has a higher hydration energy than Li-7 which gives it its higher degree of mobility. The ratio of diffusion rates of Li-6 to Li-7 in aqueous solution is much smaller than the 5.4 -8.5% observed isotopic ratio in biological systems. But one can not compare the two directly since transport of ions across a membrane is more complicated than mere diffusion of ions in an aqueous system. NMR results showed that Li^+- Li^+ exchange is faster than just lithium uptake by human erythrocytes (10).

The two isotopes are also known to exert different behavioral effects on biological systems (11-15). Spontaneous motor activity of experimental animals is known to decrease after treatment with Li^+ (11). Rats given the naturally occurring mixtures of isotopes of lithium up to ten days showed a significant decrease in exploratory behavior and motility (11). While both isotopes decreased motility of the rats, Li-6 initially produced a more profound effect than Li-7 (11). This differential behavioral effect of the isotopes was time dependent; the effect was most evident on the third day and disappeared on the fifth day (11). ^6LiCl and ^7LiCl showed maternal behavioral effects and early offspring development in rats (12). ^6LiCl treated rats were more alert, groomed themselves and their pups more than natural LiCl and ^7LiCl treated rats and controls (12). Development of LiCl treated pups was delayed compared to untreated controls (12).

When administered in isotopically pure form, ^6LiCl was more toxic after acute intake than ^7LiCl; LD_{50} of Li-6 in Swiss-Webster mice was 13.2 mEq/kg as opposed to 15.9 mEq/kg for Li-7 (13). The mortality rate of rats on Li-6 was higher than rats on Li-7 (14). In contrast, rats maintained on small quantities of Li-6 showed no obvious signs of toxicity and human subjects have received Li-6 without any ill effects (15, 16).

I.C   Medical and Industrial Applications of Lithium

Lithium is used in the treatment of manic depressive patients. It is administered to patients as lithium carbonate tablets (2). Patients receiving lithium take anywhere between 500 - 1900 mg a day to reach the therapeutic level of 0.5 - 1.2 mM in the plasma. Care is also taken not to reach the toxicity level of 2.0 mM in the plasma. Lithium has adverse effects on the kidneys, heart and thyroid (2).

Manic depression, currently known as bipolar affective disorder, is a psychiatric illness characterized by recurrent episodes of disabling mood swings. Mania, a condition during which one's mood changes from its normal state to an extremely overactive state is often marked by a feeling of elation, expansiveness and euphoria, a state described as being "on top of the world." Depression, on the other hand, is a condition during which one's mood changes from its normal state to that of being very low, blue and unhappy. Bipolar disorder affects one in every one thousand individuals in the USA (2). Even though the exact cause of manic depression is not characterized, it is hypothesized to be the result of an inherited chemical imbalance. Egeland and colleagues (17) reported evidence supporting the existence of a gene conferring a strong predisposition to bipolar affective disorder linked to two loci present in the short arm of chromosome 11, Harvey-ras-1 oncogene locus (HRAS) and insulin (INS) locus, in an Old Order Amish pedigree. However, a more recent study on a larger population of the same Old Order Amish pedigree showed no linkage between chromosome 11 and manic depression (18). This more recent result was interpreted as being either due to the existence of heterogeneity in the Old Order Amish family or, if it is assumed that the illness in the original family and the new extension is genetically homogeneous, that there is no evidence for linkage of bipolar affective disorder to the two marker genes in chromosome 11 (18). Moreover, other

studies in non-Amish populations showed that the inheritance of manic depression is not associated with chromosome 11 (19, 20).

Lithium is also used to treat granulocytopenic (low white blood cell count) conditions, hyperthyroidism and certain types of headaches. The ability of lithium to increase the WBC count has been utilized in the area of cancer chemotherapy where anti-cancer drugs often reduce the WBCs count to dangerously low levels. Lithium is also effective in the treatment of Herpes Simplex Virus (2). Lithium has also been used in conjunction with azidothymidine (AZT) to treat acquired immune deficiency syndrome (AIDS) patients (21). A four fold decrease in viral titer was observed when administered to a HIV positive patient with no AIDS related symptoms (21). Lithium is also used in dermatology (22). It has two different effects on the skin depending on how it is ingested. If it is taken orally, it exacerbates dermatological disorders. On the other hand, when applied topically on the skin surface it exhibits anti-inflammatory actions (22). The divergent clinical effect of Li^+ on the skin is not understood.

The major industrial use of lithium is in the form of lithium stearate as a thickener for lubricating greases (23). These all-purpose greases replace a multitude of specialized greases, and they have captured about one-third of the total automotive grease market. Another important use of lithium compounds is in ceramics, specifically in porcelain enamel formulation. The major action of the lithium ion in ceramics is as a flux. In ceramic mixtures, lithium carbonate readily undergoes the reaction shown below, yielding Li_2O as one constituent of the oxide mixtures of which most ceramics are composed of (23).

$$Li_2CO_3 \text{ ---> } Li_2O + CO_2$$
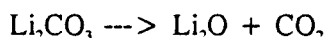
LiOH is used as an additive to give longer life and higher output in the alkaline storage batteries known as Edison cells. LiCl and LiF are used in welding and brazing fluxes; lithium-copper and lithium-silver alloys are used as self-fluxing brazing alloys. $LiClO_4$ has been

suggested as an oxidizer for solid-propellant rocket mixtures; it offers a higher percentage of available oxygen than any other perchlorate due to the low atomic weight of lithium (23, 24). ^6Li is used in neutron activation to produce tritium (4).

I.D   Techniques of Lithium Analysis

Several analytical methods have been used to monitor lithium in biological tissues and in aqueous solution. Some of these include AA, FE, UV/VIS, fluorescence, ion-selective electrodes and neutron activation analysis (25, 26). These methods require physical separation of intra and extracellular compartments and lysing of cell membranes to obtain intracellular Li^+ concentrations (27, 28). These methods only provide information about total intra- and extracellular Li^+ concentrations. The processing required by most conventional methods results in a loss of information about initial Li^+ transport movement and is very time consuming.

Absorption of radiation in AA and emission of radiation in FE involves electronic transition within atoms. In emission spectroscopy radiation is emitted by atoms which are in excited energy states, whereas in absorption spectroscopy atoms which can absorb energy from a hallow cathode lamp are in the ground state. Flame emission and absorption measurements are generally made with a flame temperature below 3000 °C, and consequently most atoms are in the ground state. It has therefore been argued that absorption should be virtually independent of temperature, whereas the number of excited atoms and hence the emission intensity varies exponentially with temperature. However, the dissociation processes which result in the production of atoms from the sample molecules are also temperature-dependent. Because of this the number of ground state atoms, and hence the amount of absorption will change with temperature although not to the same extent as emission. Absorption measurements are less prone to inert-element interference effects. Each element, including lithium, emit or absorb

radiation at a wavelength specific to that element.

Alkali and alkaline earth metals including lithium are not colored; therefore, optical and fluorescent dyes have been used (25). The major drawback of these techniques is that they do not discriminate between Li^+ and Na^+ ions satisfactorily. In blood plasma Na^+ concentration is 140 mM, whereas Li^+ is in the range 0.5 - 1.2 mM. Due to the drastic difference in concentration and high similarity in chemical and physical properties between Na^+ and Li^+, discrimination between the two ions is difficult using optical and fluorescent dyes (25). However, Li^+ ion-selective electrodes have been used successfully for selectively monitoring Li^+ action in the presence of a high Na^+ concentration (29-36).

Neutron activation methods are based upon the measurement of radioactivity that has been induced in samples by irradiation with neutrons or charged particles, such as protons or deuterium or helium-3 ions (26). Thermal neutrons from a reactor or from a small radioactive decay source are by far the most commonly used particles for inducing radioactivity in a sample. The most common neutron reaction involves capture of a neutron by ^7Li to give an isotope with a mass number greater by one accompanied by γ ray emission,

$$^7_3Li + {}^1_0n \longrightarrow {}^8_3Li + {}^0_0\gamma$$
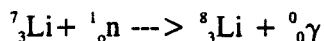
The other technique for Li^+ detection that is non invasive in nature is NMR spectroscopy. It is a technique that detects nuclear spin reorientation in an applied magnetic field (37). Radiofrequency is applied to the sample followed by detection of the transient signal from the nuclear spins. This transient is Fourier transformed to give the NMR spectrum. NMR spectroscopy is very selective. Each nucleus has its specific resonating frequency and gyromagnetic ratio. The NMR parameters are chemical shift (δ), spin-spin coupling constant (J), area or intensity of the signal, linewidth, and two relaxation times, spin-lattice (T_1) and spin-spin (T_2). The applications of NMR to biological systems are various and widespread. They

include the measurement of the concentration and isotopic composition of molecules in intact tissue, intracellular pH, pKa values of individual groups on macromolecules, kinetics, dissociation constants of ligands bound to macromolecules, structural information about molecules, and molecular dynamics in a variety of systems including membranes. The method is sensitive to environmental changes, but relatively large, concentrated samples are required because the signals produced are very weak.

Nuclear properties of the nuclei used in this project are listed on Table 2. The two stable isotopes of lithium are NMR active. Li-7 and Li-6 have nuclear spins of 3/2 and 1, respectively, thus possessing quadrupole moments (37). Due to its spin of 3/2, Li-7 can undergo three transitions. In general, in the presence of a magnetic field all three transitions are degenerate. However, when the ^{7}Li is placed in an asymmetrical electric field, the degeneracy is lifted and only the central transition state, $+1/2 <----> -1/2$, may be visible. In a very asymmetrical environment, there may be an overall loss of 60% in intensity of the Li^+ signal (38). ^{7}Li is a high-receptivity nucleus (1540 relative to ^{13}C) making ^{7}Li NMR spectroscopy a highly sensitive tool to monitor lithium action in biological systems. ^{7}Li has a very narrow chemical shift range for the paramagnetic and diamagnetic contributions to the chemical shift tend to cancel out (38). The less abundant isotope of Li^+, ^{6}Li has a receptivity of 3.58 relative to ^{13}C (38). Isotopic enrichment of ^{6}Li is generally necessary to enhance its sensitivity to the point that it can be conveniently monitored by ^{6}Li NMR spectroscopy. In general, quadrupolar relaxation predominates over dipole-dipole and rotational relaxation mechanisms for nuclei that possess a quadrupole moment (39).

Table 2. NMR Properties of Some Nuclei.[a]

Nucleus	NMR Frequency (MHz) at 7.0 Tesla	Nuclear Spin (I)	Natural Abundance	Gyromagnetic ratio (γ)[b]	Receptivity[c]
H-1	300.0	1/2	99.9	26.75	1.00
Li-6	44.3	1	7.4	4.96	6.30×10^{-4}
Li-7	116.4	3/2	92.6	10.40	0.27
C-13	74.6	1/2	1.1	6.73	1.76×10^{-4}
Na-23	79.4	3/2	100.0	7.08	9.25×10^{-2}
P-31	121.5	1/2	100.0	10.83	6.64×10^{-2}
Cl-35	29.4	3/2	75.4	2.62	3.55×10^{-3}

[a]Taken from references 37-40. [b]unit in 10^7 rad T^{-1} s^{-1}. [c]Includes contributions from γ, I, and natural abundance.

However, ^{6}Li has a small quadrupole moment which makes the quadrupolar relaxation contribution negligible and thus making its detection possible even when bound to asymmetric environments such as those most likely provided by biological ligands.

Discrimination between intra- and extracellular Li$^+$ pools in Li$^+$-loaded human RBCs was achieved by two distinct ^{7}Li NMR methods. One NMR method involved the incorporation in the suspension medium of cell-impermeable shift reagents, such as Dy(PPP)$_2^{7-}$ (dysprosium(III) triphosphate), or Dy(TTHA)$^{3-}$ (dysprosium(III) triethylenetetraminehexaacetate), and recording a standard one dimensional FT-NMR spectrum of the ^{7}Li$^+$ nucleus (41-43). The other NMR approach took advantage of the different relaxation properties of the two Li$^+$ pools and involved a modified inversion recovery (MIR) pulse sequence (41).

I.E   Lithium Ionophores

Increasing attention is being focused on Li$^+$ ionophores as tools for biological applications. Some ionophores are directly incorporated into biological media to speed up lithium transport and to calculate selectivity ratios between Li$^+$ and Na$^+$ in synthetic vesicles (44-46) or RBC suspensions (our laboratory). They are also used as extraction photometric reagents for Li$^+$ bearing chromophores, such as nitrophenol and azophenol, that can selectively extract Li$^+$ and its extraction can be monitored spectrophotometrically (47). Li$^+$ ionophores have also been used to construct ion selective electrodes to monitor Li$^+$ activity in biological and environmental systems (29-36).

Ionophores are molecules that selectively transport ions across artificial or biological membranes. Ionophoric materials can be divided into two categories, anionic and neutral. The anionic ionophores have an ionizable group, generally a carboxylic acid or hydroxyl group, and

can thus form a metal/ionophore complex which is electrically neutral. Neutral ionophores have no ionizable groups and thus form a charged complex with the metal ions. Some of the Li^+ selective ionophores include crown ethers, polyether open chain compounds, and cyclic compounds with amide functional groups (Figure 1). Crown compounds are more effective carriers than open-chain compounds. Crown ethers are neutral ionophores that have high selectivity for Li^+. 14-crown-4 crown ethers form 1:1 complexes with Li^+. On the other hand, the sizes of Na^+ and K^+ exceed that of the cavity. Therefore, they are likely to form 2:1 (cation-metal) sandwich type complexes, especially at high crown ether concentration (48, 49). This selectivity can be attributed to several factors. The first is the often quoted size of cavity versus size of ion argument, which states that the ion that best fits the crown ether's cavity will be the most tightly bound. Table 3 shows the diameters of crown ether cavities and their corresponding ion selectivities. Cryptands constitute another example of neutral ionophores with bicyclic ring structures (Figure 2). Cryptands have three-dimensional cavities that can accommodate a metal ion of suitable size and form an inclusion complex. These compounds demonstrate improved complexing behavior toward alkali metal ions (50). The cavity size of cryptand 211 (C211) is consonant with the dimension of Li^+; therefore, the C211.Li^+ complex is more stable than C222 and C221 lithium complexes (51, 52). The disadvantage of this high stability complex is its poor dissociative ability. Therefore, C211 is not the best ionophore to deliver Li^+ across membranes (43).

Recent studies (32, 47, 50) have shown that the selectivity behavior is very susceptible to solvent interaction, the side chain on the crown ether, and the stability of the ion-pair complex. The complexation of cations by crown ethers has been attributed to the electrostatic attraction between the cation's positive charge and the negative dipolar charges on the hetero atoms in the polyether ring.

Figure 1. Structures of Some Li$^+$ Selective Ionophores

   A) dodecylmethyl-14-crown-4

   B) dibenzo-18-crown-6.

   C) N,N'-diheptyl-N,N'-5,5-tetramethyl-3,7-dioxaazelaamide

A
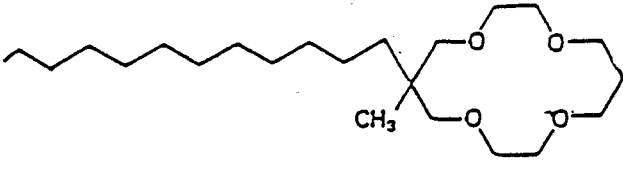
B
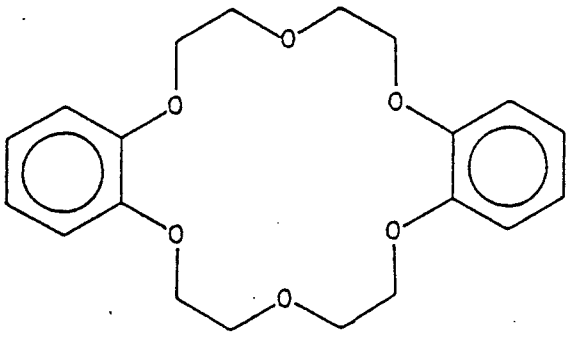
C
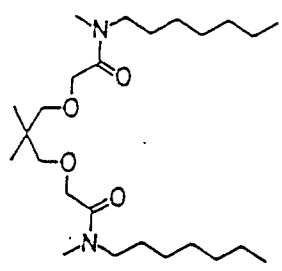
Table 3. Cavity Size and Metal Ion Selectivity of Crown Ethers and Cryptands[a].

Crown Ethers	Cavity Diameters/ Å	Metal ion Selectivity
12-Crown-4	1.2	$Li^+ > Na^+ > K^+$
14-Crown-4	1.2-1.5	$Li^+ > Na^+ > K^+$
15-Crown-5	1.7-2.2	$Na^+, K^+ > Cs^+$
C211	0.8	$Li^+ > Na^+$
C221	1.2	$Na^+ > K^+$
C222	1.4	$K^+ > Cs^+$

[a]Taken from reference 4, 5, and 50.

Figure 2.   Structures of Some Cryptands.

1) C211 ($l=1$, $m=n=0$)

2) C221 ($l=m=1$, $n=0$)

3) C222 ($l=m=n=1$)
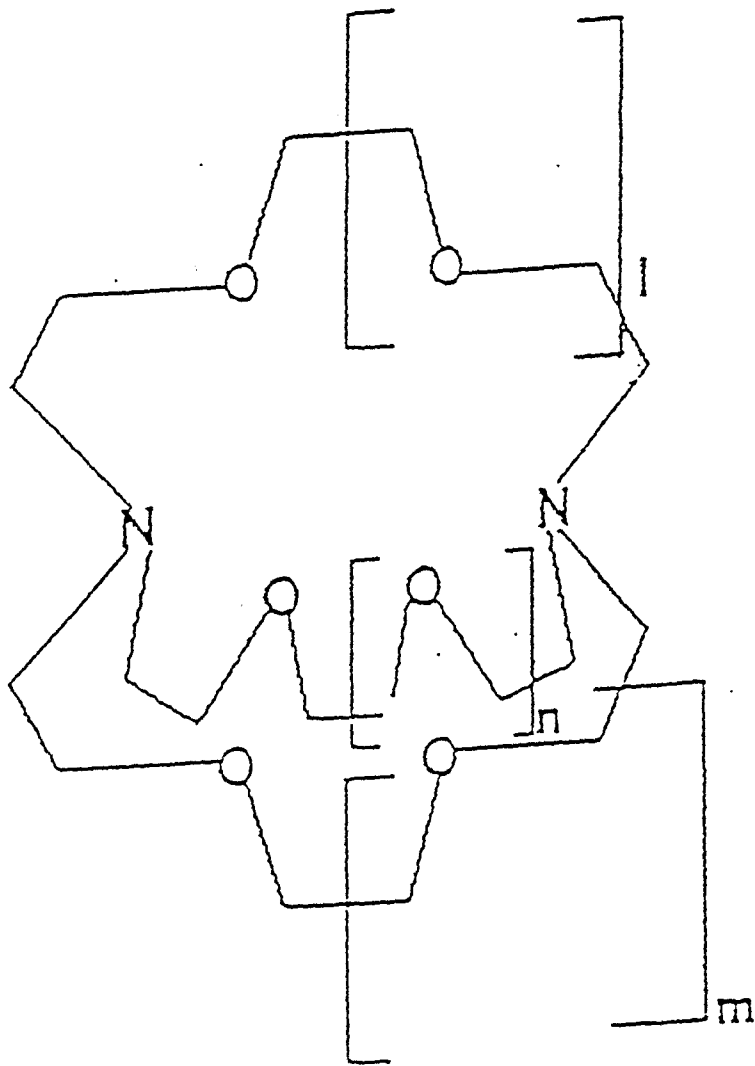
A cobalt complex ionophore directly incorporated in a synthetic PC vesicle showed a Li^+/Na^+ selectivity ratio of 40 (44). Using different side chains, carrier induced Li^+ kinetic analysis fits a pseudo-first-order reaction (45). Lipophilic 14-crown-4 derivatives bearing nitrophenol or azophenol chromophores gave extraction equilibrium constants for Li^+ that were two orders of magnitude higher than Na^+ (47).

Body fluids are complex mixtures containing a wide variety of diverse substances. The determination of the Li^+ composition of these fluids is essential for establishing a patient's metabolic condition and for facilitating the diagnosis of altered states. The use of Li^+ ion-selective electrodes in clinical medicine has grown rapidly in recent years. Using Li^+ ion-selective electrodes in human serum, artificial serum and aqueous solution, Li^+/Na^+ selectivity ratios ranged between 10-300 (29-36).

I.F   Modes of Action of Lithium

Several studies have been conducted on the possible effects of lithium salts in biological systems. Some of the hypotheses that have been put forward include: competition between Li^+ and other metal ions, binding of Li^+ to cell membranes, and interaction of Li^+ with second messenger systems. Each of these hypotheses is described in detail below.

1) Competition of Li^+ with Na^+, K^+, Ca^{2+} and Mg^{2+} (53-55).

Na^+, K^+ and Ca^{2+} are involved in interneuronal communication. Intracellular K^+ is involved in maintaining the capacity of cells to depolarize. Intracellular Na^+ is involved in depolarizing the membrane, or discharging stored membrane energy. Intracellular Ca^{2+} is involved in executing the purpose of the neuron's depolarization, or release of neurotransmitters. Mg^{2+} activates ATP, the source of

energy, and GTP, the regulator of neurotransmitter stimulation of the second messenger.

Some studies have shown that Li^+ competes for Mg^{2+} binding sites (54, 55). However, it is not clear whether competition between Li^+ and Mg^{2+} ions is related to the mode of action of Li^+. The chemical similarity between Li^+ and Mg^{2+} arises from the diagonal relationship that exists between them in the periodic table. Reactions catalyzed by ATP-dependent enzymes generally require divalent cations such as Mg^{2+} for activity. Mg^{2+} is the predominant cation in mammalian cells ranging in total concentration from 2.5 - 8.5 mM in various cell types (56-58). ATP is the universal currency of free energy in biological systems. Eighty percent of ATP exist as Mg-ATP, which is the active form of ATP. Mg^{2+} interacts with both the α- and β-phosphates of ADP and the α-, β- and γ-phosphates of ATP. However, Mg^{2+} coordination to the α-phosphate of ATP is weaker than to the β- and γ-phosphates of ATP due to steric hinderance (59, 60). Mg-ATP can have seven different structural isomers, (α-, β- and γ-) monodentate, ($\alpha \beta$-, $\beta \gamma$- and $\alpha \gamma$-) bidentate and ($\alpha \beta \gamma$-) tridentate (59). Binding of metal ions to nucleotides is pH, temperature and ionic strength dependent (61-63). Lithium is known to inhibit Mg^{2+} activated enzymes such as adenylate cyclase, phosphofructokinase and pyruvate kinase (64-66). Therefore, magnesium binding sites in biomolecules are potential sites for lithium interaction.

In considering the role of ATP as an energy carrier, we can focus on its triphosphate moiety. ATP is an energy rich molecule because its triphosphate unit contains two phosphate anhydride bonds (Figure 3). A large amount of free energy is liberated when ATP is hydrolyzed to ADP and orthophosphate (Pi) or when it is hydrolyzed to AMP and pyrophosphate (PPi). Phosphates are non selective metal ion binders. They are especially important and among the most effective groups in attracting alkali and alkaline earth metal ions (67). Several workers have noted an increase in both serum magnesium and calcium a short time following lithium

Figure 3. Structures of ATP (A) and ADP (B).
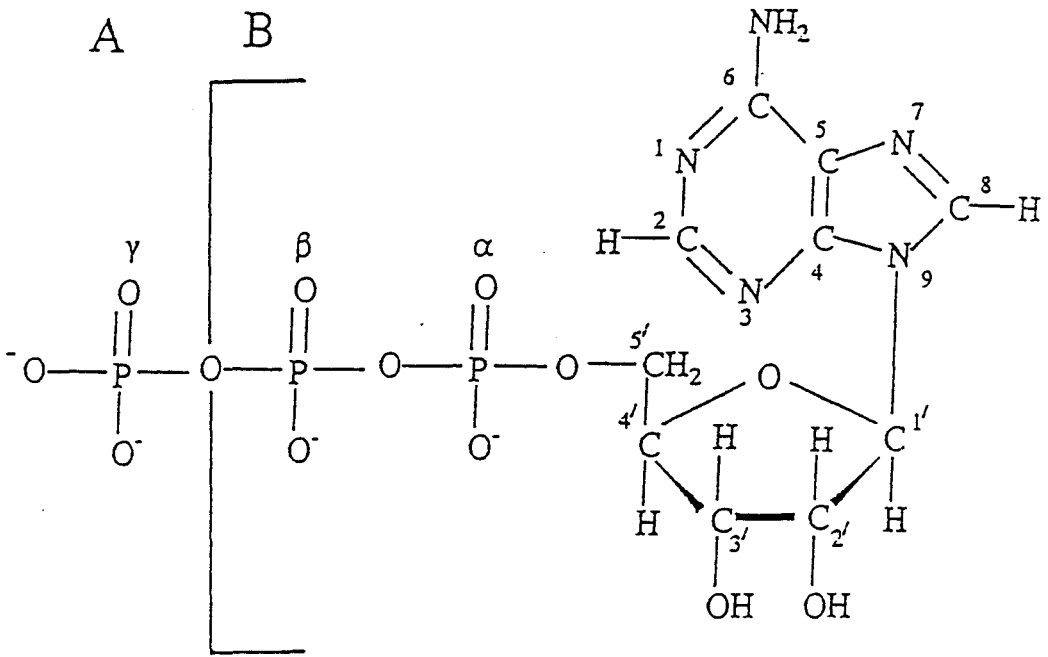
administration to humans (68-71). A general sedating effect with decreased manic behavior was observed when two acute manic patients were administered with Mg^{2+} by infusion (68). Blood samples showed an increase in plasma calcitonin, a small decrease in serum calcium, and an increase in serum Mg^{2+} (68). Therefore, it was hypothesized that magnesium could be responsible for the antimanic effect of lithium administration (68). It is known that Li^+ displaces Mg^{2+} from ATP binding sites in human RBCs (55). Therefore, this increase of serum Mg^{2+} may be due to Mg^{2+} being displaced by Li^+.

2) Binding of Li^+ to Cell Membranes. Its effects on membranes have been studied (72-86). Most of the investigations on interaction of Li^+ with membranes have been conducted with human red cell membranes because they represent a good model system for the investigation of lithium action, due to their well known morphology, simplicity, and easy access (78-80). It is also known that Li^+ transport in red cells has similar characteristics to that present in nerve tissue (27). In an *in vitro* study, Ramasamy and Mota de Freitas (55) showed that Li^+ displaced Mg^{2+} from ATP binding sites in human RBCs and that the displaced Mg^{2+} was presumably binding to the membrane (55).

Li^+ and Mg^{2+} binding to human cell membranes may be a potential site for lithium action. Interaction of metal ions with human RBC membranes and synthetic membranes made up of phospholipids, such as PC, PI and PS, has been studied using ^7Li, ^{31}P, ^2H NMR, AA, fluorescence spectroscopy and neutron diffraction (72-86). The binding of metal ions causes motional rigidity and small conformational changes of the phospholipid head groups which is reflected in changes in relaxation times, chemical shifts, chemical shift anisotropy (CSA), and in distinct changes of the quadrupole splittings.

The strength of metal ion interaction increases with increasing charge and metal ion concentration. PC is one of the predominant phospholipids in membranes. Thus, a large fraction of most membrane surfaces is occupied by PC groups. The interaction of metal ions with the uncharged PC bilayer can be expected to be relatively weak compared to those with negatively charged lipids, such as PI and PS, which are minor constituents of membranes.

Previous studies have shown that the extent of binding of Ca^{2+}, Mg^{2+}, Li^+, Na^+ and K^+ to deuterated bilayers of POPC and POPS decreased when going from Ca^{2+} to K^+ (74). Results obtained with pure DMPS and mixed bilayers with PC and PE at various NaCl or LiCl concentrations indicate that interactions with Na^+ and Li^+ have very different effects on the head group quadrupole splittings (75). CSA of resealed RBC ghosts is reported to be 45 ppm (81). This value shows the extent of immobilization of the phosphate head group in resealed human RBC ghosts. The strength of metal ion interaction with PC increased when going from monovalent to trivalent cations such as Na^+, Ca^{2+} and La^{3+} (82). The extent of Ca^{2+} binding to PC was examined using ^2H NMR and AA spectroscopy (83). A linear relationship existed between the quadrupole splitting and the amount of Ca^{2+} bound per PC head group. The quadrupole splitting at the saturation point corresponded to a binding stoichiometry of one Ca^{2+} per two POPC (83). Addition of lanthanide shift reagents, such as La^{3+} and Eu^{3+}, and $K_3Fe(CN)_6$ to a PC bilayer changed the ^{31}P NMR CSA and ^2H NMR quadrupole splittings dramatically (84). The shift reagents are in direct contact with the PC membrane. Therefore, they cause paramagnetic broadening. The addition of Ca^{2+} to PS causes rigid lattice ^{31}P NMR spectra which corresponds to a strong and specific head group immobilization by the Ca^{2+} ion (85). At pH 7.4 the hydrated PC from egg yolk and PS from human erythrocytes adopted the bilayer phase while lowering the pH below 4.0 resulted in a transition from bilayer to the

hexagonal (H_{II}) configuration, which is an indication of a conformational change of the phospholipid (85). Using differential scanning calorimetry and x-ray diffraction, it has been shown that Li^+ interacting with liquid-crystalline PS bilayers forms a highly ordered crystalline complex which retains the bilayer structure (86). The stability of the complex is indicated by the high crystal to liquid-crystal transition temperature of about 90 °C and the high transition enthalpy $\Delta H = 16.2$ kcal/mol (86). It is clear that the interaction of PS with Li^+ mimics that of Ca^{2+} and Mg^{2+} (86).

Li^+ interaction with cell membranes can also be studied via ^7Li spin-lattice (T_1) and spin-spin T_2 relaxation times (72, 76, 77). These two measurements are obtained with the inversion recovery and Carl-Purcell-Meiboom-Gill pulse sequences (87), respectively. Intracellular $^7Li^+$ T_1 values in Li^+-loaded RBCs are much higher than the corresponding T_2 values (72, 76). It is well established that slow motions contribute only toward T_2 (87). Thus, the large difference between T_1 and T_2 values is indicative of Li^+ binding to RBC components (76). A viscosity contribution was ruled out because for Li^+ in water/glycerol mixtures with viscosity adjusted to that of intracellular RBC showed no significant difference between T_1 and T_2 relaxation times (72, 76). The observed relaxation times represent a weighted average of bound and free lithium ions. Little or no change was observed on the ^7Li T_1's and T_2's of ATP-containing ghosts and ATP-depleted ghosts indicating that the interaction between Li^+ and ATP is weak and is not responsible for the drastic difference between T_1 and T_2 relaxation times (76). Moreover, the fact that the difference in relaxation times is present in both intact RBCs and RBC ghosts indicates that this Li^+ relaxation behavior has to do with Li^+ binding to RBC membrane and not to intracellular metabolites, such as ATP and hemoglobin, or membrane proteins, such as spectrin-actin.

Studies carried out with human red blood cells postulated a membrane dysfunction

hypothesis for manic depression (88-91). Some studies have shown characteristic changes in the PL composition of bipolar patients (88). Manic depressive patients have lower PC and PS and higher PE content than normal controls (88). It was previously suggested that Li^+ may interact with phospholipids (92) or a membrane protein (93). Clinically relevant concentrations of Li^+ significantly altered molecular dynamics on the erythrocyte membrane surface (73). It could be that the hydrated Li^+ ion alters the electrostatic interaction of membrane surface molecules, as well as the surrounding water structure, with a resultant increase in the molecular motion of these molecules. Li^+ induced alteration in the molecular dynamics of normal erythrocyte membranes may provide new insights into a possible molecular mechanism for the therapeutic action of lithium given the previous findings of a possible membrane abnormality in bipolar affective disorder (88-90).

A cell membrane dysfunction could alter Li^+ interaction with the membrane, and hence the rate of Li^+ transport across the membrane. Indeed, we and others (94-97) have found that the Na^+-Li^+ countertransport rate is lower for manic depressive patients receiving lithium carbonate than for matched controls. In contrast, some investigators failed to find a significant difference between patients and controls (98-103). Interindividual differences (99, 101), as well as intraindividual (104, 105) variations, have resulted in overlapping Na^+-Li^+ countertransport rates for patients and controls. Thus, decreased activity of erythrocyte Na^+-Li^+ countertransport may not be a reliable "biochemical marker" for affective disorder. Bimodal distribution of a gene encoding for a Na^+-Na^+ exchange protein having a binding site for Li^+ could explain the published discrepancies for the rates of RBC Na^+-Li^+ countertransport (93, 104). Differences in RBC Na^+-Li^+ countertransport rates were observed between the white and black populations; the rate constant for Li^+ efflux through this pathway was found to be larger in whites than in blacks (106). Thus, some of the interindividual variations may be related to racial dissimilarities

in the cellular metabolism involving cation transport (96). Sodium-lithium countertransport increased with aging in normal subjects (107). This increase is due to a phloretin insensitive component that was not present in young erythrocytes and due to a marked increase in the phloretin insensitive component upon aging (107). Ostrow et. al. (108) have demonstrated that maximal Na^+-Li^+ countertransport rate is unaffected by storage of erythrocytes for up to five days in a buffered isosmolar KCl solution, but the intracellular sodium concentration decreased. Since sodium-lithium countertransport rate measurements conducted using ^7Li NMR or AA spectroscopy showed a positive correlation (94), methodological variations were ruled out.

In human RBCs, Li^+ ion transport takes place via some of the transport pathways used by the Na^+ ion since Li^+ and Na^+ have similar chemical and physical properties. Na^+-Li^+ countertransport is the major pathway when Li^+ is transported out of the cell. This pathway is inhibited by phloretin, furosamide, and quinine (109). On both sides of the membrane the affinity of Li^+ is 15 to 18 times greater than Na^+ (110). This means that in the plasma of patients receiving lithium carbonate where Na^+ is maintained at 140 mM and Li^+ is approximately 1 mM, the external transport site will predominantly be Na^+. On the other side of the membrane, the Na^+ to Li^+ concentration ratio (8 mM vs. 0.5 mM) more closely matches the affinity ratio so the Li^+ is likely to be carried out of the cell. It is this efflux which maintains intracellular lithium levels lower than in the plasma (27, 110-112). The energy needed to move Li^+ against an electrochemical gradient, as found in Li^+-loaded RBCs, is derived from the large Na^+ gradient which is maintained by the Na^+-K^+ pump. Other pathways responsible for Li^+ efflux are the leak pathway and the Na^+-pump (89, 112). Li^+ is transported into the cell via a passive leak pathway, and the chloride exchange (or band three) protein (89, 112). The latter pathway is not shared by Na^+ for Li^+ is transported as an anion complex of carbonate, $LiCO_3^-$, exchanging for Cl^-.

3) Interaction of lithium with the two prominent second messengers systems, adenylate cyclase and phosphatidylinositol turnover. The neurotransmitter-sensitive adenylate cyclase is a transmembrane signaling system, which consists of five functional proteins. Stimulatory receptors (β-adrenergic-, dopamine D_1, serotonin 5-HT$_{1A}$-, vasopressin- and glucagon receptors) and inhibitory receptors ($\alpha 2$-adrenergic-, dopamine D_2-, opiod- and muscarine M_2 receptors) either stimulate or inhibit adenylate cyclase activity (113,114). Urine levels of cAMP are reported to be elevated in mania, and reduced in severe depression (115). Palmer et al. (116) showed that lithium *in vitro* at a concentration of 2 mM reduced noradrenaline-stimulated cAMP accumulation in rat brain slices. β-adrenergic adenylate cyclase, which is sensitive to lithium at therapeutic levels, may play an important role in the therapeutic action of lithium, while those enzymes less sensitive to lithium, e.g., dopamine-stimulated adenylate cyclase, might be linked to the adverse effects occurring at higher lithium levels. On the other hand, a dampening of dopaminergic neurotransmission may be involved in the action of antimanic drugs (117).

Several neurotransmitter receptors are coupled to the hydrolysis of phosphatidylinositol-4,5-biphosphate (PIP$_2$) yielding inositol 1,4,5-triphosphate (1,4,5-IP$_3$) and diacylglycerol (DG), which perform second messenger roles in cells (118). It has been shown that lithium treatment reduces the levels of inositol in the brain and that this reduction is accompanied by an increase in IP$_1$ (118). Inhibition of inositol-1-phosphatase leads to a depletion of inositol, the precursor in the resynthesis of PIP$_2$. Reduction of the resynthesis of PIP$_2$ may affect the signaling mechanisms operating through the phosphoinositide system. Lithium decreased apparent interaction of neurotransmitter receptors with G-proteins (119). It was found that Li$^+$ blocks the activity of two types of guanine nucleotide binding proteins (G proteins), G$_s$ and G$_i$ or G$_o$. These two different types of G proteins may provide a common site for both the antimanic and

antidepressant therapeutic effects of lithium (119). Li^+ at therapeutic levels (0.6 mM) completely blocked isoproterenol effects on GTP binding to G_s, with no effect on basal GTP binding (120). Atropine-blockable, carbamylcholine-induced increases in GTP binding capacity were found to be abolished by lithium (120). Since the muscarinic system is known to be coupled to G proteins other than G_s, i.e., G_i and G_o, lithium abolishment of carbamylcholine effect on GTP binding reflects its interaction with the latter G proteins (120). Li^+ could interfere with the activity of G-proteins by competing with Mg^{2+} ions, which are essential for the binding of GTP to G-proteins.

In summary, the modes of biological action of lithium may involve competition with other electrolytes, binding to membrane receptor sites, and/or influencing second messenger systems such as adenylate cyclase and phosphatidylinositol turnover. It is not known at the present time which of these mechanisms are responsible for the therapeutic effects of lithium. Lithium action is likely to be felt in different organs and to different degrees. However, at a molecular level a simple competition between Li^+ and Mg^{2+} ions may account for most Li^+ interactions in biological tissues.

CHAPTER II

STATEMENT OF THE PROBLEM

The purpose of this investigation is three fold: 1) to propose methods by which the slow onset of Li^+ action can be enhanced, 2) characterize the competition between Li^+ and Mg^{2+} ions for biomolecules, and 3) to find correlations among slow Na^+-Li^+ countertransport rate, amount of Li^+ bound to cell membrane, abnormal membrane makeup, and free intracellular Mg^{2+} levels in manic depressive patients that would lend support to a membrane dysfunction theory.

It takes 5-14 days for lithium to reach its effective therapeutic level (2). The characteristically slow onset of lithium action may necessitate the enrichment of lithium carbonate tablets in ^6Li isotope and the temporary use of a faster acting antipsychotic drug. Naturally occurring lithium carbonate salt consist of 93% ^7Li and 7% ^6Li. Using atomic absorption spectroscopy, it has been shown that the quantity of ^6Li that entered the erythrocytes is greater than ^7Li, with a concentration ratio of ^6Li/^7Li ranging from 5.4 - 8.5% (6). Using magnetic field gradients, the ratio of diffusion rates of ^6Li to ^7Li in aqueous solution is calculated to be 1.003% (9). Several studies have shown that ^6Li is more toxic than ^7Li, thus exerting different behavioral effects (11-13). Since lithium-6 is known to diffuse into the red blood cell faster than lithium-7, obviously the intracellular concentration of lithium-6 is going to be higher than

lithium-7 for the same dosage and period of medication. In fact, lithium toxicity should be compared for the same starting intracellular Li^+ concentrations and not the same starting extracellular Li^+ concentrations. I will show using ^6Li and ^7Li NMR spectroscopy that enriching lithium carbonate tablets with the ^6Li isotope can enhance Li^+ absorption into tissues and speed up the slow onset of Li^+ action in human RBCs.

The therapeutic level of lithium in serum is 0.5 - 1.2 mM and the toxic level is 2.0 mM. Na^+ concentration in human serum is 140 mM. Due to the high similarity in chemical and physical properties and drastic difference in concentrations between Na^+ and Li^+, discrimination between the two ions is difficult. Over the years several ion selective ionophores have been studied (29-36, 44-48). 14-crown-4 crown ether ionophores are known to be the most selective for Li^+ of all reported ionophores (31, 48, 49). The selectivity ratios of Li^+/Na^+ using these ionophores range between 10-300 (29-36). Previous ionophore studies were conducted using a synthetic membrane (44) or used ionophores to measure serum lithium level by constructing Li^+ selective electrodes. The goal of this project is to identify a molecule that can selectively pick up Li^+ and transport it rapidly across the red blood cell membranes. A non-toxic drug delivery system that is isostructural with the 14-C-4 ionophores may then be incorporated in the lithium carbonate tablets and improve Li^+ absorption in tissues.

Several studies show that Li^+ competes with Mg^{2+} for biological ligands (54, 55). Besides the fact that Li^+ and Mg^{2+} have similar chemical properties due to the diagonal relationship that exists between them in the periodic table, it is also known that Li^+ inhibits Mg^{2+} activated ATP dependent enzymes, such as adenylate cyclase, DNA polymerase and phosphofructokinase (64-66). Eighty percent of ATP exists as Mg-ATP, which is the active form. Therefore, my study of Li^+/Mg^{2+} interactions with ATP and ADP in aqueous solution represents a simple model system that can partially depict what goes on in RBCs and nerve

tissues. I hypothesize that one of the mechanisms by which Li^+ exerts its antimanic effect is by competing with Mg^{2+}. The first step would be to determine whether Li^+ and Mg^{2+} bind to the phosphate groups of ATP and ADP using ^{31}P NMR spectroscopy. Due to their high negative charge, phosphate groups are expected to attract alkali and alkaline earth metal ions (67) and be the major binding sites in ATP and ADP. ^{13}C and ^1H NMR studies would show if there is any binding of Li^+ and Mg^{2+} to the base or sugar moieties of ATP and ADP. ^7Li NMR relaxation times would confirm whether there is displacement or ternary complex formation of Li^+ and Mg^{2+} with adenine nucleotides.

It was previously shown in an *in vitro* study done on human RBCs that Li^+ displaced Mg^{2+} from ATP and the displaced Mg^{2+} was presumably bound to the membrane (55). I tested this hypothesis directly. Using ^{31}P NMR spectroscopy, I studied the mode of binding of Li^+ and Mg^{2+} to human RBC membranes.

It has been hypothesized that Mg^{2+} could be responsible for the antimanic effect of Li^+ (68). Therefore, monitoring free intracellular Mg^{2+} levels of patients and of matched controls is ideal to interpret the effect of Li^+ on Mg^{2+} distribution or vice versa. Studies carried out with human red blood cells suggest a membrane cell dysfunction in manic depression (88-91). Characteristic changes in the membrane phospholipid composition of bipolar patients have been reported (88). Manic depressive patients have lower PC and PS content and higher PE content than normal controls (88). Some investigations show that Na^+-Li^+ countertransport rate for manic depressive patients is lower than normal controls (94-97). I hypothesize that if there is higher anionic phospholipid content in the inner leaflet of the RBC membrane, the extent of intracellular Li^+ interaction with the cell membranes may be stronger resulting in lower rates of Li^+ transport across the membrane and higher free intracellular Mg^{2+} due to displacement by Li^+. In order to understand the above problem I characterized the interaction of Li^+ with human

RBC membranes using ^{7}Li NMR relaxation times, monitored free Mg^{2+} level by ^{31}P NMR chemical shifts, measured Na^+-Li^+ countertransport rates using AA, and determined phospholipid composition using ^{31}P NMR.

CHAPTER III

EXPERIMENTAL METHODS

III. 1. Materials

III. 1A. Reagents

Tris salts of adenosine triphosphate (ATP) and adenosine diphosphate (ADP), Tris

chloride, Tris base, sucrose, glucose, choline chloride, Chelex-100 cation exchange resin,

ouabain, 4,4'-diisothiocyanostilbene-2,2'-disulfonic acid (DIDS), and phosphatidylcholine (PC)

were purchased form Sigma. Lithium chloride (LiCl) 99.999%, magnesium chloride ($MgCl_2$)

hexahydrate 99.999%, potassium chloride (KCl), tetramethylammonium hydroxide

[$(CH_3)_4NOH$], tetramethylammonium chloride [$(CH_3)_4NCl$], sodium chloride (NaCl), D_2O 98.8%,

trimethyl phosphate (TMP), trimethyl silane (TMS), tertiary butanol [$(CH_3)_3COH$], sodium

triphosphate (Na_5PPP), dysprosium chloride ($DyCl_3$), and HEPES [4(2-hydroxyethyl)-1-

piperazineethanesulfonic acid], were purchased from Aldrich. Dibenzyl-14-crown-4 was

purchased from the Dojindo Laboratory, Japan. Lithium-6 chloride enriched (^6LiCl, 95.7%)

was purchased from Oak Ridge National Laboratory.

All chemicals were of the highest purity. No further purification was needed except

for Na_5PPP. Na_5PPP was recrystallized three times from 40% ethanol and dried in a rotor

evaporator.

III. 1B. Subjects

Human red blood cells (RBCs) were from Life Source, Chicago section. Whole blood samples from bipolar patients and normotensive controls were obtained with the help of Drs. J. Silberberg, W. Dorus, W. Whang, G. Borge and the nurse E. Elenz from the Department of Psychiatry, Loyola University Stritch of Medicine and Hines Veterans Administration Hospital. Bipolar patients were diagnosed according to Diagnostic and Statistical Manual of Affective Disorders (DSM-IIIR, 1990) (121). The standard procedures for experiments involving human blood were approved by the Institutional Review Boards for the Protection of Human Subjects, Loyola University of Chicago, at both Lake Shore and Maywood campuses, and by the corresponding committee at Hines Veterans Administration Hospital, Hines, IL.

III.2. Instrumentation

III. 2A. Nuclear Magnetic Resonance Spectroscopy

^1H, ^6Li, ^7Li, ^{13}C, ^{23}Na, ^{31}P, and ^{35}Cl NMR measurements were made at 300, 44.6, 116.5, 75.6, 79.1, 121.4, and 35.7 MHz, respectively, on a Varian VXR-300 NMR spectrometer equipped with a multinuclear probe. For the aqueous solution experiments, samples were locked with 16% D_2O and the spin rate was 18 Hz for the 10 mm probe and 20 Hz for the 5 mm probe. All experiments that involved blood samples were run non-spining to avoid RBC settling. All experiments were run at 37 °C. Table 4 shows some of the NMR parameters of used. T_1 and T_2 measurements were made according to published methods (87). Figure 4 shows the pulse sequences used to conduct 1-dimensional, T_1, and T_2 measurements.

TABLE 4. NMR Parameters of Nuclei Investigated at 7.0 T.

	^{1}H	^{6}Li	^{7}Li	^{13}C	^{23}Na	^{31}P	^{35}Cl
Resonating frequency /MHz	300.0	44.3	116.4	74.6	79.4	121.5	29.4
AT /s	3.8	1.7	1.2	1.3	0.15	1.5	0.15
$\Delta\nu_{1/2}$ /Hz	< 1	1	1	<1	4	5	14
PW 90 /μs	20	36	33	17.5	18	12	55
T_1 /s	0.01 - 0.03	10-160	3-20	0.01 - 1	< 0.06	0.1 - 55	10^{-4} - 0.2
NT	1	100	1	100	1	1	7

Figure 4.   Pulse Sequences for 1-D (A), T_1 (B), and T_2 (C) NMR experiments.

A
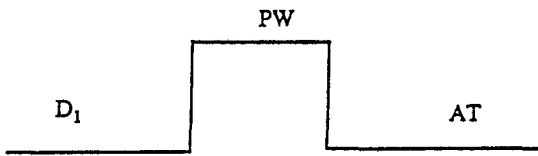
B
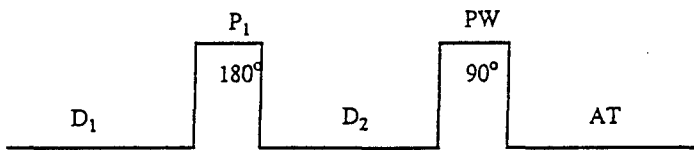
C
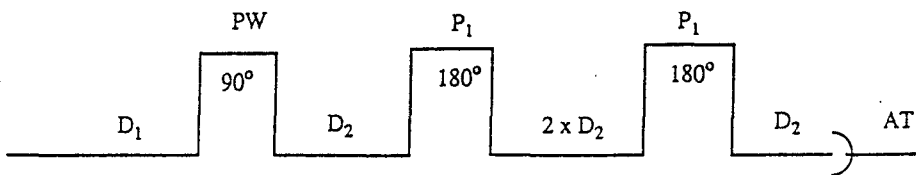
III. 2B. Atomic Absorption Spectrophotometry

Li^+, Na^+ and K^+ absorption measurements were made at 670.8, 589.0, and 766.5 nm, respectively, on a Perkin Elmer 5000 spectrophotometer equipped with a graphite furnace and flame source. Na^+-Li^+ countertransport rate measurements were done according to Canessa et al. (122). The AA parameters for Li^+, Na^+, and K^+ measurements are summarized on Table 5.

III. 2C. Flame Emission Spectrophotometer

The PFP7 is a low temperature, single channel emission flame photometer designed for routine determination of Na^+, K^+ with additional filters available for the determination of Li^+. It was also used to determine intracellular Li^+ concentrations and Na^+-Li^+ countertransport rates.

III. 2D. UV/VIS Spectrophotometer

An IBM UV/VIS 9420 spectrophotometer was used to measure the Mg-ATP affinity constant using the Mg^{2+} specific dye, antipyrylazo III, at 680 nm (61).

III. 2E. Vapor pressure Osmometer

A Wescor Vapor Pressure Osmometer model 5500 was used to measure the osmolarity of all suspension media. The osmolarity of all suspension media was adjusted to 295 $\pm$ 5 mOsm using sucrose.

III. 2F. Hemofuge

Cell volume (hematocrit) was measured using a IEC model MB IM116 hemofuge.

TABLE 5.   Li$^+$, Na$^+$, and K$^+$ AA Parameters.

	Li$^+$	Na$^+$	K$^+$
Wavelength /nm	670.8	589.0	766.5
Slit width, high /nm	1.4	1.4	1.4
Fuel	C_2H_2	C_2H_2	C_2H_2
oxidant	air	air	air
fuel/oxidant flow rate	45/50	45/50	45/50
Sample volume /mL	1.5	1.5	1.5

Using micro glass capillary tubes, blood samples were drawn with a syringe and centrifuged for 3 min. Hematocrit was defined as the ratio of the volume of packed red cells to the volume of the whole suspension medium times 100. The results were read from a micro-hematocrit reader chart.

III. 2G. Refrigerated Centrifuge

Washing of blood was done using a Savant Refrigerated High Speed Model HSC10000 bench top centrifuge. Ghosts were prepared using a Beckman J2-21 refrigerated centrifuge equipped with J-20A and JA-14 fixed angle rotors.

III. 2H. pH Meter

An Orion pH meter was used to check the pH of all suspension media and samples.

III. 2I. Lyophilizer

K_5PPP and $((CH_3)_4N)_5PPP$ were prepared from Na_5PPP using a cation exchange column. The K_5PPP and $(CH_3)_4N)_5PPP$ salts were frozen and then dried using a FDX Flexi-Dry freezer dryer model 1-54.

III. 2J. Analytical Balance

A Mettler AE100 analytical balance that has the capability of weighing samples as low as a tenth of a milligram was used.

III. 3. Sample Preparation

III. 3A. Metal nucleotide complexes in aqueous solution

ATP and ADP concentrations were either 5 or 10 mM, and metal ion concentrations ranged from 5 - 150 mM for LiCl and 0.5 - 50 mM for $MgCl_2$. Nucleotide concentrations did not exceed 10 mM in order to avoid base stacking (67). The pH was adjusted to 7.4 using either tetramethylammonium hydroxide or HCl. Ionic strength was adjusted to 0.15 M using Tris/HCl, which is also used as buffer. For the ^{13}C and ^{1}H NMR experiments no Tris/HCl was added for the Tris peak was overlapping with the nucleotide peaks. All experiments were run at 37 °C.

III. 3B. Preparation of Suspension Media for:

Isotopic Effect on Lithium Kinetics

100 mM LiCl (^{6}Li or ^{7}Li), 5 mM $((CH_3)_4N)_7Dy(PPP)_2$, 10 mM glucose, and 10 mM HEPES, pH 7.4.

Ionophore Induced Li^+ Transport

140 mM NaCl (shift reagent contribution included), 5 mM LiCl, 0.3 mM dibenzyl-14-C-4, 0.1 mM Ouabain, 0.1 mM DIDS, 10 mM glucose, and 10 mM HEPES, pH 7.4 (3 mM $Na_7Dy(PPP)_2$ when needed). Suspension medium for the control experiment consisted of all of the above except for the ionophore dibenzyl-14-C-4.

Na^+-Li^+ Countertransport Rate Measurement

1) Choline Wash Medium: 112 mM choline chloride, 85 mM sucrose, 10 mM glucose, and 10 mM HEPES, pH 7.4.

2) Li^+-loading medium: 150 mM LiCl, 10 mM glucose, and 10 mM HEPES, pH 7.4.

3) Na$^+$ medium: 140 mM NaCl, 10 mM glucose, and 10 mM HEPES, pH 7.4.

4) Choline medium: 140 mM choline chloride, 10 mM glucose, and 10 mM HEPES, pH 7.4.

Human RBC Membranes

1) Washing medium: 150 mM NaCl, 5 mM HEPES, pH 7.4.

2) Lysing medium: 5 mM HEPES, pH 8.0.

3) Resealing medium: 1 mM MgCl$_2$, 5 mM HEPES, pH 8.0.

III. 3C. Li$^+$-loaded RBC

Whole blood from patients and matched controls was centrifuged at 6,000 g to separate the RBCs from the plasma and WBCs.   Packed RBCs were washed three times for 5 min each by centrifugation, at 6,000 g, at 4 °C, using choline wash solution.   Supernatant and buffy coat were removed by aspiration.   Two Li$^+$ loading procedures of RBCs were adapted from the literature: one involved incubating cells at 50% hematocrit (Hct) in a Li$^+$-loading medium for 3 hrs in a 37 °C water bath to achieve 1 - 1.5 mM intracellular lithium (94), and the other incubating the cells at 13% hematocrit to obtain 6.5 - 7.0 mM Li$^+$ inside the red blood cell (122).   After incubation was complete, the Li$^+$-loaded cells were washed five times using choline wash solution by centrifugation at 6000 g for 5 min to remove extracellular lithium.

III. 3D. Preparation of Shift Reagent

The Na$_7$Dy(PPP)$_2$ complex was prepared from DyCl$_3$ and Na$_5$PPP in a ratio of 1:2.5. Sodium triphosphate was added dropwise to DyCl$_3$ until complete formation of the complex which is indicated by the clarity of the solution (41, 42, 123). The tetramethylammonium and potassium forms of triphosphate were obtained by passing the sodium form of the triphosphate through Dowex-50W columns saturated with (CH$_3$)$_4$NCl and KCl, respectively.   The columns

respectively. The columns were rinsed with deionized water for complete removal of the ligand and freeze-dried overnight. Preparation of the K^+ and $(CH_3)_4N^+$ forms of $Dy(PPP)_2^{7-}$ were the same as for the Na^+ form as stated above.

III. 3E   Preparation of Human RBC Membranes

Washing of RBCs is the same as section III. 3C except 5 mM HEPES, and 150 mM choline chloride, pH 7.4 isotonic washing solution was used. Procedures used to prepare human RBC membranes were taken from Steck et al. (124). Washed-packed RBCs (5 mL) were lysed using 30 mL of hypotonic lysing medium, 5 mM HEPES pH 8 (5H8). The suspension medium was centrifuged three times for eight min. each at 18,000 g and 4 °C using a Beckman J2-21 centrifuge and J-20A rotor, until the white membrane was observed.

III. 3F   Preparation of Large Unilamellar Vesicles

PC from egg yolk was dried under N_2 to remove all the hexane. PC (1.4 mL) was dissolved in 20 mL of 2:1 (v/v) chloroform-methanol, and the mixture was dried to a thin film under a stream of N_2 and then put under vacuum for 5 hrs to remove the residual traces of organic solvents (125). NaCl (150 mM) or LiCl (150 mM) or a mixture (75:75 mM) of the two salts, and 10 mM HEPES, pH 7.4 (4 L) was degassed with N_2 for over 12 hrs. The lipid film was dissolved in 4.5 mL of the desired buffer and 0.3948 g octyl-β- glucopyranoside (a detergent used to fuse the vesicles) and placed in dialysis tubing. The above mixture was dialyzed twice for 12 hrs against 2 L of the desired buffer. To remove residual detergent and extracellular Li^+ and Na^+ ions, the sample was dialyzed in 150 mM KCl, 10 mM HEPES, pH 7.4 for 24 hrs. Vesicles were forced through a syringe equipped with a 0.45 μm filter to homogenize the size.

Dialysis tubing were prepared by placing strips of tubing twice in each of the following solutions for 1 hr at 60 °C. 1) 50/50 (v/v) ethanol-water; 2) 10 mM $NaHCO_3$; 3) 1 mM

Na$_2$H$_2$EDTA; 4) double distilled water; 5) 0.02% NaN$_3$.

III. 3G. Extraction and Analysis of Phospholipids

RBC membranes were prepared according to section III. 3E. RBC membranes (1 mL) was added slowly to 17 mL of methanol and mixed for 10 min. Methanol was purchased from Aldrich Chem. Co. in a sure-seal bottle and the chloroform was distilled. All extracting solvents consisted of 50 mg/L of butylatedhydroxytoluene (BHT) as an antioxidant. Chloroform (33 mL) was added and the entire mixture was mixed for 15 min (126-128). The resulting extract was filtered through a medium size sintered glass funnel. The extract was washed with 50 mL of a chloroform, methanol mixture (2:1) to reextract the residual phospholipids. The filtrate was mixed thoroughly with 0.74% KCl of 0.2 times its total volume to remove all non lipid impurities. The bottom chloroform layer was separated using a separatory funnel fitted with a teflon stopcock. The purified phospholipid was dried in a rotary evaporator at 30 °C. The final lipid extract was stored at -20 °C in 2 mL of deuterated chloroform. To this 2 mL of deuterated chloroform consisting of the lipid extract, 1 mL of 1:4 deuterated EDTA:methanol solution was added. Phospholipid analysis was done according to Glonek et. al. (128) using ^{31}P NMR. NMR suspension media were prepared as follows (128). The free acid EDTA was titrated to pH 6 using tetramethyl ammoniumhydroxide to a final concentration of 0.2 M. The sample was freeze-dried in a lyophilizer. The solid was redissolved in a minimum amount of D$_2$O and freeze-dried in order to exchange the two labile hydrogens for deuterium. The base and the acid were prepared in D$_2$O. The sample was placed in a 10 mm NMR tube and let stand for a few minutes for the aqueous phase to separate. The turbine was adjusted so that only the chloroform phase covered the NMR window. ^{31}P NMR was run at a resonating frequency of 121.5 MHz in a Varian VXR-300 MHz instrument. Spectrometric conditions used were as follows: 1-D pulse sequence, pulse width of 10 μs (45° flip angle), AT of 1.4 s, D$_1$ of 1.5 x the longest T$_1$

(2.5 s) were used. Samples were run locked on D_2O, at ambient temperature and spinning at 16 Hz.

III .4. Data Analysis

III. 4A. Determination of Mg-ATP and Mg-ADP association constants

A combination of ^{31}P and optical spectroscopy studies were used to calculate the Mg^{2+} association constants (61). The concentration of free Mg^{2+} was measured from the absorbance of the Mg^{2+}-specific dye, antipyrylazo III. The Mg^{2+} association constants K_A to ATP were given by (61):

$$K_A = ([Mg^{2+}]_f)^{-1} (1 - \phi) / \phi \qquad (1)$$

$$\phi = [ATP]_f / [ATP]_T \qquad (2)$$

$$\phi = (\delta_{\alpha\beta}obs - \delta_{\alpha\beta}MgATP) / (\delta_{\alpha\beta}ATP - \delta_{\alpha\beta}MgATP) \qquad (3)$$

where $\delta_{\alpha\beta}obs$ is the observed chemical shift difference between the α- and β- phosphate resonances in Mg^{2+}-nucleotide solutions that are not saturated with Mg^{2+}; $\delta_{\alpha\beta}ATP$ and $\delta_{\alpha\beta}MgATP$ are the maximal and minimal values of this difference without and with Mg^{2+} respectively; $[ATP]_T$ is the total ATP concentration; and $[ATP]_f$ is the sum of the concentrations of all ATP species not chelated to Mg^{2+}. Similar expressions were used to calculate Mg-ADP association constants.

Association constants of 1:1 Li^+ complexes of ATP and ADP, using the first model (stoichiometry of 1:1, Li^+:nucleotide), were calculated based on the following equations:

$$\delta_{obs} = x_{ATP} \delta_{ATP} + x_{LiATP} \delta_{LiATP} \qquad (4)$$

$$[Li^+]_{eq} + K_{LiATP}[Li^+]_{eq}[ATP]_{eq} - [Li^+]_o = 0 \qquad (5)$$

Similar equations were used to generate Li^+ association constants based on 2:1 species, using the second model (stoichiometry of 2:1, Li^+:nucleotide):

$$\delta_{obs} = x_{ATP}\delta_{ATP} + x_{Li_2ATP}\delta_{Li_2ATP} \qquad (6)$$

$$[Li^+]_{eq} + 2K_{Li_2ATP}[Li^+]_{eq}[ATP]_{eq} - [Li^+]_o = 0 \qquad (7)$$

where δ_{ATP}, δ_{LiATP}, and δ_{Li_2ATP} represent the limiting chemical shifts for the free ATP, LiATP,

and Li_2ATP species; x_{ATP}, x_{LiATP}, and x_{Li_2ATP} are the mole fractions for the same species; K_{LiATP}

and K_{Li_2ATP} are the association constants for the LiATP and Li_2ATP complexes; and subscripts

eq and o represent the equilibrium and starting Li^+ concentrations.

III. 4B. ^{6}Li and ^{7}Li NMR Determination of Li^+ concentration

Intracellular ^{6}Li and ^{7}Li concentrations, $[Li]_I$, were calculated by integrating the areas,

A_I and A_E, under the NMR intra- and extracellular resonance curves, and by taking into account

the total isotopic composition of the LiCl used, $[Li^+]_T$, and the hematocrit level, Hct:

$$[Li^+]_I = \frac{[Li^+]_T \times (1 - Hct) \times A_I}{Hct \times (A_I + A_E)} \qquad (8)$$

Initial rates of Li^+ uptake were calculated from the slopes of the plots of $[Li^+]_I$ vs. time t for

each isotope. The rate constants, k, were calculated from the equation:

$$ln\ [Li^+]_I\ /\ [Li^+]_T = -kt \qquad (9)$$

III. 4C. NMR and AA Determinations of Li^+, Na^+, K^+, and Cl^- concentrations

For the AA experiments, the extracellular Li^+, Na^+, and K^+ concentrations

were determined by placing 500 μL aliquots at 15 min intervals in precooled culture tubes.

The aliquots were centrifuged at 2000 g for 4 min at 4 °C and the supernatants were collected,

diluted with deionized water, and analyzed directly for metal ion concentration by AA. Li^+,

Na^+, and K^+ standards prepared in the SR suspension medium were used to construct calibration

curves and to determine extracellular metal ion concentrations. For the NMR experiments, intra-

and extracellular ion concentrations ($[I^+]_{in}$ or $[I^+]_{out}$) in RBC suspensions were calculated from the following equations:

$$[I]_{in} = A_{in} \times [I]_s / (A_s \times Ht \times v) \qquad (10)$$

$$[I]_{out} = A_{out} \times [I]_s / \{A_s \times (1 - Ht)\} \qquad (11)$$

where A_{in} and A_{out}, are the peak areas under the intra- and extracellular $^7Li^+$ or $^{23}Na^+$ NMR resonances, and $[I]_s$ and A_s are the concentration and peak area of the standard solutions (0.15 M LiCl or NaCl plus 5 mM DyCl$_3$) measured separately. Relative peak areas were obtained by means of the integration routines included in the software provided by the manufacturer for the Varian VXR-300 NMR spectrometer. The NMR determined concentrations of Li^+ and Na^+ take into account the hematocrit, Ht, and the visibility factor ($v = 0.8$ for ^{23}Na and 1.0 for ^7Li) for intracellular metal ion RBC resonances (41). In the case of ^{35}Cl NMR, only the extracellular Cl^- concentration could be determined because the intracellular $^{35}Cl^-$ NMR resonance is invisible in human RBC suspensions (129). The extracellular Cl^- concentration was calculated from equation (11) above where $[I^+]_s$ and A_s are the concentrations and peak areas of standard Cl^- solutions measured separately.

For RBC suspensions, the pseudo first order rate constants, k, were determined from linear regression analysis of plots of ln ($[M^+]_t/[M^+]_0$) versus time, where $[M^+]_0$ and $[M^+]_t$ represent the initial extracellular Li^+ or Na^+ concentration and those after time t. For vesicle suspensions, the pseudo first order rate constants were determined from linear regression analysis of plots of ln A_t/A_o versus time, where A_t and A_o represent the initial peak areas of the extravesicular metal NMR resonances and those after time t (44).

III. 4D. Calculation of Free and Total Mg^{2+} in Human RBCs

Free Mg^{2+} concentration was calculated using Gupta's equation (61).

$$\phi = (\delta_{\alpha\beta}RBC - \delta_{\alpha\beta}MgATP) / (\delta_{\alpha\beta}ATP - \delta_{\alpha\beta}MgATP) \quad (12)$$

$$[Mg^{2+}] = K_D / (\phi / 1 - \phi) \quad (13)$$

where $\delta_{\alpha\beta}RBC$ is the chemical shift difference between the α- and β- phosphate resonances in RBCs; $\delta_{\alpha\beta}ATP$ and $\delta_{\alpha\beta}MgATP$ are the maximal and minimal values of this difference without and with Mg^{2+} in aqueous solution, respectively (5 mM ATP and 15 mM $MgCl_2$); Mg^{2+} is the free magnesium concentration, and K_D (50 μM) is Mg-ATP dissociation constant calculated using equations in section III. 4A (61). Total intracellular Mg^{2+} was measured by the standard addition method using AA.

III. 4E. Quantitation of Phospholipids in Human RBC Membranes Using ^{31}P NMR

Phospholipids were extracted from human RBC membranes using procedures in section III. 3G (126-128). The peak areas under the ^{31}P NMR spectra were integrated using the integration software of the NMR spectrometer. Each phospholipid peak in the RBC membranes was identified either by running standards alone or spiking the samples with standards purchased from Sigma Chemical Co.

III .4F. Protein Determination

Determination of protein was done using the Bradford Assay (130). To summarize the method briefly, standards of protein, 2.5 - 15 μg/μL, were prepared from 1mg/mL bovine albumin serum (BSA) in a Bradford working buffer (final vol. 2 mL). The Bradford working buffer consisted of H_2O, 95% ethanol, 88% phosphoric acid, and Bradford stock solution purchased from Bio-Rad Chem. Co. After proper dilution, samples were mixed with the Bradford working buffer and the absorbance was read at A_{595} using UV/VIS spectroscopy.

III. 4G. Statistical Analysis

The statistical significance of the differences between the transport data for the stable isotopes of Li^+, and for the Li^+ transport parameters between bipolar patients and matched controls were analyzed using a Student's t-test. Correlation among Li^+ transport, phospholipid composition, and $[Mg^{2+}]$ parameters for RBCs from bipolar patients and matched controls were obtained using a Pearson correlation matrix.

CHAPTER IV

RESULTS

IV.1 <u>**Isotopic Differences Between ^{7}Li and ^{6}Li Ions in Transport Across Human Red Blood Cell Membranes**</u>

IV. 1A ^{7}Li and ^{6}Li NMR Spectra of Human RBCs

Figure 5 shows ^{7}Li (5A) and ^{6}Li (5B) NMR spectra of human RBCs in ^{7}LiCl and ^{6}LiCl containing media at 1, 5 and 11 h of loading. The horizontal axis is in ppm units which represent the chemical shift of the extracellular Li^+ (Li_E) resonance from that of intracellular Li^+ (Li_I) arbitrarily placed at zero. Figure 6 is a plot of intracellular concentrations of the two Li^+ isotopes *vs* time. Table 6 shows the intracellular $^6Li^+$ and $^7Li^+$ concentrations at time t. The data given in Figure 5 and 6 and Table 6 clearly show that Li-6 diffuses faster inside the RBCs than Li-7.

During the NMR measurements on these suspensions, the sample temperature was maintained at 37 °C. The NMR spectra were obtained with a single pulse sequence, D-P-AQ, where D is the delay time between successive signal acquisitions, P is the radiofrequency excitation pulse (60°), and AQ is the time (1 s) during which the emitted radiofrequency

Figure 5. ^{7}Li (A) and ^{6}Li (B) NMR spectra of human RBC suspended at 26% hematocrit in 100 mM LiCl, 5 mM((CH_3)$_4$N)$_7$Dy(PPP)$_2$, 10 mM glucose and 10 mM HEPES, pH 7.4. The intracellular resonances are labeled I while the extracellular ones are labeled E. ^{7}LiCl (92.6% ^{7}Li) and ^{6}LiCl (95.7% ^{6}Li) were used in Figure A and B, respectively. The intensity scale for ^{6}Li NMR spectra is 1.033 (95.7/92.6) lower than that for ^{7}Li NMR spectra to take into account for the difference in isotopic composition.
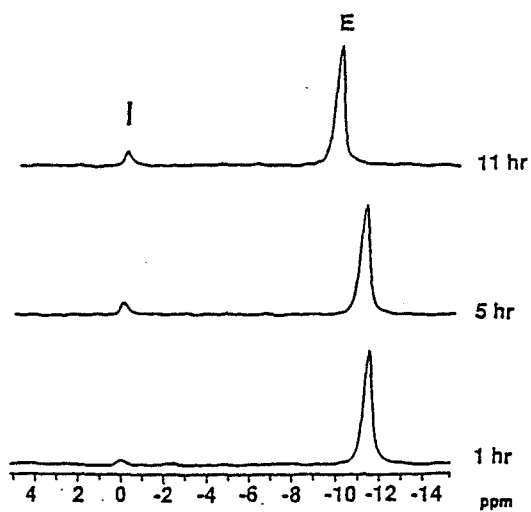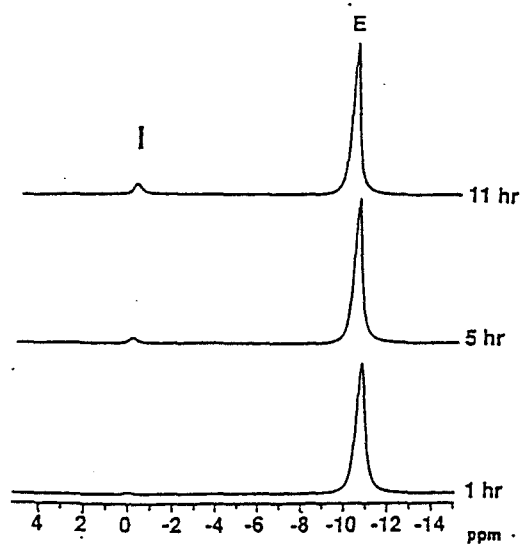
Figure 6. A Plot of intracellular $^6Li^+$ and $^7Li^+$ concentrations in RBCs vs time. Each point represents the average of three experiments performed on separately prepared samples. The error bars indicate the range of concentration values obtained. Open squares denote $^6Li^+$ and closed circles $^7Li^+$.
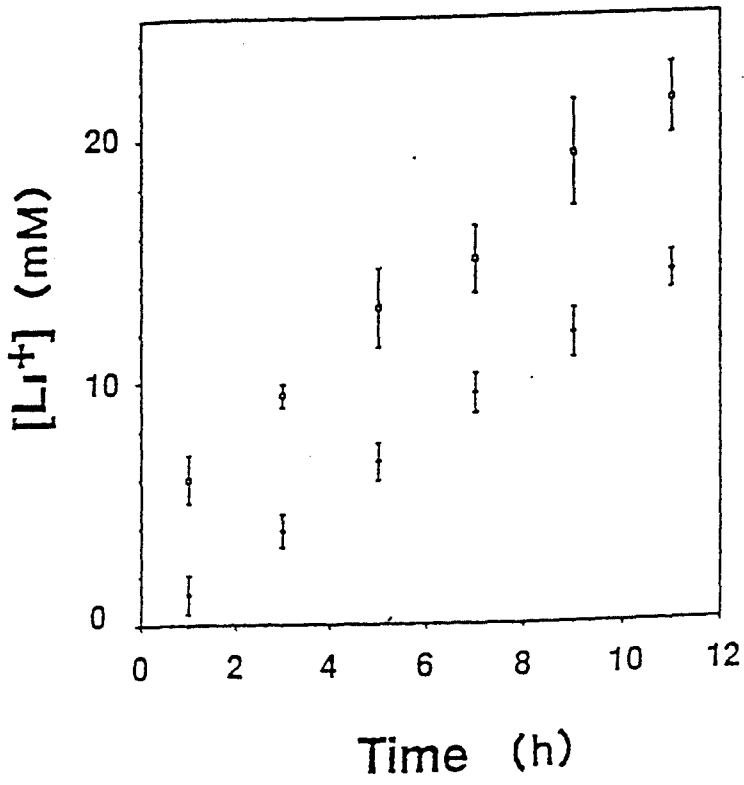
Table 6. Time Dependence of Intracellular $^6Li^+$ and $^7Li^+$ concentrations Using NMR[a].

Time /h	$[^6Li^+]$ /mM	$[^7Li^+]$ /mM
1	6.01 ± 0.99	1.24 ± 0.81
3	9.39 ± 0.47	3.82 ± 0.66
5	13.01 ± 1.64	6.66 ± 0.77
7	15.00 ± 1.38	9.47 ± 0.83
9	19.32 ± 2.20	11.88 ± 1.04
11	21.49 ± 1.44	14.39 ± 0.78

[a]Human RBCs were suspended at 26% hematocrit either in 100 mM ^7LiCl or ^6LiCl, 5 mM $((CH_3)_4N)_7Dy(PPP)_2$, 10 mM glucose and 10 mM HEPES, pH 7.4. Osmolarity was maintained at 295 ± 5 mOsm. Triplicate samples were prepared.

signals are collected. The D values used (15 s for ^{7}Li and 60 s for ^{6}Li) allowed for complete relaxation of the intracellular ^{7}Li$^+$ and ^{6}Li$^+$ NMR resonances before the next pulse P was applied. ^{7}Li and ^{6}Li NMR spectra were obtained after 450 and 120 scans, respectively, each requiring a total of 2 h. The delay time and the total number of scans used in ^{6}Li NMR spectra were changed to accommodate the longer relaxation time for the ^{6}Li nucleus. The intensity scale for ^{6}Li NMR spectra is 1.033 (95.7/92.6) lower than that for ^{7}Li NMR spectra to take into account the different isotopic compositions of the LiCl salts used. Lithium influx was measured every 2 h over a 12 h period. Each spectrum represents the midpoint for each 2 h of accumulation time extending over 12 h.

Uptake of ^{6}Li$^+$ by RBC was significantly faster than that of ^{7}Li$^+$. The initial rates of transport Li$^+$ in RBCs for the ^{6}Li and ^{7}Li isotopes are 1.56 $\pm$ 0.12 and 1.32 $\pm$ 0.14 mmol Li$^+$/(l of RBCs x h), respectively. The rate constants for the ^{6}Li and ^{7}Li isotopes are (6.92 $\pm$ 0.57) x 10^{-3}/h and (5.93 $\pm$ 0.64) x 10^{-3}/h, respectively. ^{7}Li and ^{6}Li have a mass ratio of 1.167 (7/6), and we found their rate and rate constant ratio to be 1.182 (1.56/1.32) and 1.167 (6.92 x 10^{-3}/5.93 x 10^{-3}), respectively. The more rapid uptake of ^{6}Li$^+$ relative to ^{7}Li$^+$ across the human RBC membrane is associated with the lower mass of the ^{6}Li isotope, the consequent higher charge-to-mass ratio, and the resulting higher hydration energy. The masses of the two isotopes differ by 16.7%. The difference between the two isotopes calculated from either the rates (18.2%) or the rate constants (16.7%) is similar to the difference in mass.

IV.1B Viability of Human Erythrocytes Incubated with ^{7}LiCl and ^{6}LiCl

When studying ion transport in human RBCs, monitoring cell viability is very important. Some of the changes RBCs could undergo include cell volume, levels of some

metabolites, such as ATP and DPG, and pH.

Cell volume was measured using a hemofuge at the beginning and at the end of the 12 h period. At the beginning of the experiment cell volume was 26 $\pm$ 0.5% and at the end of the 12 h period it was 28 $\pm$ 0.7% (n=3). Figure 7 shows ^{31}P NMR spectra of human RBCs at the beginning (7A) and at the end (7B) of 12 h period in ^{7}LiCl medium, and at the beginning (7C) and at the end (7D) of 12 h period in ^{6}LiCl medium. The ATP level was maintained throughout the experiment and there was a slight decrease in the DPG level. The increase in the Pi peak was mainly due to the hydrolysis of the shift reagent Dy(PPP)$_2^{7-}$ and corresponding formation of inorganic phosphate, and to a smaller extent from the hydrolysis of DPG. More DPG hydrolysis and increased Pi peak intensity is observed in Figure 7D. This is presumably due to the faster transport of ^{6}Li$^+$ than ^{7}Li$^+$. More intracellular ^{6}Li$^+$ accumulation may lead to cell toxicity.

The measurement of pH provides an important contribution to our understanding of *in vivo* metabolism. For example, hydrogen ions play a direct part in many enzyme-catalyzed reactions, and from this point of view the hydrogen ion can be regarded as an important metabolite (87). Metal ions could alter intracellular pH by competing with H$^+$. ^{31}P NMR provides a tool for measuring intracellular pH (87). The chemical shift separation between Pi and Pα of ATP ($\delta_{Pi\alpha}$) was used as an indicator of intracellular pH. Human RBCs suspended in either ^{6}LiCl or ^{7}LiCl showed no changes in $\delta_{Pi\alpha}$ separation over the 12 h period. Thus, there was no change in intracellular pH.

IV.1C Effect of Dy(PPP)$_2^{7-}$ on Lithium Transport Across Human RBCs Using AA

^{31}P and ^{19}F NMR measurements of the membrane potential of Li$^+$-free RBCs revealed that Dy(PPP)$_2^{7-}$ changed the membrane potential (42). The rate of Na$^+$-Li$^+$ exchange in

Figure 7. ^{31}P NMR spectra of human RBCs at the beginning (A) and at the end of the 12

h period (B) in 100 mM ^{7}LiCl; at the beginning (C) and at the end (D) of the 12 h period in

100 mM ^{6}LiCl.   RBCs were suspended either in 100 mM ^{7}LiCl or 100 mM ^{6}LiCl, 5 mM

$((CH_3)_4N)_7Dy(PPP)_2$, 10 mM glucose, 10 mM HEPES, pH 7.4.   Peak assignments are as

follow: a = DPG, b = Pi, c = γ-ATP, d = α-ATP, and e = β-ATP.
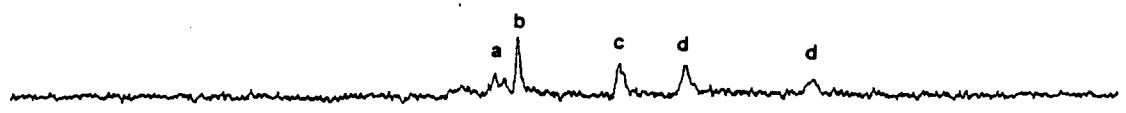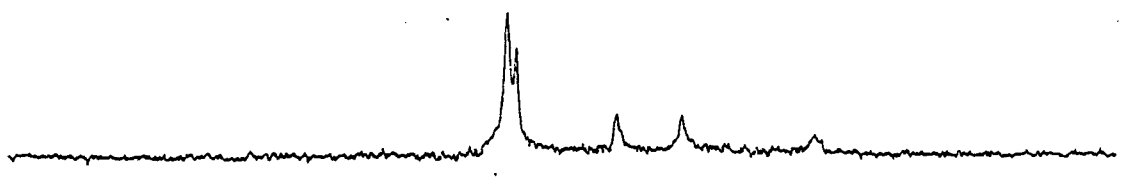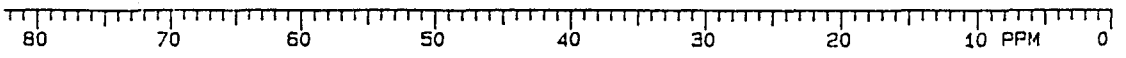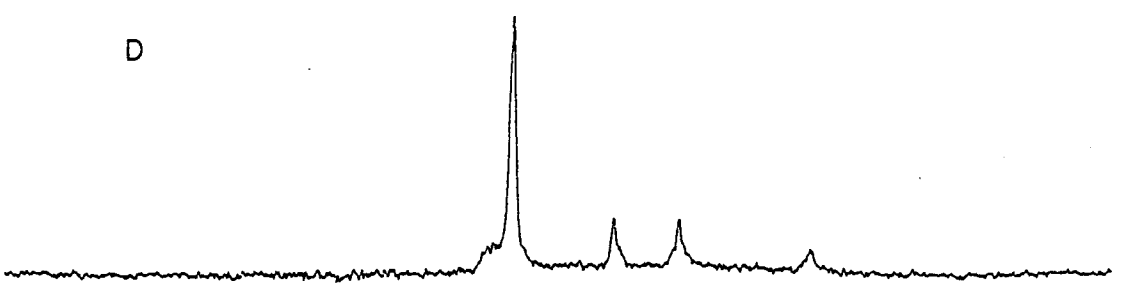
Li$^+$-loaded RBCs measured by ^{7}Li NMR spectroscopy in the presence of Dy(PPP)$_2^{7-}$ were significantly higher than the rates measured in the absence of shift reagents by atomic absorption (42). To investigate the effect of the shift reagent on Li$^+$ influx, control experiments were conducted. Table 7 depicts control experiments of human RBCs with and without 5 mM ((CH$_3$)$_4$N)$_7$Dy(PPP)$_2$, suspended in 100 mM ^{7}LiCl. In fact, in the presence of shift reagent there is a decrease of 3.48% in the rate of ^{7}Li$^+$ uptake, respectively. This is due to the electrostatic interaction between the negatively charged shift reagent and Li$^+$ ions. Most of the Li$^+$ ions are coordinated to the second coordination sphere of the complex (131). Thus, a small decrease in Li$^+$ influx is observed upon incorporation of SR in the media. Figure 5 shows that the magnitude of the shift change is greater for extracellular ^{6}Li$^+$ than ^{7}Li$^+$ because the amount of ^{6}Li$^+$ competing with other cations in the suspension medium and interacting with shift reagent is less than that of ^{7}Li$^+$ (132).

IV. 2 Dibenzyl-14-Crown-4 Induced Lithium Transport in Normal Human Erythrocytes and PC Vesicles

IV. 2A Transport of Li$^+$, Na$^+$, K$^+$ and Cl$^-$ Ions Across Human RBC Membranes

Crown ethers, such as 14-C-4, are known to be Li$^+$ selective ionophores (29-31, 33, 47, 49, 50). Figure 8 shows the structure of dibenzyl-14-Crown-4, the crown ether used in my project. Figure 9 shows ^{7}Li (part A) and ^{23}Na (part B) NMR spectra of human RBCs at 7.5, 37.5, and 67.5 min in the presence and absence of DB-14-C-4. In the presence of ionophore and at the end of 75 min, the intracellular Li$^+$ concentration was 3.0 mM, whereas in its absence it was 0.3 mM (Figure 9). At the end of the same period, the peak area

Table 7. Time Dependence of Intracellular lithium concentrations of human RBCs in the presence and absence of 5 mM $Dy(PPP)_2^{7-}$ Using AA.[a]

	$[Li^+]$ /mM	
Time /h	With $Dy(PPP)_2^{7-}$	Without $Dy(PPP)_2^{7-}$
0	0	0
2	4.75 $\pm$ 0.25	5.35 $\pm$ 0.65
4	7.95 $\pm$ 0.15	8.65 $\pm$ 0.15
6	10.30 $\pm$ 0.50	11.25 $\pm$ 0.25
8	11.45 $\pm$ 0.15	13.15 $\pm$ 0.25
10	12.45 $\pm$ 0.35	13.78 $\pm$ 0.65
12	15.50 $\pm$ 0.40	16.05 $\pm$ 0.45

[a]RBCs were suspended at 26% hematocrit in a medium that consists of 100 mM ^7LiCl, 10 mM glucose, and 10 mM HEPES, pH 7.4. Samples were prepared in triplicate.

Figure 8. Structure of Dibenzyl-14-Crown-4
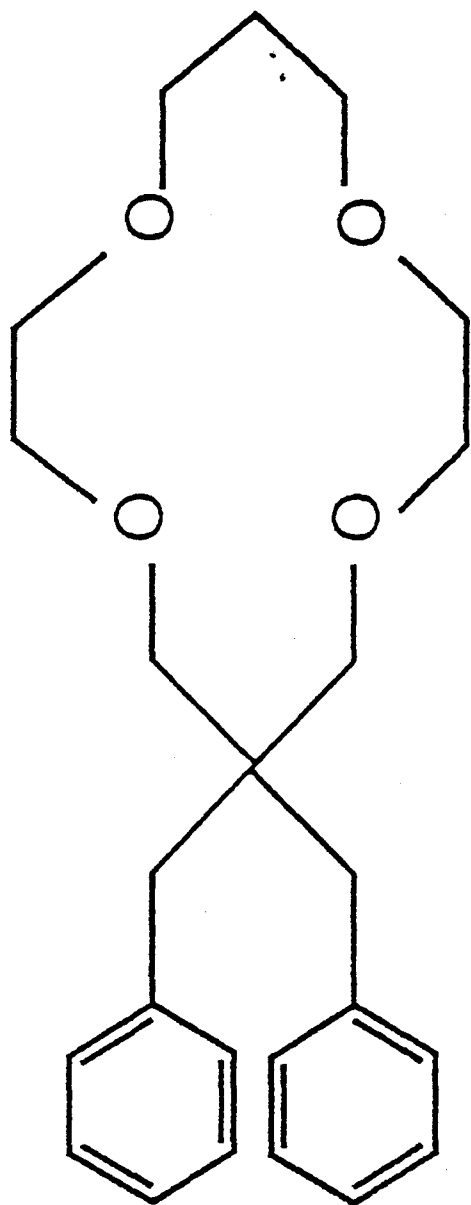
Figure 9. ^{7}Li **(A)** and ^{23}Na **(B)** NMR spectra of human RBCs in the presence and absence of 0.3 mM DB-14-C-4 at 7.5, 37.5, and 67.5 min, and in in its absence at 67.5 min. In parts (A) and (B), the bottom three spectra are for samples containing ionophore, whereas the top spectrum is for a sample without ionophore. RBCs were suspended at 26% hematocrit in 140 mM NaCl (shift reagent contribution included), 5 mM LiCl, 5 mM Na$_7$Dy(PPP)$_2$, 0.1 mM ouabain, 0.1 mM DIDS, 10 mM glucose and 10 mM HEPES, pH 7.4. Osmolarity of suspension media was maintained at 295 $\pm$ 5 mOsm.   The peaks at 0 ppm represent intracellular Li$^+$ or Na$^+$ ions, whereas the extracellular peaks are upfield.
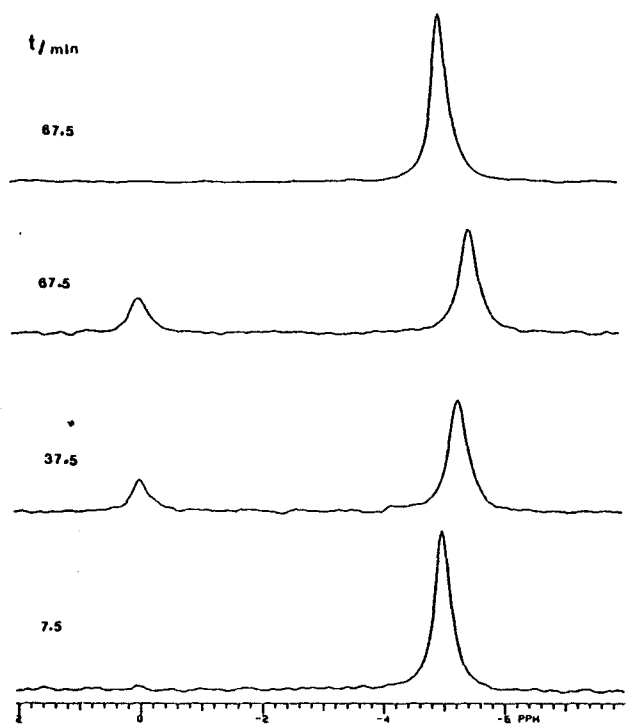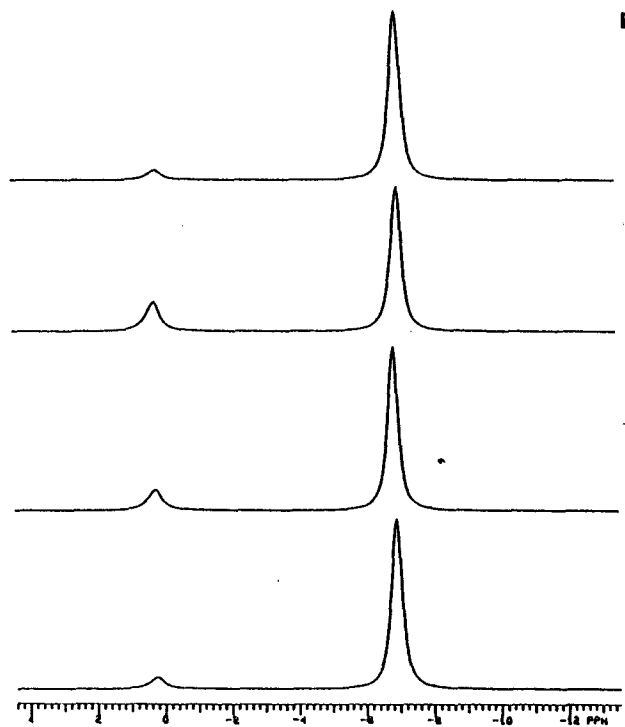
corresponding to the intracellular $^{23}Na^+$ NMR resonance increased in the presence of ionophore, but not in its absence. The intracellular Na^+ concentrations at the end of 75 min in the presence and absence of ionophore were 45.0 and 9.0 mM, respectively (Figure 9). Figure 10 shows changes in extracellular Na^+, K^+, and Cl^- concentrations in the presence (part A) and in the absence (part B) of 0.3 mM DB14C4. It is clearly shown that transport of ions was induced mainly by the ionophore.

I calculated pseudo-first-order rate constants and Li^+/Na^+ selectivity ratios for Li^+ and Na^+ transport in human RBC suspensions from AA measurements of extracellular ion concentrations. The pseudo-first-order rate constants, k, were determined from linear regression analysis of plots of ln $([M^+]_t/[M^+]_0)$ versus time, where $[M^+]_0$ and $[M^+]_t$ represent the initial extracellular Li^+ or Na^+ concentration and that at time t. In the presence of 0.30 mM ionophore in an SR-free medium containing 0.1 mM DIDS and 0.1 mM ouabain, Li^+ and Na^+ transport had rate constants of 0.18 $\pm$ 0.01 and 0.12 $\pm$ 0.02 h^{-1}, respectively. The Li^+/Na^+ selectivity ratio was 1.47 $\pm$ 0.10. Ouabain and DIDS are known inhibitors of the Na^+-K^+ pump and band 3 protein, respectively (133, 134a). Similar experiments conducted without the inhibitors, in the suspension media showed large Na^+, K^+ and Cl^- movements across the membrane. Incorporation of DB14C4 at different concentrations (0.25, 0.30, and 0.35 mM) in the human RBC suspension medium (free of SR, DIDS, and ouabain) led to pseudo-first-order rate constants (k values) for Li^+ transport of 0.15 $\pm$ 0.02, 0.18 $\pm$ 0.02, and 0.24 $\pm$ 0.01 h^{-1}, respectively. The ratio k/[ionophore], which represents the second-order rate constant for Li^+ transport, was approximately constant and equal to 627 $\pm$ 33 M^{-1} h^{-1}. Similarly, the k values for transport of Na^+ across the RBC membrane were 0.16 $\pm$ 0.01, 0.18 $\pm$ 0.01, and 0.26 $\pm$ 0.03 h^{-1} for ionophore concentrations 0.25, 0.30, and 0.35

Figure 10. Changes in extracellular Na^+, K^+ and Cl^- concentrations with time in the presence of 0.3 mM DB-14-C-4 (A) and in the absence (B). Conditions are the same as for Figure 9. Circles, triangles and squares represent K^+, Cl^- and Na^+ ion concentrations, respectively.
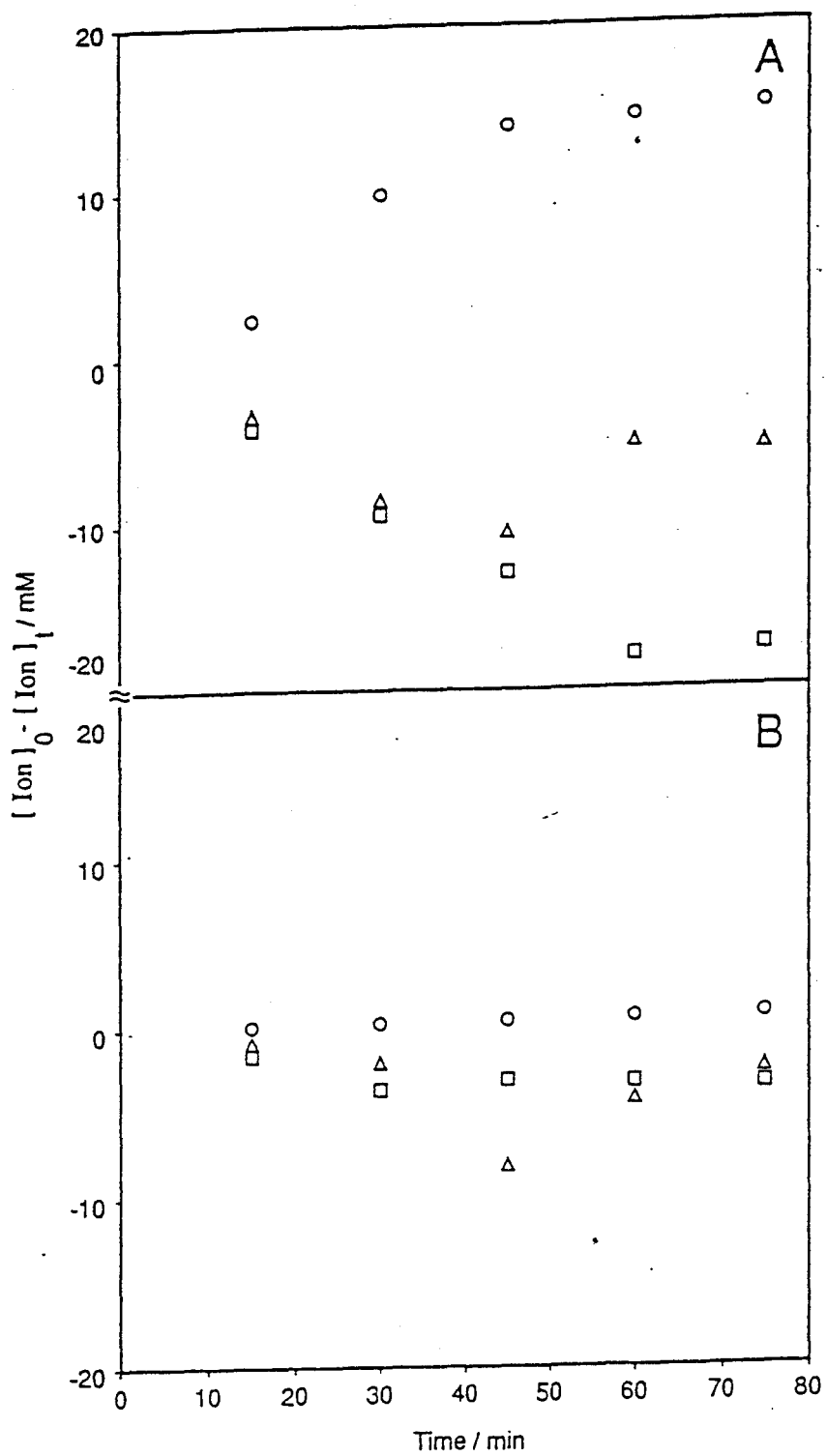
mM, respectively, giving a k/[ionophore] ratio of 653 ± 60 $M^{-1}h^{-1}$. In the presence of 0.30 mM ionophore, addition of 0.1 mM DIDS and 0.1 mM ouabain had no significant effect on the rates of Li^+ transport. However, the pseudo-first-order rate constant for Na^+ transport induced by 0.30 mM ionophore decreased from 0.18 ± 0.01 to 0.12 ± 0.02 h^{-1} upon addition of transport inhibitors. The difference in rates of Na^+ transport upon addition of inhibitors is presumably related to inhibition of Na^+ transport by ouabain. There was no apparent effect of ouabain on the rates of Li^+ transport because Li^+ uptake in human RBC suspensions is mediated by a leak pathway, and not by Na^+,K^+-ATPase (27).

In the presence of 5 mM $Na_7Dy(PPP)_2$ and 0.30 mM DB14C4 in a medium containing DIDS and ouabain, the rates constants for transport of Li^+ and Na^+ were 0.15 ± 0.02 and 0.12 ± 0.05 h^{-1}, whereas in the absence of SR the rate constants for transport of Li^+ and Na^+ were 0.18 ± 0.01 and 0.12 ± 0.02 h^{-1}. The Li^+/Na^+ selectivity ratios in the absence and presence of SR were 1.47 ± 0.10 and 1.19 ± 0.01, respectively. The SR decreased the rate constants for transport of Li^+ but not of Na^+. The slight decrease in the Li^+/Na^+ selectivity ratio from 1.47 ± 0.10 in the absence of $Dy(PPP)_2^{7-}$ to 1.19 ± 0.01 in the presence of SR suggests that less Li^+ than Na^+ transport occurs across the human RBC membrane when the triphosphate SR is present in the suspension medium. The SR binds more strongly to Li^+ ions, resulting in slower rates of Li^+ transport in SR-containing medium. This SR-specific effect is consistent with the previously reported effects of $Dy(PPP)_2^{7-}$ on membrane potential, Na^+-Li^+ exchange rates, and Li^+ and Na^+ transmembrane ratios in human RBC suspensions (41,42).

IV.2B Viability of RBCs in the Presence of Ionophore

Figures 11 A and B show ^{31}P NMR of normal human erythrocytes in the presence of 0.3 mM DB-14-C-4 at the beginning and at the end of the 1.25 h period. ATP and DPG levels were maintained throughout the experiment. Cell viability was therefore preserved during the course of the ionophore-induced ion transport experiment. The chemical shift separation between Pi and Pα of ATP ($\delta_{\alpha\beta}$) were the same at the beginning and at the end. Thus, intracellular pH was also maintained during these experiments and the mechanism of ionophore induced ion transport does not involve exchange between intracellular H$^+$ and extracellular alkali metal cations as previously reported for other Li$^+$ ionophores (44).

Table 8 also shows changes in cell volume in the presence of DB-14-C-4. Cell volume was monitored every 15 min for over the 1.25 h period using a hemofuge. Cell volume increased by 23% by the end of 1.25 h period. Hydrated Na$^+$ and Li$^+$ ions transported by the ionophore carried water that caused the cells to swell. In contrast, Table 9 shows no appreciable increase in cell volume and concentrations of ions in the absence of the ionophore.

IV. 2C Lithium and Sodium Transport in Synthetic PC Vesicles

In an attempt to compare the Li$^+$/Na$^+$ selectivity of DB14C4 with that of other Li$^+$ ionophores (44), I conducted ion transport experiments with PC vesicles loaded with 150 mM LiCl, or 150 mM NaCl, or a mixture of 75 mM LiCl and 75 mM NaCl suspended in a K$^+$-containing medium. Large unilamellar PC vesicles were prepared according to section III .3F (125).

Figure 12 shows Li$^+$ and Na$^+$ transport across PC vesicle membrane in the presence of 0.3 mM DB-14-C-4, at time 7.5, 37.5 and 67.5 min.

Figure 11. ^{31}P NMR spectra of human RBCs at the beginning **(A)** and at the end **(B)** of the 1.25 h period. Suspension medium consists of 140 mM NaCl, 5 mM LiCl, 0.3 mM DB-14-C-4, 5 mM Na$_7$Dy(PPP)$_2$, 10 mM glucose and 10 mM HEPES, pH 7.4. Samples were run unlocked and non-spining in 10 mm NMR tubes. RBCs were suspended in the above medium at 26% hematocrit. Sample temperature, pH and osmolarity were maintained at 37 °C, 7.4, and 295 mOsm, respectively. Peak assignments are the same as for Figure 7.
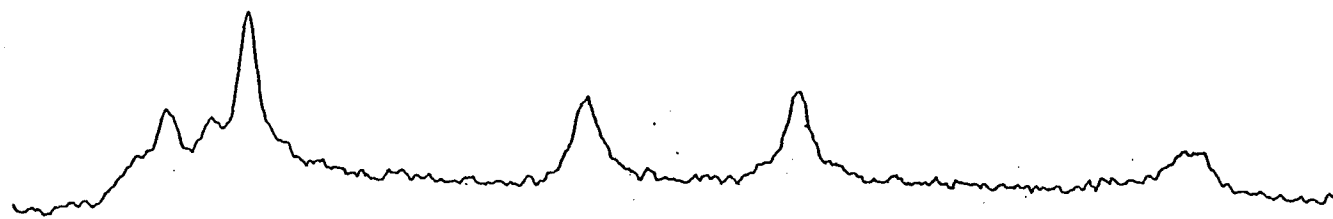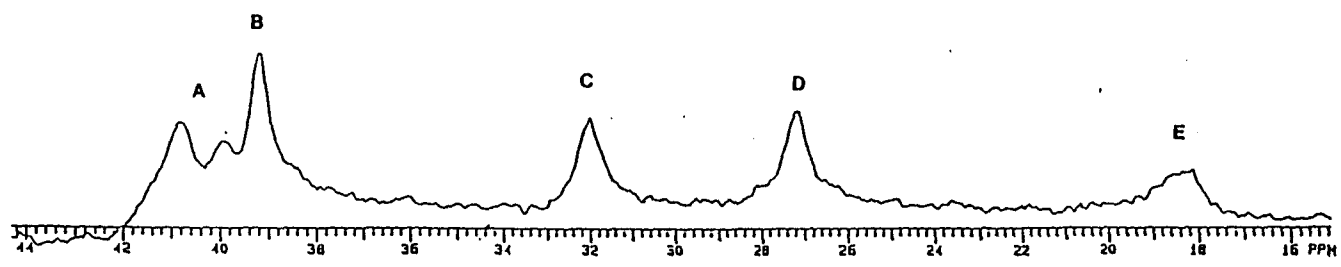
Table 8. Time Dependence of Extracellular Li^+, Na^+, K^+ and Cl^- concentrations (mM) and cell volume in the presence of 0.3 mM dibenzyl-14-C-4.[a]

Time /h	[Li^+]	[Na^+]	[K^+]	[Cl]	Hct %
0.09	5.06 $\pm$ 0.02	137.50 $\pm$ 1.50	0.28 $\pm$ 0.02	147.62 $\pm$ 5.58	26.80 $\pm$ 0.79
0.26	4.92 $\pm$ 0.13	135.00 $\pm$ 3.00	2.36 $\pm$ 0.30	143.12 $\pm$ 5.63	26.10 $\pm$ 0.14
0.50	4.31 $\pm$ 0.01	128.00 $\pm$ 2.00	10.09 $\pm$ 1.11	138.52 $\pm$ 2.47	27.58 $\pm$ 0.22
0.77	3.97 $\pm$ 0.04	124.50 $\pm$ 1.50	14.19 $\pm$ 0.33	147.18 $\pm$ 6.07	28.83 $\pm$ 0.20
1.00	3.95 $\pm$ 0.02	119.50 $\pm$ 1.50	14.73 $\pm$ 0.04	147.60 $\pm$ 3.90	29.45 $\pm$ 0.46
1.27	4.10 $\pm$ 0.02	120.00 $\pm$ 2.00	15.29 $\pm$ 0.08	146.39 $\pm$ 6.07	31.01 $\pm$ 0.35

[a]Normal human RBCs were suspended at 26% Hct in 140 mM NaCl, 5 mM LiCl, 0.3 mM DB-14-C-4, 0.1 mM ouabain, 0.1 mM DIDS, 5 mM Na$_7$Dy(PPP)$_2$, 10 mM glucose and 10 mM HEPES, pH 7.4. The data shown represent an average of three separately prepared samples.

Table 9. Time Dependence of extracellular of Li^+, Na^+, K^+ and Cl^- concentrations (mM) and cell volume in the absence of dibenzyl-14-C-4.[a]

Time /h	$[Li^+]$	$[Na^+]$	$[K^+]$	$[Cl^-]$	Hct %
0.08	5.03 ± 0.02	140.67 ± 2.05	0.15 ± 0.02	147.64 ± 0.67	27.75 ± 0.56
0.25	4.97 ± 0.05	139.00 ± 2.62	0.21 ± 0.03	144.89 ± 2.71	27.75 ± 0.66
0.50	5.02 ± 0.05	133.00 ± 4.55	0.33 ± 0.04	145.27 ± 2.65	28.38 ± 0.41
0.75	5.01 ± 0.07	137.50 ± 3.50	0.46 ± 0.02	143.45 ± 3.11	27.36 ± 0.49
1.00	4.96 ± 0.02	143.00 ± 5.10	0.62 ± 0.04	142.83 ± 1.53	27.88 ± 0.54
1.25	4.89 ± 0.01	143.00 ± 4.97	0.82 ± 0.04	144.86 ± 2.73	27.33 ± 0.56

[a]Conditions are the same as for Table 8 with the exception that no ionophore was present.

Figure 12. ^{7}Li **(A)** and ^{23}Na **(B)** NMR spectra of PC vesicles at time 7.5, 37.5, and 67.5 min. Intravesicullar Li$^+$ or Na$^+$ concentrations are 150 mM, and extracellular medium consists of 150 mM KCl (shift reagent contribution included), 0.3 mM DB-14-C-4, 3.5 mM K$_7$Dy(PPP)$_2$ and 10 mM HEPES, pH 7.4. Transport of ions was monitored every 15 min over a period of 75 min.
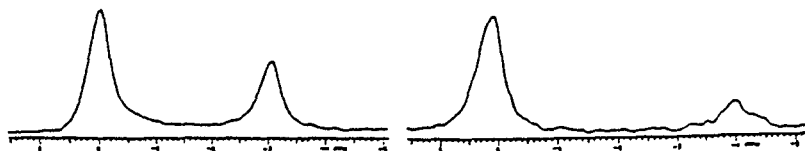
For vesicles loaded with 75 mM LiCl and 75 mM NaCl suspended in an SR-containing K^+ medium, and in the presence of 0.30 mM DB14C4, the pseudo-first-order rate constants for Li^+ and Na^+ transport were 0.99 $\pm$ 0.07 and 0.44 $\pm$ 0.01 h^{-1}, respectively. However, for vesicles loaded with either 150 mM LiCl or 150 mM NaCl, the rate constants for Li^+ and Na^+ transport were 1.34 $\pm$ 0.02 and 0.16 $\pm$ 0.01 h^{-1}, respectively. The pseudo-first-order rate constants were determined from linear regression analysis of plots of ln $[A_i/(A_i + A_o)]$ versus time, where A_i and A_o represent the peak areas of the intra- and extravesicular ^7Li and ^{23}Na NMR resonances, as previously reported (44). The Li^+/Na^+ selectivity ratio calculated for PC vesicles loaded with either LiCl or NaCl alone was 8.48 $\pm$ 0.02, whereas the selectivity ratio calculated for PC vesicles loaded with an equimolar mixture of LiCl and NaCl was 2.26 $\pm$ 0.07. The decrease in Li^+/Na^+ selectivity ratios when equimolar concentrations of Li^+ and Na^+ ions used is due to the competition of these ions for the ionophore.

IV. 3   Competition Between Li^+ and Mg^{2+} for ATP and ADP in Aqueous Solution

IV. 3A ^7Li NMR T_1 measurements of ATP and ADP

^7Li T_1 measurements were used to investigate the mode of interaction of Li^+ with ATP and ADP in the absence and presence of Mg^{2+}. Because the $^7Li^+$ nucleus is known to have a narrow chemical shift range (38), the ^7Li NMR chemical shifts were insensitive to binding. Figure 13 and Table 10 show ^7Li T_1 relaxation times of ATP and ADP in the absence and presence of Mg^{2+}. ^7Li T_1 relaxation times decreased in LiCl solutions in the presence of increasing amounts of ATP or ADP, indicating that T_1 values are sensitive to Li^+

FIGURE 13. ^{7}Li T_1 values for Li-ATP (open symbols) and Li-ADP (closed symbols) complexes in the presence of increasing amounts of Mg^{2+}. Nucleotide concentrations: circles, 3 mM; squares, 5 mM; and triangles, 7 mM. The Li^+ concentration was 5 mM in all samples. Each value is an average of two readings made on separately prepared samples.
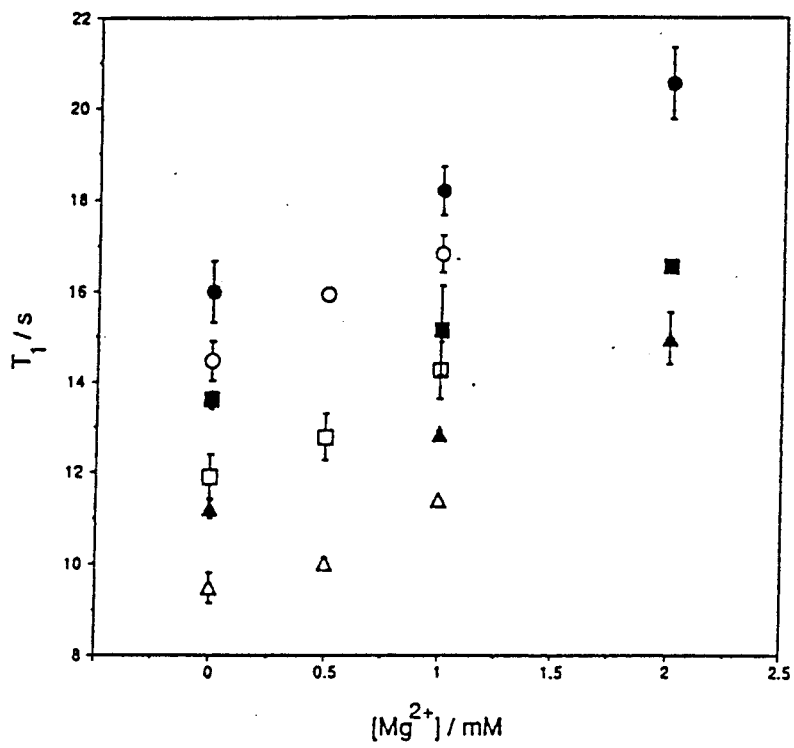
Table 10. ^{7}Li NMR T_1 Values for Li-ATP and Li-ADP Complexes in the Presence of Increasing Amounts of Mg^{2+}.

	$[Mg^{2+}]$ /mM		
[ATP] / mM	0	0.5	1.0
3	14.47 ± 0.44	15.93 ± 0.06	16.80 ± 0.40
5	11.91 ± 0.51	12.80 ± 0.51	14.26 ± 0.63
7	9.50 ± 0.33	10.05 ± 0.10	11.40 ± 0.02

	$[Mg^{2+}]$ /mM		
[ADP] / mM	0	1.0	2.0
3	16.00 ± 0.66	18.17 ± 0.53	20.53 ± 0.80
5	13.63 ± 0.20	15.14 ± 0.97	16.53 ± 0.06
7	11.22 ± 0.21	12.86 ± 0.10	14.95 ± 0.57

binding to nucleotides. Upon addition of Mg^{2+}, the ^7Li T_1 values increased because of displacement of Li^+ by Mg^{2+} from ATP or ADP binding sites.

IV. 3B ^1H and ^{13}C NMR chemical shift measurements

Diamagnetic metal ions generally produce small shifts in the ^1H and ^{13}C NMR spectra of the base and sugar moieties of nucleotides, except at NH or OH groups that are directly involved in metal ion binding. NH or OH protons are not visible in ^1H NMR spectra in aqueous solution because rapid exchange with the solvent protons occurs. Figure 14 shows the ^1H NMR spectrum of ATP. Table 11 shows ^1H NMR chemical shifts in the presence of saturating concentrations of LiCl or $MgCl_2$. The H_8 and H_2 proton resonances of the base and the H_1' resonance of the ribose moieties of ATP and ADP showed no significant changes in chemical shifts upon addition of either excess $MgCl_2$ or excess LiCl. No simultaneous binding of Li^+ and Mg^{2+} to the phosphate groups and to the base or sugar groups of ATP and ADP occurred. Figure 15 shows a typical ^{13}C NMR spectrum of ATP. Table 12 shows the changes in ^{13}C NMR chemical shifts of ATP and ADP upon metal ion binding. The chemical shift changes that occurred upon addition of excess $MgCl_2$ or LiCl were too small to account for direct binding of the cations to the sugar or base moieties of the nucleotides. Indeed, they are probably due to a change in nucleotide conformation or in metal ion proximity to the sugar or base residues.

IV. 3C ^{31}P NMR chemical shift and optical spectroscopy studies of ATP and ADP

Figure 16 shows ^{31}P NMR spectra of ATP. The separation between the α and β resonances of ATP ($\delta_{\alpha\beta}$) decreased as saturating amounts of Li^+ and/or Mg^{2+} were added. The chemical shift separation between the α- and β- phosphate resonances of ATP reflects the

Figure 14. ^{1}H NMR spectrum of ATP in the absence of metal ions. The sample was prepared in 95% D_2O, adjusted to pH 7.4 and was run at 37 °C. t-butanol was used as a reference. A presaturation technique was used for suppression of the water resonance. H_8 and H_2 are proton resonances from the base; H_1' is due to a sugar proton. The resonances at 4.79, 3.84 and 3.31 ppm are from H_2O, Tris, and tetramethylammonium hydroxide peaks respectively. Refer to Figure 3 for structure assignments.
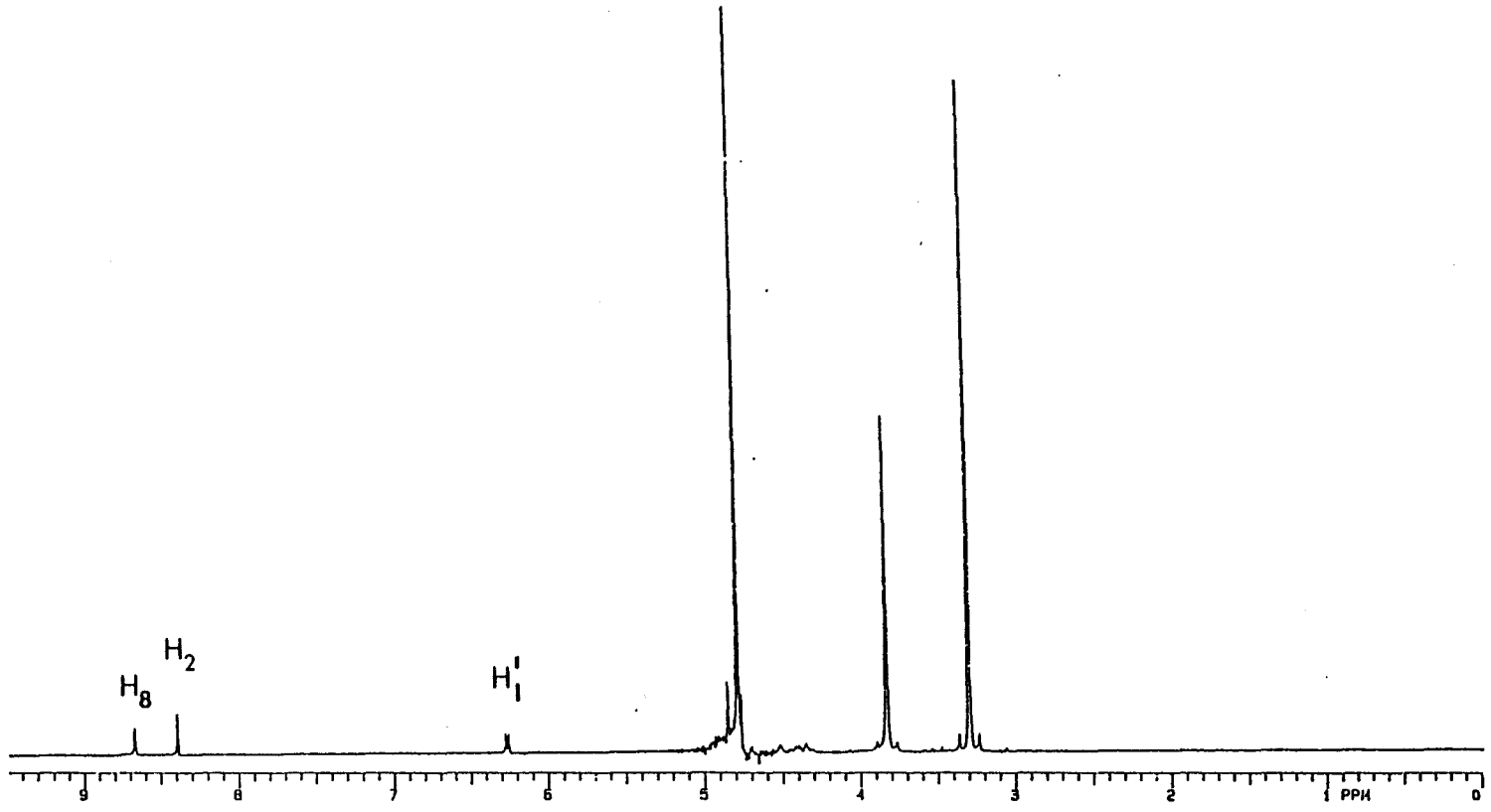
TABLE 11. ^{1}H NMR chemical shifts of ATP and ADP alone and with saturating levels of Li^+ and Mg^{2+}.[a]

Sample	H_2	H_8	H_1'
10 mM ATP	8.40	8.67	6.28
10 mM ATP + 50 mM MgCl$_2$	8.35	8.58	6.24
10 mM ATP + 150 mM LiCl	8.39	8.65	6.24
10 mM ADP	8.40	8.66	6.28
10 mM ADP + 50 mM MgCl$_2$	8.34	8.60	6.23
10 mM ADP + 150 mM LiCl	8.36	8.63	6.27

[a]All experiments were conducted at pH 7.4 and at 37 °C. All samples were prepared in 95% D_2O, and t-butanol was used as a reference. A presaturation technique was used for suppression of the water resonance. H_8 and H_2 are proton resonances from the base; H_1' is due to a sugar proton.

Figure 15. ^{13}C NMR spectrum of ATP. All experiments were done at pH 7.4 and 37 °C. Tetramethyl silane (TMS) was used as a reference. C_2, C_4, C_5, C_6, and C_8 are the base carbons; C_1' to C_5' are sugar carbons. Refer to Figure 3 for structure assignments.
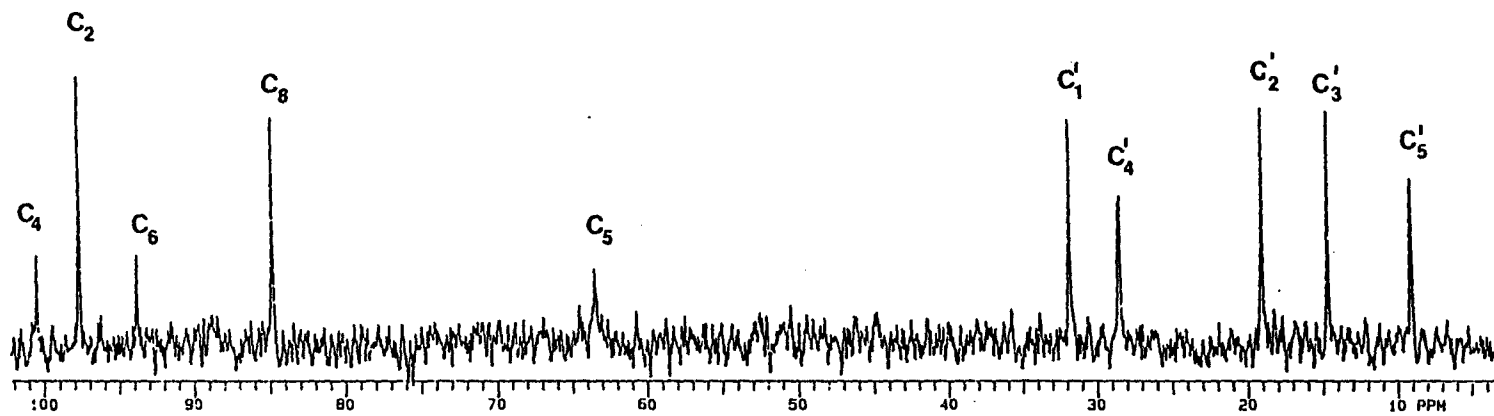
TABLE 12. ^{13}C NMR chemical shift changes of ATP and ADP alone and in the presence of saturating levels of Li$^+$ and Mg^{2+}.[a]

Sample	C_2	C_4	C_5	C_6	C_8	C_1'	C_2'	C_3'	C_4'	C_5'
1	-0.01	-0.16	0.03	-0.10	-0.26	0.47	0.03	0.02	-0.32	0.30
2	0.13	0.04	0.11	0.07	0.41	0.23	0.06	0.04	-0.08	0.12
3	-0.02	-0.13	-0.12	-0.17	-0.04	0.20	-0.16	-0.04	-0.40	0.24
4	0.05	0.01	-0.01	-0.04	0.02	0.12	-0.04	-0.07	-0.14	0.01

[a]All experiments were done at pH 7.4 and 37 °C. All shifts are reported relative to free ATP or ADP. Samples 1 and 2 consisted of 10 mM ATP with 50 mM MgCl$_2$ and 10 mM ATP with 150 mM LiCl, respectively. Samples 3 and 4 consisted of 10 mM ADP with 50 mM MgCl$_2$ and 10 mM ADP with 150 mM LiCl, respectively. C_2, C_4, C_5, C_6, and C_8 are the base carbons; C_1' to C_5' are sugar carbons. Refer to Figure 3 for structure assignments.

Figure 16. ^{31}P NMR (121.4 MHz) spectra of ATP for the following: (A) 5.0 mM TRIS-ATP, (B) 5.0 mM TRIS-ATP with 150 mM LiCl, (C) 5.0 mM TRIS-ATP with 0.5 mM MgCl$_2$ and 150 mM LiCl, and (D) 5.0 mM TRIS-ATP with 50 mM MgCl$_2$. No line broadening was used, and trimethyl phosphate was the external reference. Ionic strength, pH, and temperature were maintained at 0.15 M, 7.4, and 37 °C, respectively.
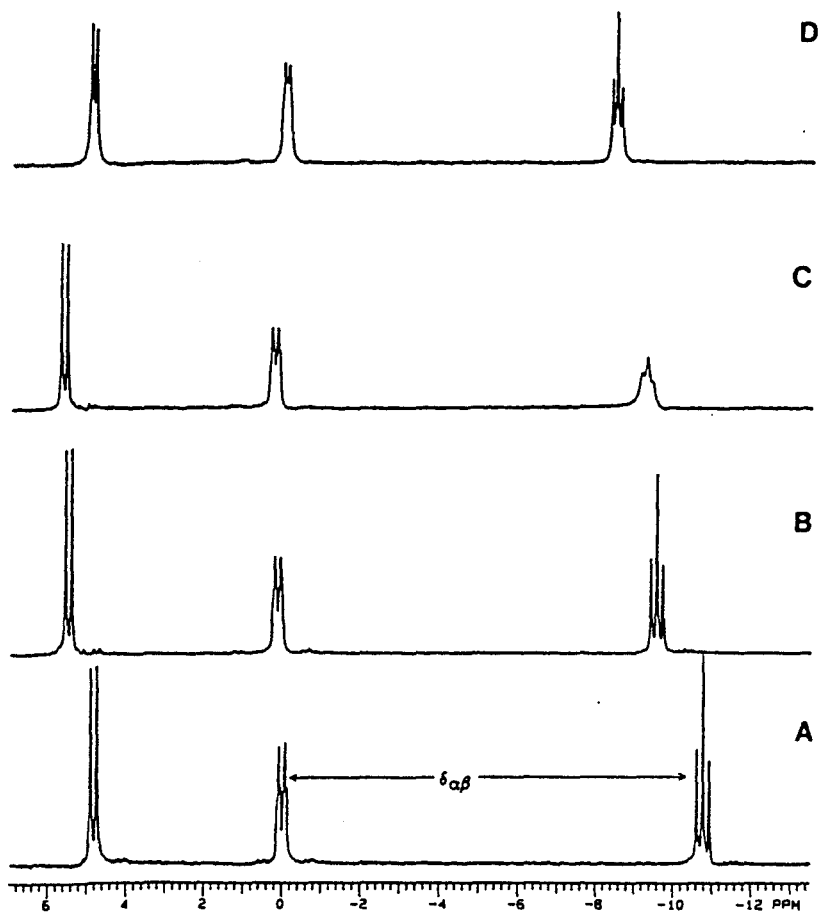
state of metal complexation of ATP (55, 61). The value of $\delta_{\alpha\beta}$ changed from 10.82 ppm in free ATP (Figure 16A) to 9.80 ppm in Li^+-saturated ATP (Figure 16B) and 8.43 ppm in Mg^{2+}-saturated ATP (Figure 16D). For the mixture of Li^+ and Mg^{2+} salts with ATP (Figure 16.C), an intermediate value of $\delta_{\alpha\beta}$, 9.43 ppm, was observed, suggesting that competition of the ions for ATP-phosphate binding sites was occurring.

In ion competition experiments, ^{31}P NMR chemical shifts for the phosphate resonances of ATP and ADP in the absence or presence of LiCl or $MgCl_2$ alone and for $LiCl/MgCl_2$ mixtures were measured (Table 13-18). Nucleotide concentrations were kept constant at 5 mM while the concentrations of Li^+ and Mg^{2+} ranged from 0 to 100 mM and from 0 to 15 mM, respectively. Because of the lower affinity of Li^+ relative to Mg^{2+} for both ATP and ADP, an excess amount of Li^+ ions was used in order to obtain an appreciable change in chemical shift. ^{31}P chemical shifts measured for Li^+-ATP or Li^+-ADP solutions were fitted to three different models, that assumed either the formation of 1:1 or 2:1 species alone or a mixture of 1:1 and 2:1 species, by means of non-linear least-squares approximations.

Tables 19 shows association constants for Li-ATP, Li-ADP, Mg-ATP, and Mg-ADP in the presence of either LiCl or $MgCl_2$. Table 20 shows association constants for Li-ATP and Li-ADP and ^{31}P NMR experimental and theoretical limiting chemical shifts for the phosphate resonances of ATP and ADP in the presence of both LiCl and $MgCl_2$. All calculations were done using equations 1-7 in the methods section.

Due to its higher charge density, Mg^{2+} has a higher affinity for ATP and ADP than Li^+. Since ATP is more electronegative than ADP at physiological pH, its affinity constants for Mg^{2+} and Li^+ are higher than ADP.

Table 13. ^{31}P NMR Chemical Shifts of Li-ATP in the Absence of Mg^{2+}.[a]

[Li$^+$] /mM	γ	α	β
0	-9.701 ± 0.048	-14.198 ± 0.081	-25.115 ± 0.133
15	-9.307 ± 0.003	-14.143 ± 0.012	-24.610 ± 0.081
30	-9.113 ± 0.031	-14.087 ± 0.013	-24.296 ± 0.080
45	-8.963 ± 0.074	-14.051 ± 0.036	-24.056 ± 0.078
60	-8.810 ± 0.068	-13.958 ± 0.002	-23.857 ± 0.078
75	-8.617 ± 0.016	-13.909 ± 0.006	-23.678 ± 0.077
100	-8.448 ± 0.077	-13.888 ± 0.043	-23.411 ± 0.077

[a]ATP concentration was 5 mM. n = 3. Ionic strength, temperature, and pH were kept constant at 0.15 M, 37 °C, and 7.4, respectively.

Table 14. ^{31}P NMR Chemical Shifts of Li-ATP in the Presence of 0.5 mM MgCl$_2$,[a].

[Li$^+$] /mM	γ	α	β
0	-9.227 ± 0.002	-14.123 ± 0.003	-24.784 ± 0.004
15	-9.139 ± 0.082	-14.000 ± 0.056	-24.351 ± 0.023
30	-8.953 ± 0.064	-13.927 ± 0.057	-24.128 ± 0.041
45	-8.817 ± 0.023	-13.873 ± 0.046	-23.876 ± 0.038
60	-8.634 ± 0.033	-13.814 ± 0.005	-23.691 ± 0.023
75	-8.534 ± 0.044	-13.775 ± 0.047	-23.581 ± 0.007
100	-8.349 ± 0.063	-13.713 ± 0.034	-23.234 ± 0.011

[a]Conditions are the same as for Table 13.

Table 15. ^{31}P NMR Chemical Shifts and Optical Spectroscopy Data of Mg-ATP[a].

$[Mg^{2+}]_T$ /mM	ϕ	$[Mg^{2+}]_F$ /μM	$\delta_{\alpha\beta}$
0	1	0	10.92 ± 0.04
1.5	0.65 ± 0.10	59 ± 9	10.00 ± 0.02
2.5	0.49 ± 0.08	69 ± 10	9.57 ± 0.12
3.5	0.23 ± 0.09	173 ± 43	8.89 ± 0.04
5.0	0.091 ± 0.03	271 ± 80	8.32 ± 0.01

[a]ATP concentration was 5 mM. $[Mg^{2+}]_T$ and $[Mg^{2+}]_F$ are the total and free Mg^{2+} concentrations in the solution. ϕ and $\delta_{\alpha\beta}$ are defined in section III .4D.

Table 16. ^{31}P NMR Chemical Shifts of Li-ADP in the Absence of Mg^{2+}.[a]

[Li$^+$] /mM	α	β
0	-9.490 ± 0.010	-13.751 ± 0.011
15	-9.437 ± 0.021	-13.651 ± 0.021
30	-9.404 ± 0.030	-13.592 ± 0.012
45	-9.321 ± 0.013	-13.470 ± 0.000
60	-9.169 ± 0.011	-13.374 ± 0.023
75	-9.084 ± 0.00	-13.211 ± 0.000
100	-8.898 ± 0.001	-13.055 ± 0.000

[a]ADP concentration was 5 mM. Ionic strength, temperature and pH were kept constant at 0.15 M, 37 °C, and 7.4, respectively.

Table 17. ^{31}P NMR Chemical Shifts of Li-ADP in the Presence of 0.5 mM MgCl$_2$[a].

[Li$^+$] /mM	α	β
0	-9.436 ± 0.001	-13.680 ± 0.010
15	-9.426 ± 0.010	-13.651 ± 0.011
30	-9.411 ± 0.000	-13.563 ± 0.020
45	-9.330 ± 0.011	-13.461 ± 0.000
60	-9.269 ± 0.000	-13.402 ± 0.023
75	-9.222 ± 0.003	-13.222 ± 0.000
100	-9.131 ± 0.012	-13.121 ± 0.001

[a]Conditions are the same as for Table 16.

Table 18. ^{31}P NMR Chemical Shifts and Optical Spectroscopy Data of Mg-ADP[a].

$[Mg^{2+}]_T$ /mM	ϕ	$[Mg^{2+}]_F$ /μM	$\delta_{\alpha\beta}$
0	1	0	4.261 ± 0.011
3	0.436 ± 0.062	220 ± 35	4.142 ± 0.022
3.5	0.355 ± 0.060	273 ± 44	4.132 ± 0.010
4.0	0.275 ± 0.043	292 ± 67	4.111 ± 0.011
5.0	0.134 ± 0.031	343 ± 77	4.090 ± 0.048

[a]ADP concentration was 5 mM. $[Mg^{2+}]_T$ and $[Mg^{2+}]_F$ are the total and free Mg^{2+} concentrations in the solution. ϕ and $\delta_{\alpha\beta}$ are defined in section III .4D.

TABLE 19. Association constants for Li-ATP, Li-ADP, Mg-ATP, and Mg-ADP in the presence of either LiCl or MgCl$_2$ alone.

	ATP			ADP	
	α	β	γ	α	β
A) LiCl alone[a]					
1:1 species only (M^{-1})	7	4	4	5	9
Σ^2	0.0017	0.0102	0.0037	0.0395	0.0351
2:1 species only (M^{-2})	597	416	450	85	182
Σ^2	0.0009	0.0190	0.0070	0.0017	0.0044
1:1 and 2:1 species					
1:1 (M^{-1})	14	4	11	61	78
2:1 (M^{-2})	845	477	738	489	489
Σ^2	0.0011	0.0165	0.0092	0.0062	0.0049
B) MgCl$_2$ alone[b] (M^{-1})	20,010 $\pm$ 400			9605 $\pm$ 707	

[a]Association constants Li-ATP and Li-ADP as determined by ^{31}P NMR. Σ^2 values are the corresponding sums of square deviations. The nucleotide concentration was kept constant at 5 mM; the LiCl concentration ranged from 0 to 100 mM. [b]Association constants for Mg-ATP and Mg-ADP as determined by optical and ^{31}P NMR spectroscopies. The nucleotide concentration was kept constant at 5 mM; the MgCl$_2$ concentration ranged from 0 to 15 mM.

TABLE 20. Association constants for Li-ATP and Li-ADP and ^{31}P NMR experimental and theoretical limiting chemical shifts (in ppm) for the phosphate resonance of ATP and ADP in the presence of both LiCl and MgCl$_2$.[a,b]

	ATP			ADP	
	α	β	γ	α	β
A) 1:1 species only					
K (M^{-1})	73	52	71	6	5
Σ^2	0.0232	0.3152	0.0651	0.0079	0.0196
B) 2:1 species only					
K (M^{-2})	2475	1541	2901	269	187
Σ^2	0.1121	0.1390	0.0372	0.0035	0.0042
C) 1:1 and 2:1 species					
1:1 K (M^{-1})	2	0.25x10^{-9}	41	366	e
δ_{theor}[c]	-13.94	-25.98	-9.11	-9.50	e
2:1 K (M^{-2})	701	462	2256	1966	e
δ_{theor}[c]	-13.71	-23.18	-8.18	-8.04	e
δ_{obs}[d]	-13.85	-23.61	-8.34	-8.90	-13.05
Σ^2	0.0011	0.0223	0.0192	0.0017	e

[a]Σ^2 values are the sums of the square deviations for each calculation. [b]For the competition experiments, [nucleotide] = 5.0 mM, [Mg^{2+}] = 0.5 mM, and [Li$^+$] ranged from 0 to 100 mM. [c]δ_{theor} were calculated using equations 1 and 3. [d]δ_{obs} were measured from ^{31}P NMR spectra for [Li$^+$] = 100 mM. [e]No convergence was found.

At the pH and ionic strength used, 2:1 and 1:1 species of the Li^+-ATP and Li^+-ADP complexes were present, with the 2:1 species predominating. In contrast, 1:1 species predominated for the Mg^{2+}-ADP and Mg^{2+}-ATP complexes.

IV. 4 Interaction of Li^+ and Mg^{2+} With Human RBC Membrane

IV. 4A ^{31}P NMR Chemical Shift Anisotropy Measurements of Human RBC Membranes

I have shown in detail that Li^+ competes for ATP and ADP binding sites in aqueous solution (135a). It has also been shown in our lab that Li^+ displaces Mg^{2+} from ATP in human RBCs (55) and the displaced Mg^{2+} was speculated to bind to the membrane. ^{31}P NMR has been a useful and powerful method to study membrane structure. The P-31 nucleus is 100% naturally abundant. Using chemical shift anisotropy (CSA) as a probe, I conducted ^{31}P NMR measurements to investigate the degree of Li^+ and Mg^{2+} interaction with human RBC membranes. Due to the motional rigidity of this phosphate groups, the recorded broad spectrum comprises of all the motions of these atoms in the x, y, and z directions; hence, the name anisotropy. The observation of CSA provides informations about the structural, motional and environmental properties of the molecule to which the P atom is bonded. The phosphorus atom is found in the phosphate head group of the phospholipids located at the surface of the membrane.

Human RBC membranes were prepared according to section III. 3E. All suspension media consisted of 10 mM HEPES, pH 7.4 for the membrane alone and different Li^+ and Mg^{2+} concentrations for the metal ion experiments. Li^+ and Mg^{2+} concentrations ranged from

25-200 and 3-20 mM, respectively. Since Mg^{2+} is divalent and Li^+ is a monovalent metal ion, less Mg^{2+} concentration is sufficient to saturate the membrane binding sites. ^{31}P NMR spectra were recorded at an operating frequency of 121.6 MHz on a Varian VXR-300 MHz spectroscopy. Samples were run in 10 mm NMR tubes spinning at 16 Hz and at 37 °C. A ratio of 2:1 suspension to RBC membranes was used. Figure 17 shows ^{31}P NMR spectra of human RBC membrane with a CSA value of 51.3 ppm. Since our NMR spectrometer is not equipped to do Hans spin echo measurements (81), all experiments were done using one dimensional ^{31}P NMR pulse sequence as opposed to Hahn spin echo which is the conventional technique for CSA measurements. Nevertheless, the value I got for human RBC membranes alone, 51.3 ppm, is consistent with the literature value of 45 ppm obtained using the Hahn spin echo method (81).

Table 21 shows changes in CSA values upon addition of different amounts of Li^+ and Mg^{2+} ions. Upon addition of metal ions the CSA values increased from 51.3 ppm for membrane alone to 69.2 and 83.7 ppm in the presence of excess amounts of Mg^{2+} and Li^+, respectively. Despite the large experimental errors involved in CSA measurements, it is clearly shown that metal ion binding to membranes causes further motional rigidity of the phosphate head groups which is reflected in broadening of the peak. Protein concentrations in mg/ml are also reported in Table 21 for changes in CSA are also dependent on the metal ion to membrane ratio. Protein analysis were done using Bradford's Assay according to section III .4G (130).

IV .4B [7]Li T_1 measurements of Human RBC Membranes

Table 22 shows [7]Li T_1 values of the Li^+-membrane complex upon addition of increasing Mg^{2+} concentrations. All samples consisted of 10 mM HEPES, pH 7.4 membrane

Figure 17. ^{31}P NMR Spectrum of Human RBC Membrane.
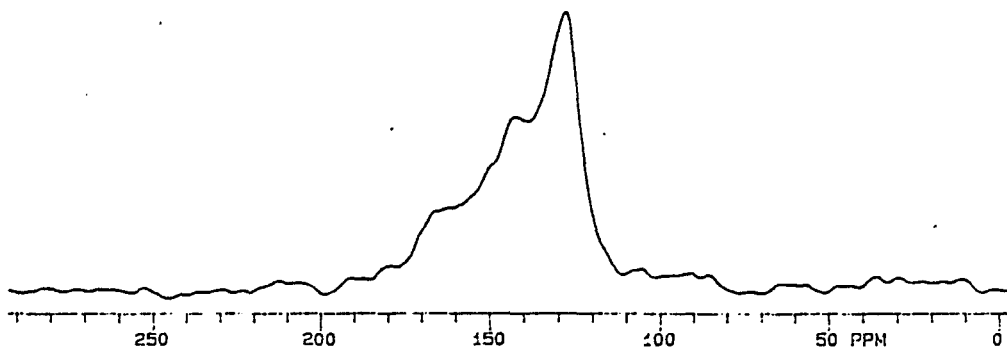
Table 21. ^{31}P NMR CSA Measurements of Human RBC Membranes[a].

[Li$^+$] /mM	[Mg^{2+}] /mM	CSA /ppm	[Prot.] /mg/ml
-	-	51.3 ± 3.0	6.0 ± 1.5
-	3	54.6 ± 4.3	6.7 ± 0.8
-	6	57.8 ± 2.1	7.7 ± 1.8
-	10	59.4 ± 1.6	8.0 ± 1.5
-	15	65.8 ± 3.0	7.2 ± 1.9
-	20	69.2 ± 3.3	6.9 ± 1.0
25	-	53.6 ± 3.7	8.4 ± 2.6
50	-	57.1 ± 4.5	8.4 ± 2.6
75	-	63.7 ± 8.3	6.5 ± 0.7
100	-	69.0 ± 4.4	6.5 ± 0.7
150	-	76.1 ± 7.9	9.1 ± 3.6
200	-	83.7 ± 5.2	9.1 ± 3.6

[a]All samples consisted of membrane suspensions and 10 mM HEPES, pH 7.4. Samples were run in 10 mm NMR tube at 37 °C, spinning at 16 Hz.

TABLE 22. ^{7}Li NMR T_1 Values for Li$^+$-Human RBC Membranes in the presence of Increasing Amounts of Mg^{2+a}.

[Li$^+$] /mM	[Mg^{2+}] /mM	T_1 /sec
5.0	0.0	13.9 ± 0.8
"	0.25	16.0 ± 0.3
"	0.50	16.9 ± 0.2
"	1.0	18.9 ± 0.8
"	2.0	19.5 ± 0.3

[a]Conditions are the same as for Table 21.

suspension and were run spinning at 16 Hz at 37 °C. A ratio of 2 mL of suspension to 1 mL human RBC membranes was used. LiCl (5 mM) in water has a T_1 value of 20 sec. Upon addition of membrane the T_1 relaxation time dropped to 13.9 sec. This is due to the binding of Li^+ to the membrane and the high viscosity of the membrane solution. Li^+ ions in water tumble faster than in membrane containing solution which is viscous, thus the higher T_1 value in water. But upon titration of this solution with increasing amounts of Mg^{2+}, T_1 values started to increase from 13.9 sec in the absence of Mg^{2+} to 19.5 sec in the presence of 2.0 mM Mg^{2+}. This is an indication of a competition between Li^+ and Mg^{2+} for the RBC membrane binding sites. As the Mg^{2+} concentration increases more and more Li^+ is being displaced; hence, approaching the free Li^+ T_1 relaxation time value.

IV .5 Na^+-Li^+ Countertransport Rates, Phospholipid Composition, ^7Li T_1 and T_2 Relaxation Times, and Free and Total [Mg^{2+}] Analyses in Bipolar Patients and Normal Matched Controls

IV. 5A Demography of Patients and Controls

Whole blood cells from 10 bipolar patients receiving lithium carbonate and 10 matched normal controls were obtained from Dept. of Psychiatry, Loyola University Medical Center or Hines Veterans Administration Hospital. Patients received anywhere from 200 - 1600 mg of lithium carbonate per day. The patients had been taking lithium carbonate for a minimum of 3 weeks or for as long as 17 yrs. Patients were diagnosed according to the Diagnostic and Statistical Manual of Mental Disorders, 3rd Edition (121). Na^+-Li^+ countertransport rates were known to increase with hypertension (122); therefore blood pressure was taken at the

time of blood drawing and subjects suffering from hypertension were excluded from this study. Table 23 and 24 show the demography of patients and controls, respectively. Controls were matched according to sex, race, age, and weight. In addition to lithium carbonate, patients were taking a wide variety of psychotropic drugs, such as halcion, klonopine, dripramine, dilantinnavane, synthroid, thorazine, stelazine, and carbamazepine.

IV. 5B Na$^+$-Li$^+$ Countertransport Rate Measurements

For determination of Na$^+$-Li$^+$ countertransport rates, washed packed RBCs were loaded with Li$^+$ by incubating the cells in a medium containing 150 mM LiCl, 10 mM glucose, 10 mM HEPES, pH 7.4 at 37 °C at 13% hematocrit according to Canessa et. al. (122). Under this loading condition, intracellular lithium concentrations were 7.5 $\pm$ 1.0 mM. To remove extracellular Li$^+$, Li$^+$ loaded RBCs were then washed five times with isotonic choline wash solution. The cells were suspended at 7% hematocrit in either Na$^+$ medium (150 mM NaCl, 10 mM glucose, 0.1 mM ouabain, 10 mM HEPES, pH 7.4) or choline medium (112.5 mM choline chloride, 85 mM sucrose, 10 mM glucose, 0.1 mM ouabain, and 10 mM HEPES, pH 7.4) and incubated at 37 °C for over 75 min period. Ouabain was added to inhibit any Li$^+$ transport through (Na$^+$-K$^+$)-ATPase (133). Aliquots were taken every 15 min from each of the Li$^+$ loaded RBC suspensions and collected into precooled polyethylene tubes. The aliquots were centrifuged at 6000 g for 2 min at 4° C and the supernatants were collected and analyzed by AA. Li$^+$ standards (10 - 0.2 μM Li$^+$) prepared in both Na$^+$ and choline medium were used to construct calibration curves. Li$^+$ transport that takes place in the choline medium is due to the leak pathway. The rate of Li$^+$ transport in the Na$^+$ medium is made up of the Na$^+$-Li$^+$ countertransport pathway and the leak pathway.

Table 23 Demography of Bipolar Patients[a].

Patients	Sex	Race	Age	Weight	B.P.	$[Li^+]_s$	Smoker	I.P.
P1	M	W	47	205	140/82	0.073	Y	N
P2	F	W	69	242	124/60	0.074	N	Y
P3	F	B	43	230	125/75	0.010	N	N
P4	M	W	41	152	106/78	0.163	Y	Y
P5	M	W	42	236	107/64	0.434	Y	Y
P6	M	W	39	148	109/64	0.400	Y	Y
P7	M	W	58	123	118/77	0.327	Y	Y
P8	M	W	52	193	140/90	0.133	Y	Y
P9	M	W	61	191	124/70	0.690	Y	Y
P10	M	W	57	163	171/98	0.210	Y	Y

[a]M = male, F = female, W = white, B = black, B.P. = blood pressure, I.P. = inpatient, Y = yes, N = no, $[Li^+]_s$ = starting intracellular Li^+ concentration in mM.

Table 24. Demography of Matched Controls[a].

Controls	Sex	Race	Age	Weight	Blood Pressure	Smoker
C1	M	W	46	170	128/80	N
C2	F	W	65	149	134/78	N
C3	F	B	42	127	112/72	N
C4	M	W	39	151	110/70	Y
C5	M	W	43	189	130/80	Y
C6	M	W	37	210	124/90	N
C7	M	W	65	165	110/80	Y
C8	M	W	52	180	120/75	N
C9	M	W	63	185	160/70	N
C10	M	W	55	197	160/100	N

[a]Definitions are the same as for Table 23.

Thus, the rates of Na^+-Li^+ countertransport were obtained by subtracting the measured rates of Li^+ in a choline medium from the Na^+ medium.

Figure 18 shows the time dependence of extracellular Li^+ concentration versus time for normal individual 8 in Table 26. All regressions had correlations of $r > 0.93$. Li^+ transport follows first-order kinetics as it is apparent from the linearity of the plots on Figure 18. Linear plots of RBC Li^+ efflux within the first hr were reported previously (27, 94).

Table 25 and 26 show Na^+-Li^+ countertransport rates, phospholipid composition, free and total Mg^{2+} concentrations, and ^7Li T_1 relaxation times of intact RBCs, for 10 bipolar patients and 10 matched normal controls, respectively. The observed rates measured by AA were found to be significantly lower for bipolar patients vs normal controls (0.13 ± 0.01 vs 0.20 ± 0.05, mean $\pm$ SD, paired Student's t-test, $t = 4.176$, $p < 0.0025$). The mean interindividual coefficients are 8% for the patients and 25% for the controls. Some studies have shown that patients have lower Na^+-Li^+ countertransport rates than normals (94-97) even though, others have not (98-103).

Table 27 shows Pearson's correlation analysis of all the parameters on Tables 25 & 26 for patients and controls. The purpose of this statistical analysis was to see if there was any correlation between Na^+-Li^+ countertransport rate and PL composition, intracellular free and total Mg^{2+} levels, and ^7Li T_1 and T_2 relaxation times in intact RBCs. Therefore, I focus only on the data bolded on Table 27. Using Pearson's correlation statistics, for a degree of freedom of 18 and a probability (α) of 0.05 any number above 0.4 is accepted (134b). Therefore, Na^+-Li^+ countertransport rate shows a positive correlation with PC and PI, a negative correlation with PS and Sph and no correlation with Mg^{2+} levels, and very weak correlation with ^7Li T_1 measurements.

Figure 18. Plot of Extracellular Li$^+$ Concentration vs Time For Normal Control 8 in Table 26.
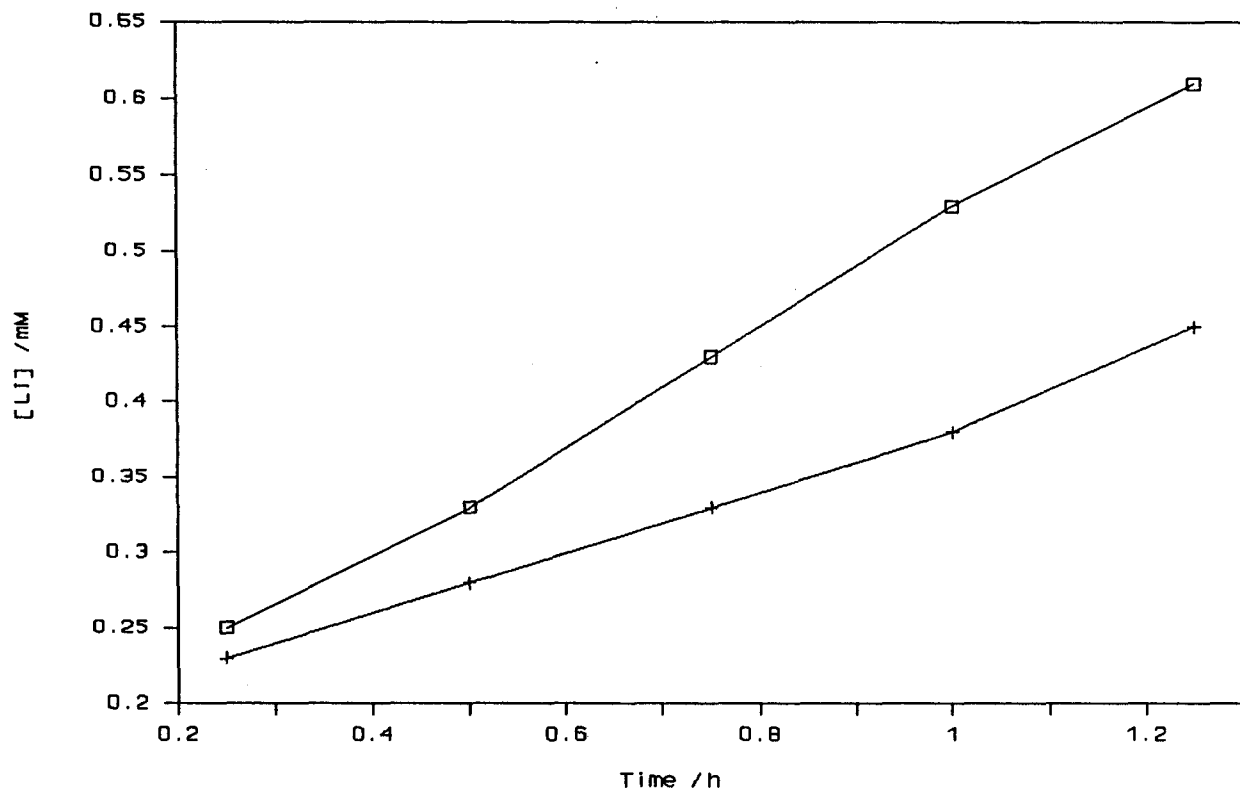
Table 25. Na^+-Li^+ Countertransport Rates, Phospholipid Compositions, Free and Total Intracellular Mg^{2+} Concentrations, and ^7Li T_1 Relaxation Measurements of Patients[a].

Patients	Na^+-Li^+	PC	PS	PI	PE	Sph	$[Mg^{2+}]_f$	$[Mg2+]_t$	^7Li T_1	^7Li T_2
P1	0.11	32.57	13.24	2.13	26.49	25.57	0.275	2.30	4.96	0.252
P2	0.12	30.68	16.28	1.87	26.59	24.59	0.287	2.15	5.54	0.153
P3	0.13	33.58	14.41	1.38	24.94	25.69	0.383	2.19	5.98	0.127
P4	0.15	30.07	17.25	2.00	23.45	27.23	0.287	2.51	5.42	0.106
P5	0.13	27.35	16.83	1.44	25.14	29.24	0.287	2.62	5.34	0.128
P6	0.14	28.19	17.74	1.70	27.70	24.70	0.275	2.31	5.43	0.102
P7	0.11	28.65	18.80	2.81	26.54	23.20	0.275	2.19	5.02	0.095
P8	0.11	29.35	16.97	1.60	28.45	23.64	0.400	2.34	4.70	0.195
P9	0.14	33.29	16.30	1.64	25.07	23.70	0.338	2.13	4.81	0.206
P10	0.14	32.04	16.89	2.05	24.15	24.87	0.275	2.98	4.86	0.104

[a] Na^+-Li^+ countertransport rates are in m moles of Li^+ /(L x RBCs h); phospholipid compositions are in %; Mg^{2+} concentrations are in mM, and ^7Li T_1 and T_2 relaxation times are in sec for intracellular $[Li^+]$ of 2.19 ± 0.37 mM.

Table 26. Na^+-Li^+ Countertransport Rates, Phospholipid Compositions, Free and Total Intracellular Mg^{2+} Concentrations, and ^7Li T_1 Relaxation Measurements of Matched Controls[a].

Controls	Na^+-Li^+	PC	PS	PI	PE	Sph	$[Mg^{2+}]_f$	$[Mg^{2+}]_t$	^7Li T_1	^7Li T_2
C1	0.16	28.73	17.16	2.05	27.43	24.63	0.383	1.92	5.54	0.155
C2	0.15	29.92	16.48	2.46	26.33	24.81	0.275	2.48	6.10	0.111
C3	0.15	26.70	14.00	2.30	26.40	30.50	0.383	2.43	5.19	0.161
C4	0.19	31.13	13.89	2.71	28.10	24.17	0.383	2.27	5.58	0.090
C5	0.32	34.90	14.09	3.69	26.85	20.47	0.275	2.37	5.76	0.111
C6	0.17	31.90	13.43	2.43	25.75	26.49	0.210	2.09	5.55	0.211
C7	0.18	33.03	14.06	2.29	25.49	25.37	0.275	2.51	5.18	0.112
C8	0.23	33.15	15.13	1.67	23.14	26.92	0.275	2.77	5.42	0.257
C9	0.26	32.25	14.91	2.71	27.64	22.49	0.275	2.26	5.03	0.132
C10	0.19	32.66	14.57	2.51	26.88	23.37	0.275	2.50	5.91	0.134

[a]Conditions are the same as for Table 25.

Table 27. Pearson Correlation Matrix For RBC Parameters in Bipolars and Matched Controls.

	Type	PC	PS	PI	PE	Sph	Na^+-Li^+	$[Mg^{2+}]_f$	$[Mg^{2+}]_t$	T_l
PE	-1.00									
PC	0.193	1.000								
PS	**-0.535**	-0.539	1.000							
PI	**0.567**	0.257	-0.299	1.000						
PE	0.191	-0.255	-0.031	0.346	1.000					
Sph	-0.073	-0.513	-0.080	-0.519	-0.459	1.000				
Na^+-Li^+	**0.687**	**0.522**	**-0.426**	**0.645**	0.044	**-0.408**	1.000			
$[Mg^{2+}]_f$	-0.053	-0.269	0.067	-0.283	0.304	0.089	-0.211	1.000		
$[Mg^{2+}]_t$	-0.025	0.073	0.034	-0.092	-0.538	0.279	0.118	-0.269	1.000	
T_l	**0.414**	0.138	-0.225	0.203	-0.008	-0.026	0.282	-0.077	-0.105	1.000

The negative correlation implies that as the PS level increased the rate decreased. By the same token, the positive correlation means that as the PI and PC levels increased the rate increased. Therefore, the underlying conclusion may be that Li^+ binding to the negatively charged PS could be the reason for the variation in rates between bipolars and controls.

IV .5C   Analysis of Phospholipid Composition

Figure 19 shows the five PLs in human RBC membranes studied in this project. PC and Sph are the two main neutral PL constituents of the exterior part of the lipid bilayer. PS and PI are negatively, and PE is neutrally charged PLs and are located mainly in the interior part of the membrane. Phospholipids are essential structural components in the membranous structure of cells. Many theories have been proposed for the anatomic localization of the lipids within the membranes but their precise disposition in mental illness is still unknown. Sengupta et al. (88), using TLC, showed characteristic changes in the lipid composition of blood cellular fraction of different types of mental patients and the clinical response to medications, taking into account any changes in the lipid profile after in vivo administration of drugs. PS and PC contents decreased, and PE content increased in bipolar patients compared to normals (88). There was no change in PI and Sph contents (88). No significant alteration was found in lipid profile of mental defectives when compared to drug free conditions (88).

Figure 20 shows ^{31}P NMR spectrum of phospholipids extracted from human RBC membranes. In human RBC membranes, there is just as much PE plasmologen as there is PE. PE has an alkyl ether on the glyceride backbone; whereas, PE plasmologen has an alkenyl ether instead (135b). ^{31}P NMR is sensitive enough to differentiate between these two types of PLs ; whereas, other conventional techniques, such as TLC, HPLC, and

Figure 19. The Five Main Phospholipid Components of Human RBC Membranes. Structural assignments are as follows: Phosphatidyl serine (A), Phosphatidyl ethanolamine (B), Phosphatidyl choline (C), Phosphatidyl inositol (D), and Sphingomyelin (E).

A

$$R-\overset{\overset{O}{\|}}{C}-O-CH_2$$
$$R'-\overset{\overset{O}{\|}}{C}-O-CH$$
$$H_2C-O-\overset{\overset{O}{\|}}{\underset{O^-}{P}}-O-CH_2-\overset{\overset{H}{|}}{\underset{COO^-}{C}}-NH_3^+$$

B

$$R-\overset{\overset{O}{\|}}{C}-O-CH_2$$
$$R'-\overset{\overset{O}{\|}}{C}-O-CH$$
$$H_2C-O-\overset{\overset{O}{\|}}{\underset{O^-}{P}}-O-CH_2-CH_2-NH_3^+$$

C

$$R-\overset{\overset{O}{\|}}{C}-O-CH_2$$
$$R'-\overset{\overset{O}{\|}}{C}-O-CH$$
$$H_2C-O-\overset{\overset{O}{\|}}{\underset{O^-}{P}}-O-CH_2-CH_2-\overset{+}{N}(CH_3)_3$$

D

$$H_2C-O-\overset{\overset{O}{\|}}{C}-R$$
$$HC-O-\overset{\overset{O}{\|}}{C}-R'$$
$$CH_2$$

(inositol ring with OH, OH, H, H, OH, H, HO, H, H, OH substituents linked to O—P(O)(O⁻)—O—CH₂)

E

$$CH_3(CH_2)_{12}\overset{}{C}=\overset{H}{}$$
$$\overset{H}{}=C-CHOH$$
$$CHNH\overset{\overset{O}{\|}}{C}(CH_2)_{22}CH_3$$
$$CH_2OP\overset{\overset{O}{\|}}{\underset{O_-}{}}OCH_2CH_2\overset{+}{N}(CH_3)_3$$
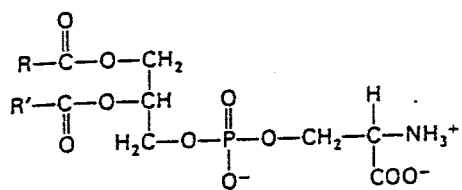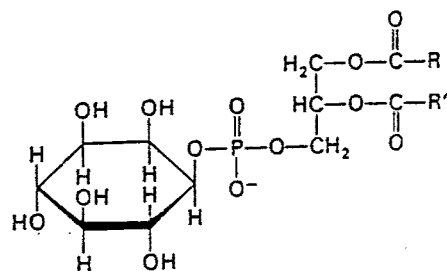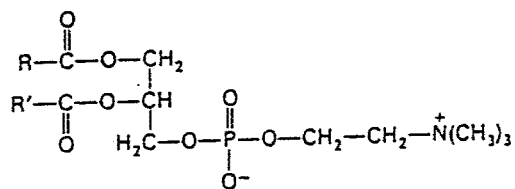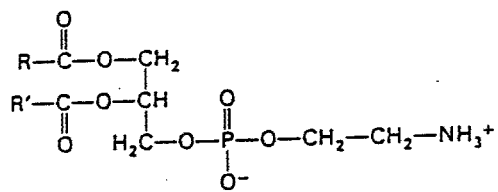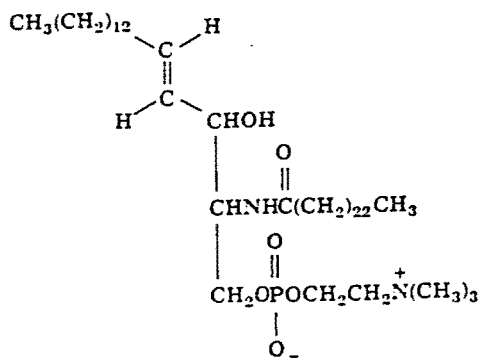
Figure 20. ^{31}P NMR spectrum of Phospholipids Extracted from Human RBC Membranes. Assignments of peaks are as follow: PE (A), PE plasmalogen (B), PS (C), Sph (D), PI (E), and PC (F).
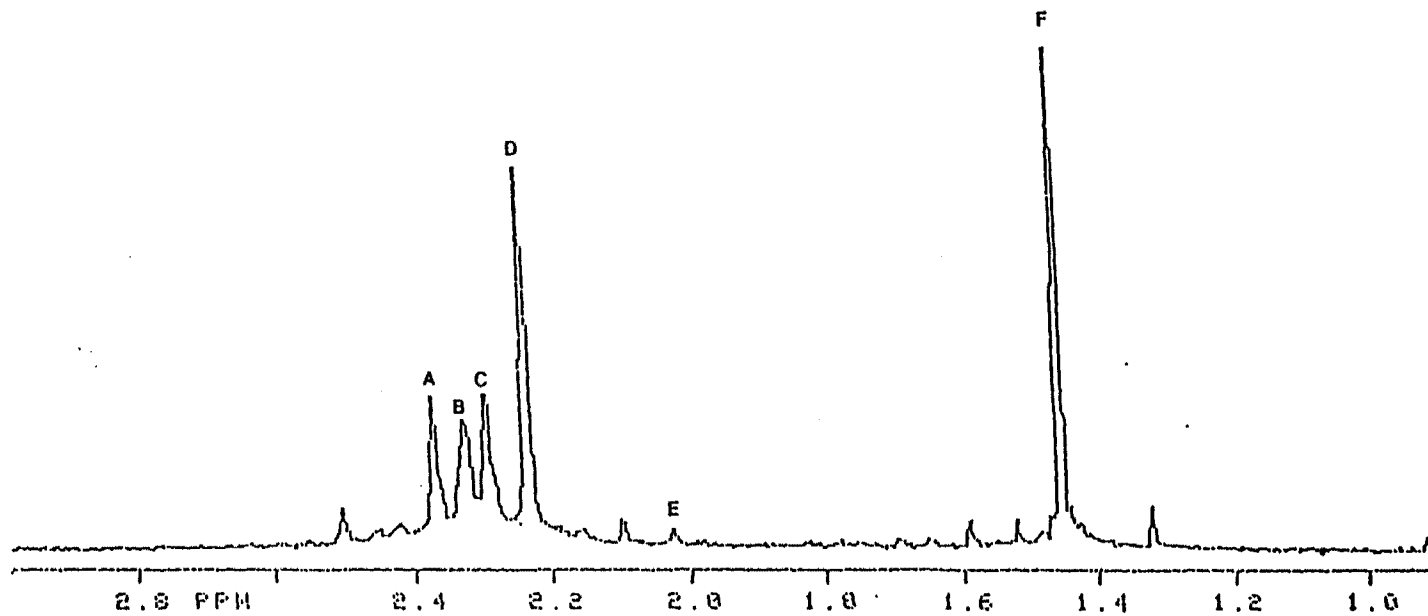
GC give the total composition of the two groups. ^{31}P and ^{1}H NMR techniques have been used to determine PL compositions in earth worm, soybean, amniotic fluid, and bovine brain white matter (128, 136, 137). To the best of my knowledge, our group is the first one to use ^{31}P NMR for phospholipid analysis of human RBC membranes. Phospholipid extractions were done according to section III .4G (127, 128). Assignments of PLs were made by running standard phospholipids or spiking the samples with standards. Chemical shift assignments were made relative to an external reference of 85% phosphoric acid. However, PC was also used as an internal reference for its relative chemical shift was constant. ^{31}P NMR experiments were done at an operating frequency of 121.6 MHz on a Varian VXR-300 NMR spectrometer. Spectrometeric conditions used were as follows: one dimensional pulse sequence, 9 μsec pulse width (45° spin-flip angle), D1 + AT = 4 sec, ambient temperature, spin rate of 16 Hz, high power decoupler of 55 db, and NT of 10,000. Reported relaxation time for PC is 2.3 s (136); therefore, a value of 4 sec (D1 + AT) was enough time for the magnetization to relax back fully.

Table 25 and 26 show PL compositions of patients and their matched controls. Reported PL composition data are similar to other finding in RBCs (88, 126). A Student's t-test was done to compare all the individual PLs in the patient and control groups. PS composition was slightly higher for patients than normals (16.47 $\pm$ 1.51 vs 14.77 $\pm$ 1.14, mean $\pm$ SD, df = 9, t = 2.130, p < .10). The PI composition in patients was slightly lower than normals (1.86 $\pm$ 0.40 vs 2.48 $\pm$ 0.50, mean $\pm$ SD, df = 9, t = 2.608, p < 0.05). In contrast, no significant difference was found in PC, PE and Sph between patients and controls.

IV. 5D Free and Total Intracellular Mg^{2+} Levels

Magnesium ions are important metal ions in biological systems. Intracellular Mg^{2+} exists either free (Mg^{2+}_f) or bound (Mg^{2+}_b) to biological ligands, such as RNA, ATP, and Mg^{2+}- activated enzymes (138). Mg^{2+} regulates the activity of Mg^{2+}-activated enzymes involved in protein synthesis, ion transport, glycolysis, muscle contraction, and respiration.

Tables 25 and 26 show the amount of free and total intracellular Mg^{2+} concentrations for patients and matched controls. Intracellular total and free Mg^{2+} concentrations were measured using AA and ^{31}P NMR spectroscopy. No significant difference was found in free and total Mg^{2+} levels between patients and controls. In addition, statistical analysis shows no correlation between Na^+-Li^+ countertransport rates and Mg^{2+} levels. Patients had free and total Mg^{2+} levels of 0.308 $\pm$ 0.045 mM and 2.37 $\pm$ 0.25 mM, whereas the free and total $[Mg^{2+}]$ for controls were 0.301 $\pm$ 0.057 mM, and 2.36 $\pm$ 0.23 mM (mean $\pm$ SD), respectively. Reported intracellular free Mg^{2+} levels are 0.188 mM, and 0.311 mM using ^{31}P NMR and null-point titration methods, respectively (139, 140). Total plasma Mg^{2+} levels were measured in 59 patients who had various primary affective disorders and 303 normal individuals using AA (141). Although men had significantly higher Mg^{2+} levels than did women, no difference occurred between patients and normal individuals (141).

IV. 5E ^7Li T_1 and T_2 Relaxation Times in intact RBCs

^7Li T_1 and T_2 value of intact RBCs are generally around 5 and 0.2 sec, respectively; whereas LiCl in water has a T_1 and T_2 relaxation times of 20 and 17 sec, respectively. This big difference in relaxation times observed in Li^+-loaded RBCs is due to Li^+ binding and viscosity. Thus, Li^+ binding to cell membranes can be studied using relaxation times

measurements. Intracellular ^{7}Li T_1 values in Li$^+$-loaded RBCs are much higher than the corresponding T_2 values (72, 76). It is well established that slow motions contribute only toward T_2 (87). Thus, the large difference between T_1 and T_2 values is indicative of Li$^+$ binding to RBC components (76).

Tables 25 and 26 show ^{7}Li T_1 and T_2 relaxation times of patients and controls, respectively. Li$^+$ loading of RBCs was done according to section III .3C. The ^{7}Li T_1 and T_2 values reported here are for a single intracellular Li$^+$ concentration (2.19 $\pm$ 0.37). ^{7}Li T_1 measurements were obtained using inversion-recovery and Carl-Purcell-Meiboom-Gill pulse sequences. A very weak correlation was found in Na$^+$-Li$^+$ countertransport rates and relaxation times between patients and controls (Table 27). On the other hand, a Student's t-test showed a slight difference in ^{7}Li T_1 values between patients and controls (5.21 $\pm$ 0.38 vs 5.53 $\pm$ 0.32, mean $\pm$ SD, df = 9, t = 2.065, p < 0.10). There was no difference in T_2 values between patients and controls. A lower relaxation time is an indication of stronger binding. Even though, the difference in relaxation times between patients and controls is not that significant, it may be that binding of Li$^+$ to the RBC membranes and metabolites is slightly stronger for patients than normals.

CHAPTER V

DISCUSSION

Since, ^6Li and ^7Li resonate at different NMR frequencies, they are distinguishable even when the lithium salt is not enriched in ^6Li. However, the use of lithium salts enriched in ^6Li increases the otherwise low NMR sensitivity to this isotope. For a comparison of the transport behavior of these two isotopes, LiCl that was enriched in ^6Li (95.7%) was used so that the percentage of ^6Li was comparable to that of ^7Li (92.6%).

Uptake of $^6Li^+$ by RBC was significantly faster (Student's one-tailed t test, $p < 0.05$) than that of $^7Li^+$ (Figures 5 & 6). The initial rates of transport Li^+ in RBCs for the ^6Li and ^7Li isotopes are 1.56 ± 0.12 and 1.32 ± 0.14 mmol of $Li^+/(l$ of RBCs x h), respectively. The rate constants for the ^6Li and ^7Li isotopes are (6.92 ± 0.57) x $10^{-3}/h$ and (5.93 ± 0.64) x $10^{-3}/h$, respectively. These results are consistent with data for AA on RBCs (6) and cerebrospinal fluid (7). The rate of $^7Li^+$ uptake at nearly pharmacological levels by human RBC was recently measured by ^7Li NMR spectroscopy (10). The rate of Li^+ uptake from a suspension medium containing 2 mM Li^+ concentration (10) was consistent with that measured in this study from a suspension medium containing 100 mM ^7LiCl. ^7Li and ^6Li have a mass ratio of 1.167 (7/6), and we found their rate and rate constant ratio to be 1.182 (1.56/1.32)

and 1.167 (6.92 x 10^{-3}/5.93 x 10^{-3}), respectively. The more rapid uptake of $^6Li^+$ relative to $^7Li^+$ across the human RBC membrane is associated with the lower mass of the ^6Li isotope, the consequent higher charge-to-mass ratio, and the resulting higher hydration energy. The masses of the two isotopes differ by 16.7%. The difference between the two isotopes calculated from either the rates (18.2%) or the rate constants (16.7%) is similar to the difference in mass. The data obtained by AA for *in vitro* uptake of $^6Li^+$ by erythrocytes were 5.4% to 8.5% higher than those observed for $^7Li^+$ (6). The deviation from the theoretical value of 16.7% based on the difference in mass is not understood (6). The difference in the aqueous diffusion rates of the two isotopes is reported to be 0.6% (9), which is much lower than the difference reported in biological systems. Therefore, ion diffusion is only a partial contributor to the difference between $^6Li^+$ and $^7Li^+$ ions in transport across biological membranes. The agreement of our RBC data with cerebrospinal fluid data (7) indicates that RBCs may be a suitable model for the study of Li^+ action in normal individuals and for that in patients with bipolar disorders. Because ^6Li enriched salts are transported faster across cell membranes, their use may shorten the number of days needed before lithium is effective. Li^+ has a toxic effect on the kidney and the heart (2). The toxic effects of $^6Li^+$ have been established only when equivalent doses of $^6Li^+$ and $^7Li^+$ are given (14). Because $^6Li^+$ is transported more rapidly than is $^7Li^+$, giving equivalent doses does not result in equivalent intracellular concentrations. It will be more appropriate to determine whether $^6Li^+$ is more toxic than $^7Li^+$ when the two isotopes are used at the same intracellular levels.

Recently, attention has been given to Li^+ ionophores as tools for understanding Li^+ transport across biological membranes. Ionophores have been incorporated in suspension media as a means for speeding up Li^+ transport. The aim of this study was to show, by

using NMR and AA techniques, that the Li^+ ionophore dibenzyl-14-crown-4 can induce Li^+ transport across human RBC and PC vesicle membranes even in the presence of an excess of Na^+ ions.

The pseudo-first-order rate constants for Li^+ and Na^+ transport across RBC membranes are proportional to DB14C4 concentration and therefore the mechanism of ionophore-induced ion transport is first-order with respect to ionophore concentration. The good linear fit obtained for the calculations of pseudo-first-order rate constants indicates that the mechanism of ionophore-induced ion transport is also first order with respect to alkali metal ion concentration. The pseudo-first-order kinetics observed for Li^+ transport induced by DB14C4 in human RBC suspensions is consistent with the same kinetics observed for Li^+ transport induced by monensin in human RBC suspensions (43) and in synthetic vesicles (44, 47). In contrast to Li^+ transport induced by DB14C4 which took place in a physiologic Na^+-containing medium, monensin-induced Li^+ transport across the human RBC membrane was observed in a non-physiologic K^+ medium, but not in a Na^+ medium (43, 44, 77, 142).

The line widths of the intra- and extracellular $^7Li^+$ NMR resonances increased (Figure 9A) as the ionophore-induced Li^+ transport occurred because of exchange between the two pools of Li^+. Smaller increases in the line widths of the intra- and extracellular ^{23}Na NMR resonances (Figure 9B) were observed because of the larger concentrations of Na^+ relative to Li^+ ions in human RBC suspensions. For both $^7Li^+$ and $^{23}Na^+$ NMR resonances, the line broadening was more significant for the intracellular resonances. This observation is consistent with exchange between intra- and extracellular cations, with the ions present at lower concentration being broadened the most, as previously reported for Na^+ transport induced by monensin (142). The chemical shift separation between the intra- and extracellular

$^7Li^+$ NMR resonances increased as Li^+ was transported from the suspension medium into RBC. As ionophore-induced Li^+ transport occurred, the extracellular Li^+ concentration decreased, leading to an increase in the $[SR]/[Li^+]$ ratio and, consequently, an upfield shift of the extracellular $^7Li^+$ NMR resonance, as previously reported (43).

Because of the similarity between Na^+ and Li^+ ions, the ionophore transports Na^+ as well as Li^+ ions. Figure 10 shows changes in extracellular Na^+, K^+, and Cl^- concentrations in the presence (part A) and in the absence (part B) of 0.30 mM DB14C4. The ion transport illustrated in Figure 10A was induced mainly by the ionophore; a small amount of ion transport was observed upon resuspension of RBC in ionophore-free medium (Figure 10B). Similar experiments conducted without the inhibitors ouabain and DIDS in the suspension medium showed larger Na^+, K^+, and Cl^- movements across the membrane both with and without ionophore. The additional Na^+, K^+, and Cl^- transport observed in the absence of ouabain and DIDS is presumably due to movement of ions through the RBC membrane proteins Na^+,K^+-ATPase and to anion exchange (131). Balancing the ion gradient across the RBC membrane there were movements of K^+ and Cl^- ions. These RBC results are consistent with a mechanism of ionophore-induced ion transport in which uptake of Li^+ by human RBCs is accompanied by influx of Na^+ and Cl^-. The net cation influx is balanced by a K^+ efflux. Because DIDS, an inhibitor of Cl^- transport in human RBC suspensions, was present in our experiments, I presume that Cl^- was transported into RBCs ion-paired to the ionophore-cation complex. Alternatively, the amount of DIDS used in these experiments was not sufficient for complete inhibition of Cl^- transport via the anion exchange protein. For a comparison of the effect of the ionophore on the rates of Li^+ and Na^+ transport, I conducted experiments with and without the transport inhibitors DIDS and ouabain. The SR decreased the rate constants

for transport of Li^+ but not of Na^+. The SR binds more strongly to Li^+ ions, resulting in slower rates of Li^+ transport in SR-containing medium. This SR-specific effect is consistent with the previously reported effects of $Dy(PPP)_2^{7-}$ on membrane potential, Na^+-Li^+ exchange rates, and Li^+ and Na^+ transmembrane ratios in human RBC suspensions (41,42).

^{31}P NMR spectra of normal human erythrocytes in the presence and absence of DB-14-C-4 at the beginning and at the end of 1.25 h period showed that ATP and DPG levels were maintained throughout the experiment (Figure 11). Cell viability was therefore maintained during the course of the ionophore induced ion transport experiments (Figure 11). The chemical shift separation between the Pi and $P\alpha$ resonances of ATP ($\delta_{\alpha\beta}$) were the same at the beginning and at the end (Figure 11). Thus, intracellular pH was also maintained during these experiments and the mechanism of ionophore induced ion transport does not involve exchange between intracellular H^+ and extracellular alkali metal cations as previously reported for other Li^+ ionophores (44). The pH independence of Li^+ or Na^+ transport induced by DB14C4 is consistent with the absence in this ionophore of functional groups that could undergo protonation. The changes that occurred in extracellular Li^+, Na^+, K^+, Cl^- concentrations in the presence of DB14C4 were accompanied by changes in cell volume (Table 8). Hematocrit measurements indicated that cell volume increased by 23% by the end of 1.25 h period (Table 8). In contrast, no appreciable changes in cell volume and intracellular ion concentrations were observed in the absence of DB14C4 (Table 9). These changes in cell volume were taken into account in the calculations of ion concentrations shown in Figure 10. Because of the high hydration energy of Li^+, hydrated Li^+ ions and Na^+ transported into RBCs by the ionophore presumably drag in extracellular water across the RBC membrane causing the cells to swell.

The Li^+/Na^+ selectivity ratio calculated for PC vesicles loaded with LiCl and NaCl alone was 8.48 ± 0.02; whereas the Li^+/Na^+ selectivity ratio calculated for PC vesicles loaded with an equimolar mixture of LiCl and NaCl was 2.26 ± 0.07. In contrast, the Li^+/Na^+ selectivity ratio for DB14C4 obtained by EMF measurements of polymeric membrane electrodes was 229 (48). For an organometallic ionophore the Li^+/Na^+ selectivity ratio calculated for PC vesicles loaded with either 150 mM LiCl or 150 mM NaCl was approximately 4.5 whereas the ratio calculated for PC vesicles loaded with an equimolar mixture of LiCl and NaCl was 22 ± 6 (44). While DB14C4 yielded lower Li^+/Na^+ selectivity in mixtures of LiCl and NaCl than in suspensions of the pure Li^+ or Na^+ salts, the cobalt organometallic ionophore displayed the opposite behavior (44). The difference in trends in Li^+/Na^+ selectivity ratios in PC vesicle suspensions is presumably associated with the different mechanisms of ion transport for the two ionophores. In addition to their dependence on the nature of the ionophore, Li^+/Na^+ selectivity ratios are dependent on the composition of the membrane through which the ion transport takes place, the ionic composition of the suspension medium to which the membrane is exposed, and the method of measurement used for determination of the Li^+/Na^+ selectivity ratio (33). Thus, it is not surprising that the Li^+/Na^+ selectivity ratio for DB14C4 obtained with ion-selective electrode with a polyvinylchloride membrane does not agree with the ones reported here for human RBC or PC vesicle suspensions.

The capacity of an ionophore to transport a specific ion across a membrane is dependent on the rates of association and dissociation of the ionophore-cation complex at the membrane (45, 77, 143). Because of the similar lipophilic nature of the interior of human RBC and of PC membranes, it is likely that the ratios of the stability constants for the

complexes of DB14C4 with Li^+ and Na^+ are approximately the same in the two types of lipid bilayer. The finding that the Li^+/Na^+ selectivity ratio for DB14C4 is enhanced in PC vesicle relative to human RBC suspensions suggests that the rates of cation transport are controlled by the rates of uptake and release of the ionophore-cation complex at the membrane interface. The negatively inside potential of the human RBC membrane (42), associated with the presence of anionic phospholipid in the inner leaflet of the RBC membrane, may slow down the release of Li^+ or Na^+ ions from the positively charged DB14C4-cation complex at the membrane interface. These conclusions are consistent with the increased rate of Li^+ dissociation induced by monensin at the membrane surface of PC vesicles containing 5% of the anionic phospholipid phosphatidylserine relative to vesicles containing neutral PC alone (77). Thus, the weaker interaction in PC vesicles between the DB14C4-cation complex or the neutral complex of the organometallic ligand previously reported (44) with the membrane surface may explain the enhanced Li^+/Na^+ selectivity ratios found with vesicle preparations.

I have shown that DB14C4 is an efficient carrier for Li^+ across human RBC membranes even in the presence of a background of Na^+ ions. This study constitutes the first example in which ionophore-induced Li^+ transport across a biological (as opposed to a synthetic) membrane was observed in a physiologic Na^+ medium. The uptake of Li^+ in lithium carbonate preparations by biological tissues may be enhanced not only by use of the lighter isotope, $^6Li^+$, (144) but also by Li^+-selective ionophores, leading to an improvement in the effectiveness of lithium therapy of manic-depressive patients. Although we used DB14C4, a Li^+ ionophore with one of the highest Li^+/Na^+ selectivity ratios known (229, as determined by EMF measurements of polymeric membrane electrodes) (48). DB14C4 induced considerable changes in intra- and extracellular Na^+ concentrations. Because the maintenance

of intra- and extracellular Na^+ levels is crucial for metabolic balance and the Li^+ levels in sera of bipolar patients receiving lithium carbonate are approximately five times lower than those used in our experiments, Li^+ ionophores with Li^+/Na^+ selectivity ratios considerably higher than those currently available are needed before pharmacologic applications can be contemplated.

One way Li^+ may exert its effect is by competing with Mg^{2+} for ATP and ADP binding sites. Therefore, I have examined this phenomenon in detail. Binding of metal cations to nucleotides is dependent on pH, temperature, and ionic strength (61-63, 67). In all of the experiments, the pH was adjusted to 7.4 and the ionic strength to 0.15 M with tetramethylammonium hydroxide and TRIS-Cl, respectively. The bulky organic cations which were used to adjust ionic strength and pH were selected because they were not likely to compete with the binding of Li^+ and Mg^{2+} to ATP and ADP. To avoid nucleotide base stacking (67), a maximum nucleotide concentration of 10 mM was used.

^7Li T_1 relaxation times decreased in LiCl solutions in the presence of increasing amounts of ATP or ADP, indicating that T_1 values are sensitive to Li^+ binding to nucleotides (Figure 13). Upon addition of Mg^{2+}, the ^7Li T_1 values increased because of displacement of Li^+ by Mg^{2+} from ATP or ADP binding sites (Figure 13). If simultaneous binding of Li^+ and Mg^{2+} to ATP or ADP had occurred, the ^7Li T_1 values in the presence of Mg^{2+} would be the same as in its absence; however, this was not observed.

^1H and ^{13}C NMR results showed no significant changes in chemical shifts of protons and carbons on the base and sugar moieties of ATP and ADP upon addition of either excess $MgCl_2$ or excess LiCl (Tables 11 & 12). These observations are in agreement with a previous report on metal ion binding to nucleosides in DMSO (145). Binding of Li^+ or Mg^{2+} to

nucleosides is weak in DMSO (which should enhance metal ion binding to the sugar and base moieties as a result of the poor solvation power of DMSO); their binding to the sugar and base groups in water was observed to be even weaker.

The chemical shift separation between the α- and β- phosphate resonances of ATP reflects the state of metal complexation of ATP (55, 61). The value of $\delta_{\alpha\beta}$ changed from 10.82 ppm in free ATP to 9.80 ppm in Li$^+$-saturated ATP and 8.43 ppm in Mg^{2+}-saturated ATP (Figure 16). For the mixture of Li$^+$ and Mg^{2+} salts with ATP, an intermediate value of $\delta_{\alpha\beta}$, 9.43 ppm, was observed, suggesting that competition of the ions for ATP-phosphate binding sites was occurring. The downfield shifts observed upon addition of Li$^+$ and/or Mg^{2+} probably resulted from polarization of the electron density away from the phosphorus atoms when phosphates are associated with cations. The downfield shifts could also indicate that each phosphate contributes only one oxygen atom for coordination in the chelate ring (60). At higher than equimolar concentrations of Mg^{2+} and ATP, upfield shifts of the phosphate resonances have been reported (146).

Based on ^{31}P chemical shifts obtained for Li$^+$/Mg^{2+} mixtures of nucleotides (Tables 14 & 17), and using the three models (equations 1-7) for the predominant species in solution, the Li$^+$-nucleotide binding constants in the presence and absence of Mg^{2+} was found to be somewhat greater in the presence of Mg^{2+} than in the presence of Li$^+$ alone (Table 19). For ATP, better convergence was obtained for the third model (that assumed the presence of both 1:1 and 2:1 Li-ATP species); for ADP, while good convergence was found for the α phosphate resonances using the third model better convergence was found for the β phosphate resonances using the first or second models. However, because of the large error involved in the calculation of the binding constants, this difference may not be significant. We also

found consistency between observed and theoretical limiting ^{31}P phosphate chemical shifts for aqueous mixtures of nucleotides in the presence of both metal ions (Table 20). The small increases in Li-ATP and Li-ADP association constants in the presence of Mg^{2+} indicates that the formation of mixed complexes involving Li^+, Mg^{2+}, and the phosphate-binding sites of ATP and ADP cannot be ruled out. The small increase in Li^+ binding affinity in the presence of Mg^{2+} for ADP found by ^{31}P NMR agrees with previously reported affinity values measured by gel filtration (64).

The ^7Li T_1 relaxation times increased in the presence of Mg^{2+}, and the phosphate chemical shifts observed in the presence of varying concentrations of Li^+ and Mg^{2+} were consistent with theoretical values calculated on the basis of competitive binding to ATP or ADP of one Mg^{2+} or two Li^+ ions. ^1H and ^{13}C NMR indicated that no significant metal ion binding to the sugar and base moieties of the nucleotides occurred. Even though our findings provide evidence for competition between Li^+ and Mg^{2+} for ATP or ADP binding sites, formation of mixed complexes with phosphate binding sites can not be ruled out.

Interaction of metal ions with human RBC membranes and synthetic membranes made up of phospholipids, such as PC, PI and PS, has been studied using ^7Li, ^{31}P, ^2H NMR, AA, fluorescence spectroscopy and neutron diffraction (72-86). Using the ^{31}P NMR CSA approach, Li^+ and Mg^{2+} binding to human RBC membranes was studied. Upon addition of increasing levels of Li^+ and Mg^{2+}, the CSA values increased which was an indication of metal ions binding to the membrane (Table 21). The CSA increased from 51.3 ppm, for membrane alone, to 69.2 and 83.7 ppm in the presence of 20 $MgCl_2$ and 200 mM LiCl, respectively. The strength of metal ion interaction increases with increasing charge and metal ion concentration. The strength of metal ion interaction with PC increased when going from

monovalent to trivalent cations such as Na^+, Ca^{2+} and La^{3+} (82). Therefore, in this study an excess amount of LiCl was used to maximize the effect of Li^+ binding. The binding of Li^+ and Mg^{2+} to the membrane caused motional rigidity and small conformational changes of the phospholipid head groups which was reflected in CSA changes.

Using ^7Li T_1 and T_2 relaxation times, binding of Li^+ to RBCs and RBC ghosts was examined (76). Typical T_1 and T_2 values for Li^+-loaded RBCs are 5 and 0.2 sec, respectively. Little or no change was observed on the ^7Li T_1's and T_2's of ATP-containing ghosts and ATP-depleted ghosts indicating that the interaction between Li^+ and ATP is weak and is not responsible for the drastic difference between T_1 and T_2 relaxation times (76). Moreover, the fact that the difference in relaxation times was present in both intact RBCs and RBC ghosts indicated that this Li^+ relaxation behavior had to do with Li^+ binding to RBC membrane and not to intracellular metabolites, such as ATP and hemoglobin, or membrane proteins, such as spectrin-actin (76). A ^7Li T_1 study was conducted to investigate the mode of Li^+ and Mg^{2+} binding to the membrane (Table 22). ^7Li T_1 values increased from 13.9 sec (5 mM Li^+, membrane alone) to 19.5 sec in the presence of 2.0 mM $MgCl_2$. The increase in relaxation times was due to the displacement of Li^+ by Mg^{2+} via a competitive mechanism for membrane phosphate binding sites.

It has been shown that manic depressive patients have lower Na^+-Li^+ countertransport rates than matched normals (94-97). Studies carried out with human RBCs postulated a membrane dysfunction hypothesis for manic depression (88-91). Other studies have shown characteristic changes in the PL composition of bipolar patients (88); manic depressive patients had lower PC and PS contents and higher PE content than normal controls (88). The results on Table 25 and 26 show that bipolar patients have lower Na^+-Li^+ countertransport rates than

normal controls. The observed rates measured using AA were 0.13 ± 0.01 and 0.20 ± 0.05 m moles Li^+ /(L of RBC x h), respectively. A Student's t-test with $p < 0.0025$ showed that there was a distinct difference between the two groups. Pearson correlation statistics showed Na^+-Li^+ countertransport rates being positively correlated with PC and PI and negatively correlated with PS (Table 27). This means that as the PS composition increases the rate decreases. In contrast, as PC and PI compositions increase the rate also increases. A Student's t-test ($p < 0.10$) showed that PS composition in patients were slightly higher than normals. PI content in patients were slightly lower than normals ($p < 0.05$). On the other hand, no difference in PC, PE and Sph was observed between patients and normals. Sengupta et al. (88) using TLC showed that PS and PC contents were lower and PE content was higher in manic depressive patients than normals. Using ^{31}P NMR, my results showed that PS content was higher and PI content was lower in manic depressive patients than normals and no difference was found in PE and Sph contents. The difference in results between my study and the other group may be attributed to the different sensitivities of the techniques used in the two studies.

Several neurotransmitter receptors are coupled to the hydrolysis of phosphatidylinositol-4,5-biphosphate (PIP_2) yielding inositol 1,4,5-triphosphate (1,4,5-IP_3) and diacylglycerol (DG), which perform second messenger roles in cells (118). It has been shown that lithium treatment reduces the levels of inositol in the brain and that this reduction is accompanied by an increase in IP_1 (118). Inhibition of inositol-1-phosphatase leads to a depletion of inositol, the precursor in the resynthesis of PIP_2. Reduction of the resynthesis of PIP_2 may affect the signaling mechanisms operating through the phosphoinositide system. Therefore, the explanation for the decrease in PI content could be due to depletion by lithium.

Because PS is a negatively charged PL, its interaction with Li^+ is expected to be strong. Hence, since PS composition in patients was found to be higher than controls, Li^+ could bind stronger to the membrane of patients than controls which could lead to lower Li^+ transport rates in patients than normals.

One way Li^+ could exert its antimanic effect is by competing with Mg^{2+} binding sites in biomolecules (55, 135). Several workers have noted an increase in both serum magnesium and calcium a short time following lithium administration to humans (68-71). A general sedating effect with decreased manic behavior was observed when two acute manic patients were administered with Mg^{2+} by infusion (68). Blood samples showed an increase in plasma calcitonin, a small decrease in serum calcium, and an increase in serum Mg^{2+} (68). Therefore, it was hypothesized that magnesium could be responsible for the antimanic effect of lithium administration (68). Intracellular free and total Mg^{2+} concentrations examined in 10 patients and 10 matching controls showed no significant difference between the two groups, and no correlation with Na^+-Li^+ countertransport rates using Student's t-test and Pearson correlation analysis (Table 27). Using AA, total plasma Mg^{2+} levels measured in 59 patients who had various primary affective disorders and 303 normal individuals showed no difference (141). Thus, our findings on total Mg^{2+} levels are consistant with those reported previously (141). Intracellular free Mg^{2+} concentrations in human RBCs determined by ^{31}P NMR spectroscopy were measured in 26 individuals who had fasted overnight (57). The data showed a strong correlation between intracellular free Mg^{2+} level and both diastolic and systolic blood pressure. The lower the free Mg^{2+} levels, the higher were the diastolic and systolic blood pressure. In contrast, Woods et al. (147) found only a weak positive association between free Mg^{2+} and blood pressure (147). The contradicting results between

the different groups could be due to the effect of diet (148); it is known that intracellular free Mg^{2+} may be affected by the presence of glucose (148). In our study, the patients and controls did not fast overnight. Therefore, future studies should take into account the effect of glucose to determine whether intracellular free Mg^{2+} levels are indeed different in bipolar patients from matched controls.

Another probe used to unravel the cause for slower Na^+-Li^+ countertransport rates in manic depressive patients than normals were ^7Li T_1 and T_2 relaxation time measurements. Pearson correlation test showed very poor correlation between rates and relaxation times. Nevertheless, a Student's t-test ($p < 0.10$) showed that T_1 values for bipolars were slightly higher than normals. No difference was found in T_2 values between the two groups. Since the reported T_1 and T_2 values were for a single intracellular Li^+ concentration (2.19 ± 0.37), it is not possible to draw a definitive conclusion. Because the PS content in patients was found to be higher than normals, it could mean that Li^+ binds stronger to the membrane of patients. Lower T_1 relaxation times are indicative of stronger binding. Therefore, the fact that patients showed lower T_1 values than normals, could be due to stronger binding of Li^+ to PS. The original experiments were done at different intracellular Li^+ concentrations. Since Li^+ binding to RBCs is complicated by the availability of several binding sites, analysis of the data was not possible. Recent relaxation studies in our laboratory (149) using RBC membrane as opposed to the intact RBCs used in this study indicate that indeed binding of Li^+ to the RBC membrane of bipolar patients receiving lithium carbonate is stronger than matched controls. It will also be useful to examine the binding of Li^+ to membrane of patients who are Li^+-free in order to establish whether abnormal Li^+ binding to RBC membranes (150) is a biochemical marker of manic depression or a signature of Li^+ therapy.

REFERENCES

1)   Johnson FN (1975) Lithium. In Johnson FN (ed.): "Lithium Research and Therapy", Amsterdam: Academic Press, pp. 1 -22.

2)   Jefferson JW, Greist JH and Baudhuin M (1985) Lithium in Psychiatry. In Bach RO (ed.): "Lithium: Current Applications in Science, Medicine and Technology", Wiley: New York, pp. 345-352.

3)   Johnson FN (1985) The Early History of Lithium Therapy. In Bach RO (ed.): "Lithium: Current Applications in Science, Medicine and Technology", Wiley: New York, pp. 337-344.

4)   Hart WA and Beumel OF (1973) Lithium and its Compounds. In Bailar JC, Emeleus HJ, Nyholm R and Trotman-Dickerson AF (eds.): "Comprehensive Inorganic Chemistry" vol. 1, Oxford: Pergamon Press, pp. 331-367.

5)   Birch NJ (1978) Lithium in Medicine. In Williams RJP and Frausto da Silva JRR (eds.): "New Trends in Bioinorganic Chemistry", New York: Academic Press, pp. 389-435.

6)   Lieber KW, Stokes PE and Kocsis J (1979) Characteristics of the uptake of lithium isotopes into human erythrocytes. Biol Psychiatry 14, 845-849.

7)   Stokes PE, Okamoto M, Lieberman KW, Alexander G and Triana E (1982) Stable isotopes of lithium: In vivo differential distribution between plasma and cerebrospinal fluid. Biol Psychiatry 14, 413-421.

8)   Sherman WR, Munsell LY and Hu WY (1984) Differential uptake of lithium isotopes by rat cerebral cortex and its effect on inositol phosphate metabolism. J Neurochem 42, 880-882.

9)   Renshaw PF (1987) A diffusional contribution to lithium isotopic effects. Biol Psychiatry 22, 73-78.

10)   Riddell FG, Patel A and Hughes MS (1990) Lithium uptake rate and Li^+-Li^+ exchange rate in human erythrocytes at a nearly pharmacologically normal level monitored by ^7Li NMR. J Inorg Biochem 39, 187-192.

11)   Lieberman KW, Alexander GJ and Stokes P (1979) Dissimilar effects of lithium isotopes on motility in rats. Pharmacology, Biochemistry and Behavior 10, 933-935.

12)   Sechzer JA, Lieberman KW, Alexander GJ, Weidman D and Stokes PE (1988)

Aberrant parenting and delayed offspring development in rats exposed to lithium. Biol Psychiatry 21, 1258-1266.

13) Alexander GJ, Lieberman KW, Okamoto M, Stokes PE and Triana E (1982) Lithium toxicology: Effect of isotopic composition on lethality and behavior. Pharmacology, Biochemistry and Behavior 16, 801-804.

14) Alexander GJ, Lieberman KW and Stokes P (1980) Differential lethality of lithium isotopes in mice. Biol Psychiatry 15, 469-470.

15) Birch NJ (1977) Metabolic effects of lithium. In Johnson FN and Johnson S (eds.): "Lithium in Medical Practices", Baltimore: University Park Press, pp. 89-114.

16) Birch NJ, Robinson D, Inie RA and Hullin RP (1978) Lithium-6 stable isotope determination by atomic absorption spectroscopy and its application to pharmacokinetic studies in man. J Pharmacy Pharmacology 30, 683-685.

17) Egeland JA, Gerhard DS, Paul DL, Sussex JN, Kidd KK, Allen CR, Hostetter AM and Housman DE (1987) Bipolar affective disorders linked to DNA markers on chromosome X. Nature 325, 783-787.

18) Kelos JR, Ginns EI, Egeland JA, Gerhard DS, Goldstein AM, Bale SJ, Pauls DL, Long RT, Kidd KK, Conte G, Housman DE & Paul SM (1989) Re-evaluation of the linkage relationship between chromosome 11p loci and the gene for bipolar affective disorder in the Old Order Amish. Nature 342, 238-243.

19) Hodgkinson S, Sherington R, Gurling H, Marchbanks R, Reeders S, Malley J, Mcinnis M, Pertursson H and Brynjolfson J (1987) Molecular genetic evidence for heterogeneity in manic-depression. Nature 325, 805-806.

20) Baron M, Risch N, Humburger R Mandel B, Kushner S, Newman M, Drumer D and Bellmaker RH (1987) Genetic linkage between x-chromosome markers and bipolar affective illness. Nature 326, 289-292.

21) Specter S, Lancz G and Bach RO (1990) Lithium and virus infections. In Bach RO and Gallichio VS (eds.): "Lithium and Cell Physiology", Springer-Verlag: New York, pp. 150-157.

22) Horrobin DF (1990) Lithium and dermatological disorders. In Bach RO and Gallichio VS (eds.): "Lithium and Cell Physiology", Springer-Verlag: New York, pp. 158-168.

23) Davis J and Franzese K (1987) Lithium. In Mcbride EF and Sittig M (eds.): "McGraw-Hill Encyclopedia of Science and Technology", 6th ed., vol 10, Mcgraw-Hill Book Co., New York, pp. 129-133.

24) Cotton FA and Wilkinson G (1980) Group I elements. In:" Advanced Inorganic Chemistry", 4th ed., Wiley Press, New York, pp. 253-256.

25) Xie YU and Christian GD (1987) Measurement of serum lithium levels. In Johnson FN (ed): "Depression and Man," Oxford: IRL Press, pp. 78-88.

26) Vartsky D, Lomonte A, Ellis KJ, Yasumura S and Cohn SH (1988) A method for in vivo measurement of lithium in the body. In Birch NJ (ed.): "Lithium: Inorganic Pharmacology and Psychiatric Use", Oxford: IRL Press, pp. 297-298.

27) Ehrlich BE and Diamond JM (1979) Lithium fluxes in human erythrocytes. Am J Physiol 237, C102-C110.

28) Pandey GN, Sarkadi B, Haas M, Gunn RB, Davis JM and Tosteson DC (1978) Lithium transport pathways in human red blood cells. J Gen Physiol 72, 233-247.

29) Kimura K, Oishi H, Miura T and Shono T (1987) Lithium ion selective electrode based on crown ethers for serum lithium assay. Anal Chem 59, 2331-2334.

30) Xie RY and Christian D (1986) Serum lithium analysis by coated wire lithium ion selective electrodes in a flow injection analysis dialysis system. Anal Chem 58, 1806-1810.

31) Kitazawa S, Kimura K, Yano H and Shono T (1985) Lithium selective polymeric membrane electrodes based on dodecylmethyl-14-Crown-4. Analyst 110, 295-299.

32) Sugihara H, Okada T and Hiratani K (1987) Lithium ion selective electrodes based on 1,10-phenanthroline derivatives. Chem Lett, 2391-2392.

33) Gadzekpo VPY, Hungerford JM, Kadry AM, Ibrahim YA and Christian GD (1986) Comparative study of neutral carriers in polymeric lithium ion selective electrode. Anal Chem 58, 1948-1953.

34) Gadzekpo VPY, Hungerford JM, Kadry AM, Ibrahim YA and Christian GD (1985) Lipophylic lithium ion carrier in a lithium ion selective electrode. Anal Chem 57, 493-495.

35) Metzger E, Dohner R and Simon W (1987) Lithium/sodium ion concentration ratio measurements in blood serum with lithium and sodium ion selective liquid membrane electrodes. Anal Chem 59, 1600-1603.

36) Metzger E, Ammann D, Asper R and Simon W (1986) Ion selective liquid membrane electrode for the assay of lithium in blood serum. Anal Chem 58, 132-135.

37) Brevard C and Granger P (1981) Handbook of High Resolution Multinuclear NMR. John Wiley and Sons, New York.

38) Detellier C (1983) Alkali Metals. In Laszlo P (ed.): "NMR of Newly Accessible Nuclei", New York: Academic Press, pp. 105-151.

39) Gorenstein DG (1984) Phosphorus-31 chemical shifts: Principles and Empirical Observations: In David G Gorenstein (ed.): " Phosphorus-31 NMR Principles and Applications", Academic Press INC.: New York pp. 7-36.

40) Silverstein RM, Bassler GC and Morril TC (1963) Proton and carbon magnetic resonances spectrometry. In Silverstein RM, Bassler GC and Morril TC (eds.): "Spectrometric Identification of Organic Compounds. John Wiley and Sons, New York, 4th ed., pp. 181-278.

41) Mota de Freitas D, Espanol MT, Ramasamy R, and Labotka RJ (1990) Comparison of Li$^+$ transport and distribution in human red blood cells in the presence and absence of dysprosium(III) complexes of triphosphate and triethylenetetraminehexaacetate. Inorg Chem 29, 3972-3978.

42) Ramasamy R, Mota de Freitas D, Jones W, Wezeman F, Labotka R, and Geraldes CFGC (1990) Effects of negatively charged shift reagents on red blood cell morphology, Li$^+$ transport, and membrane potential. Inorg Chem 29, 3979-3985.

43) Espanol MC and Mota de Freitas D (1987) ^{7}Li NMR studies of lithium transport in human erythrocytes. Inorg Chem 26, 4356-4359.

44) Shinar H and Navon G (1986) Novel organometallic ionophore with specificity toward Li$^+$. J Am Chem Soc 103, 5005-5006.

45) Shanzer A, Samuel D and Krenstein R (1983) Lipophilic lithium ion carriers. J Am Chem Soc 105, 3815-3818.

46) Kobuke Y and Yamamoto JY (1990) Cation transport by modified dibenzo-18-Crown-6 through lecithin liposomal membrane. Bioorg Chem 18, 283-290.

47) Kimura K, Tanaka M, Kitazawa S and Shono T (1985) Highly lithium-selective crown ether dyes for extraction photometry. Chem Lett 8, 1239-1240.

48) Kimura K, Yano H, Kitazawa S and Shono T (1986) Synthesis and selectivity for lithium of lipophilic 14-Crown-4 derivatives bearing bulky substituents or an additional binding site in the side arm. J Chem Soc Perkin Trans II, 1945-1951.

49) Kitazawa S, Kimura K, Yano H and Shono T (1984) Lipophilic crown-4 derivatives as lithium ionophores. J Am Chem Soc 106, 6978-6983.

50) Pacey GE (1985) Lithium crown ether complexes. In Bach RO (ed.): "Lithium: Current Applications in Science, Medicine and Technology", Wiley: New York, pp. 35-45.

51) Cahen YM, Dye JL and Popov AI (1975) Lithium-7 NMR study of lithium ion-lithium cryptate exchange rates in various solvents. J Phys Chem 79, 1292-1295.

52) Shamsipur M and Popov AI (1986) Lithium-7 NMR study of the kinetics of Li$^+$ ion complexation by C222 and C221 cryptates in acetonitrile, propylene carbonate, and acetone solution. J Phys Chem 90, 5997-5999.

53) El-Mallakh RS (1983) The Na, K-ATPase hypothesis for manic depression. I. General considerations. Med Hypothesis 12, 253-268.

54) Frausto da Silva JJR and Williams RJP (1976) Possible mechanism for the biological action of lithium. Nature 263, 237-239.

55) Ramasamy R and Mota de Freitas D (1989) Competition between Li$^+$ and Mg^{2+} for ATP in human erythrocytes: A ^{31}P NMR and optical spectroscopy study. FEBS Lett 24, 223-226.

56) Gupta R, Benovic J and Rose Z (1978) Determination of free magnesium in the human red blood cell by ^{31}P NMR. J Biol Chem 253, 6172-6176.

57) Resnick L, Gupta R, and Laragh J (1984) Intracellular free Mg^{2+} in erythrocytes of essential hypertension: Relationship to blood pressure and serum divalent cations. Proc Natl Acad Sci USA 81, 6511-6515.

58) Mildvan AS (1987) Role of magnesium and other divalent cations in ATP utilizing enzymes. Magnesium 6, 28-33.

59) Huang S and Tsai M (1982) Does the Magnesium (II) ion interact with the α-phosphate of ATP? An investigation by ^{7}O NMR. Biochemistry 21, 951-959.

60) Prigodich RV Haake P (1985) Association phenomena. 5. Association of cations with nucleoside di- and triphosphates studied by ^{31}P NMR. Inorg Chem 24, 89-93.

61) Gupta RK, Gupta P, Yushok DW and Rose BZ (1983) Measurement of the dissociation constants of MgATP at physiological nucleotide levels by a combination of ^{31}P NMR and optical spectroscopy study. Biochem Biophys Res Commun 117, 210-216.

62) Cohn M and Hughes TR Jr. (1960) Phosphorus magnetic resonance spectra of adenosine di and triphosphate. J Biol Chem 235, 3250-3253.

63) Sontheimer GM, Kuhn W and Kalbitzer HR (1986) Observation of Mg^{2+} ATP and complexed ATP in slow exchange by ^{31}P NMR at high magnetic field. Biochem Biophys Res Commun 134, 1379-1386.

64) Birch NJ and Goulding I (1975) Lithium-nucleotide interactions investigated by gel filtration. Anal Biochem 66, 293-297.

65) Kajda PA and Birch NJ (1981) Lithium inhibition of phosphofructokinase. J Inorg

Biochem 14, 275-278

66) Kajda PK, Birch NJ, O'Brien MJ and Hallin RP (1979) Rat brain pyruvate kinase: purification and effects of lithium. J Inorg Biochem 11, 361-366.

67) Martin RB and Mariam YH (1979) In Sigel H (ed.): "Metal Ions in Biological Systems", Marcel Dekker, New York, vol. 8, Chapter 2.

68) Pavlinac D, Langer R and Lenhard L (1979) Magnesium in affective disorders. Biol Psychiatry 14, 657-661.

69) Arnoff MS, Evens RG and Durell J (1971) Effect of lithium salts on electrolyte metabolism. J Psychiat Res 8, 139.

70) Carmen JS, Post RN, Teplitz TA and Goodwin FK (1974) Divalent cations in predicting antidepressant response to lithium. Lancet 2, 1454.

71) Mellerup ET, Lauristen B, Dam H and Rafaelsen OJ (1976) Lithium effect on diurnal rythim of calcium, magnesium and phosphate metabolism in manic-melancholic disorder. Acta Psychiat Scand 53, 360.

72) Pettegrew JW, Post JFM, Panchalingam K, Withers G and Woessner DE (1987) ^{7}Li NMR study of normal human erythrocytes. J Magn Reson 71, 504-519.

73) Pettegrew JW, Short JW, Woessner RD, Strychor S, Mskeag DW, Armstrong J, Minshew NJ and Rush AJ (1987) The effect of lithium on the membrane molecular dynamics of normal human erythrocytes. Biol Psychiatry 22, 857-871.

74) Roux M and Bloom M (1990) Ca^{2+}, Mg^{2+}, Li^+, Na^+, and K^+ distribution in the head group region of binary membranes of PC and PS as seen by deuterium NMR. Biochemistry 29, 7077-7089.

75) Roux M and Neuman JM (1986) Deuterium NMR study of head-group deuterated phosphatidylserine in pure and binary phospholipid bilayer. FEBS Lett 3552, 33-38.

76) Mota de Freitas D, Espanol M and Wittenkeller L (1991) ^{7}Li NMR relaxation studies of Li^+ binding to human erythrocyte membranes (in preparation).

77) Riddell FG and Arumugam S (1988) Surface charge effects upon membrane transport processes: the effects of surface charge on the monensin-mediated transport of lithium ions through phospholipid bilayers studied by ^{7}Li-NMR spectroscopy. Biochim Biophys Acta 945, 65-72.

78) Ehrlich BE, Diamond JM, Clausen C, Gosenfeld L and Kaufman-Diamond S (1979) The effects of lithium on cell membranes. In Cooper TB, Gershon S, Kline NS and Schou M (eds.): "Lithium: Controversies and Unresolved Issues", Int. Congr. Ser. No.478, Amsterdam-Oxford-Princeton: Excerpta Medica, pp. 758-767.

79) Pandey GN, Dorus E and David JM (1979) Lithium transport in human red cells: genetic and clinical aspects. In Cooper TB, Gershon S, Kline NS and Schou M (eds.): "Lithium: Controversies and Unresolved Issues", Int. Congr. Ser. No. 478 , Amsterdam-Oxford-Princeton: Excerpta Medica, pp. 736-757.

80) Weinstein RS (1974) The Morphology of Adult Red Cells. In Surgen DM (ed.): "The Red Blood Cells", New York: Academic Press Inc., pp. 214-268.

81) Yeagle PA (1984) Phospholipid-protein interaction and structure of the human erythrocytes membrane; NMR studies. In Yeagle PA (ed.) "Erythrocyte Membrane 3: Recent Clinical and Experimental Advances". Alan R Liss Inc.: New York, pp.153-175.

82) Akutsu H and Seeling J (1981) Interaction of metal ions with PC bilayer membranes. Biochemistry 20, 7366-7373.

83) Alten C and Seeling J (1984) Ca^{2+} binding to PC bilayers as studied by ^2H NMR. Evidence for the formation of Ca^{2+} complex with two phospholipid molecules. Biochemistry 23, 3913-3920.

84) Brown FB and Seeling J (1977) Ion induced changes in head group conformation of lecithin bilayers. Nature 269, 721-723.

85) Hope MJ and Cullis PR (1980) Effect of divalent cations and pH on phosphatidylserine model membranes: A ^{31}P NMR study. Biochem Biophys Res Commun 92, 846-851.

86) Hauser H and Shiley GG (1981) Crystallization of phosphatidylserine bilayer induced by lithium. J Biol Chem 256, 11377-11380.

87) Gadian DG (1982) NMR and its Applications to Living Systems. Clarendon Press, Oxford, pp. 23-41.

88) Sengupta N, Datta SC and Sengupta D (1981) Platelet erythrocyte membrane lipid and phospholipid pattern in different types of mental patients. Biochem Med 25, 267-275.

89) Mota de Freitas DE, Espanol MT and Dorus E (1991) Lithium transport in red blood cells of bipolar patients. In Gallichio VS (ed.):"Lithium and the Blood", Lithium Therapy Monographs, Karger and Basel Vol. 4, pp. 96-120.

90) Medels J and Frazier A (1974) Alterations in cell membrane activity in depression. Am J Psychiatry 131, 1240-1246.

91) Hokin-Neaverson M, Spiegel DA and Lewis WC (1974) Deficiency of erythrocyte sodium pump activity in bipolar manic-depressive psychosis. Life Sciences 15, 1739-1748.

92) Mendel J and Frazer A (1973) Toward a membrane theory of depression. Psychiatry Res 10, 9-18.

93) Dorus E, Cox NJ, Gibbons RD, Shaughnessy R, Pandey GN and Cloninger R (1983) Lithium ion transport and affective disorders within famillies of bipolar patients: Identification of a major gene locus. Arch Gen Psychiatry 40, 545-552.

94) Mota de Freitas D, Silberberg J, Espanol MT, Dorus E, Abraha A, Dorus W, Elenez E and Wang W (1990) Measurement of lithium transport in RBC from psychiatric patients receiving lithium carbonate and normal individuals by ^{7}Li NMR spectroscopy. Biol Psychiatry 28, 415-424.

95) Pandey GN, Ostrow DG, and Haas M (1977) Abnormal lithium and sodium transport in erythrocytes of manic patient and some members of his family. Proc Natl Acad Sci USA 74, 3607-3611.

96) Szentistvanyi I and Janka Z (1979) Correlation between lithium ratio and Na^+-dependent Li^+ transport in red blood cells during lithium prophylaxis. Biol Psychiatry 14, 973-977.

97) Zaremba D and Rybakowski J (1986) Erythrocyte lithium transport during lithium treatment in patients with affective disorders. Pharmacopsychiatry 19, 63-67.

98) Egeland JA, Kidd JR, Frazer A, Kidd KK and Neuhauser VI (1984) Amish study V: Lithium-sodium countertransport and catechol o-methyltransferase in pedigree of bipolar probands. Am J Psychiatry 141, 1049-1054.

99) Greil W, Eisenried F, Becker BF and Duhm J (1977) Interindividual differences in the Na^+ dependent Li^+ countertransport system and in the Li^+ distribution ratio across the red cell membrane among Li^+ treated patients. Psychopharmacologia 53, 19-26.

100) Mallinger AG, Mallinger J, Himmelhoch JM, Rossi A and Hanin I (1983) Essential hypertension and membrane lithium transport in depressed patients. Psychiatry Res 10, 11-16.

101) Richelson E, Snyder K, and Carlson J (1986) Lithium ion transport in erythrocytes of randomly selected blood donors and manic depressive patients: Lack of association with affective illness. Am J Psychiatry 23, 465-475.

102) Rybakowski JK, Amsterdam JD, Dyson WL, Frazer A, Winokur A and Kurt J (1989) (1989) Factors contributing to lithium-sodium countertransport activity in lithum-treated bipolar patients. Pharmacopsychiatry 22, 16-20.

103) Amsterdam JD, Rybakowski J, Gottlieb J and Frazer A (1988) Kinetics of erythrocytes of sodium-lithium countertransport in patients with affective illness before and after lithium therapy. J Affect Disord 14, 75-81.

104) Waters B, Thakar J and Lapierre Y (1983) Erythrocyte lithium transport variables as a marker for manic-depressive disorder. Neuropsychobiology 9, 94-98

105) Werstiuk ES, Rathbone MP and Grof P (1981) Phloretin-sensitive lithium transport in erythrocytes in affectively ill patients: Inter-individual reproducibility. Prog Neuropsychopharmacol 5, 503-506.

106) Weder A, Torreti BA, Julius S (1984) Racial differences in erythrocyte cation transport. Hypertension (Dallas) 6, 115-123.

107) Carr S, Thomas TH and Wilkinson R (1988) Sodium-lithium countertransport activity and its sensitivity to inhibitors with erythrocyte aging in man. Clin Chim Acta 178, 51-58.

108) Ostrow DG, Canessa M, Sparks S and Davis JM (1983) Preservation of human erythrocytes for sodium-dependent lithium efflux rate measurements. Clin Chim Acta 129, 39-44.

109) Duhm J (1982) Lithium transport pathways in red cells. In Emrich HM, Aldenhoff JB and Lux HD (eds.): "Basic Mechanisms in the Action of Lithium". Excerpta Medica, Amsterdam-Oxford-Princeton, 1-48.

110) Sarkadi B, Allimeff JK, Gunn RB and Tosteson DC (1978) Kinetics and stoichiometry of Na^+-dependent Li^+ transport in human red blood cells. J Gen Physiol 72, 249-265.

111) Haas M, Schooler J and Tosteson DC (1975) Coupling of lithium to sodium transport in human red cells. Nature (London) 258, 425-427.

112) Duhm J, Eisenried F, Becker BF and Greil W (1976) Studies on the lithium transport: a marker for manic-depressive disorder. Neuropsychobiol 9, 94-98.

113) Goldberg H, Clatman P, and Skorecki K (1988) Mechanism of Li^+ inhibition of vasopressin-sensitive adenylate cyclase in cultured renal epithelial cells. Am J Physiol 255, F995-F1002.

114) Limbird LE (1988) Receptors linked to inhibition of adenylate cyclase: additional signaling mechanisms. FASEB J 2, 2686-2695.

115) Abdulla YH and Hamada K (1970) 3', 5' cyclic adenosine monophosphate in depression and mania. Lancet 1, 378-381.

116) Palmer GC, Robinson GA, Manian AA and Sulser F (1972) Modification by psychotropic drugs of cyclic adenosine monophosphate response to norepinephrine in rat brain. Psychopharmacologia 23, 201-211.

117) Mork A (1990) Actions of lithium on second messenger activity in the brain. The adenylate cyclase and phosphoinositide systems. Lithium 1, 130-147.

118) Hallcher LM and Sherman WR (1980) The effects of lithium ion and other agents on the activity of myo-inositol-1-phosphatase from bovine brain. J Biol Chem 255, 10896-10901.

119) Avissar S, Schreiber G and Danon A (1989) Lithium inhibits adrenergic and cholinergic increases in GTP binding in rat cortex. Nature 331, 440-442.

120) Avissar SS, Schreiber G, Danon A and Belmrak RH (1988) Lithium effects on cyclic AMP and Phosphatidylinositol metabolism may promote adrenergic-cholinergic balance. In Birch NJ (ed.): "Lithium: Inorganic Pharmacology and Psychiatric Use", Oxford: IRL Press, pp. 213-216.

121) American Psychiatric Association (1987): Diagnostic and statistical Manual of Mental Disorders (ed 3), revised. washington, DC: American Psychiatric Association.

122) Canessa M, Adragna N, Solmon H, Connolly T, and Tosteson DC (1984) Increased sodium-lithium countertransport in red cells of patients with essential hypertension. New Eng J Med 302, 772-776.

123) Chu SCK, Qiu HZH, and Springer CS (1990) Aqueous shift reagents for high-resolution cation NMR. V. Thermodynamics of interaction of DyTTHA^{3-} with Na$^+$, K$^+$, Mg^{2+} and Ca^{2+}. J Magn Reson 87, 287-303.

124) Steck TL and Kant JA (1974) Preparation of impermeable ghosts and inside-out vesicles from human erythrocyte membranes. In Fleischer S and Packer L (eds.): "Methods in Enzymology" vol. 31, pp. 172-180.

125) Mimms LT, Zampighi G, Nozaki Y, Tanford C, and Reynolds JA (1981) Phospholipid vesicle formation and transmembrane protein incorporation using octyl glucoside. Biochemistry 20, 833-840.

126) Broekhuyse RM (1969) Quantitative two-dimensional thin-layer chromatography of blood phospholipids. Clin Chim Acta 23, 457-461.

127) Folch J, Lees M, and Sloane Stanley GH (1957) A simple method for the isolation and purification of total lipids from animal tissues. J Biol Chem 226, 497-509.

128) Meneses P and Glonek T (1988) High resolution ^{31}P NMR of extracted phospholipids J Lipid Res 29, 679-689.

129) Bauer M, Spread CY, Reitheiner RAF and Sykes BD (1985) ^{31}P and ^{35}Cl NMR measurements of anion transport in human erythrocytes. J Biol Chem 260, 11643-11650.

130) Bollag DM and Edelstein SJ (1991) Protein Methods. In Bollag JM and Edelstein SJ (eds.): "Protein Methods", Wiley: New York, pp. 50-55.

131) Ramasamy R, Mota de Freitas D, Geraldes CFGC and Peters JA (1991) Multinuclear NMR study of the interaction of the shift reagent lanthanide (III) bis(triphosphate) with alkali-metal ions in aqueous solution and in solid state. Inorg Chem 30, 3188-3191.

132) Ramasamy R, Espanol MC, Long KM, Mota de Freitas D and Geraldes CFGC (1989) Aqueous shift reagents for ^{7}Li NMR transport studies in cells. Inorg Chim Acta 163, 41-52.

133) Duhm J and Becker BF (1977) Studies on lithium across the red cell membrane. II. Characterization of ouabain-sensitive and ouabain-insensitive Li^+ transport effects of bicarbonate and dipyridamole. Pflugers Arch 367, 211-219.

134a) Cabantik ZI and Rothstein A (1974) Membrane proteins related to anion permeability of human red cell. I. Localization of disulfonic stilbene binding sites in proteins involved in permeation. J Membr Biol 15, 207-226.

134b) Zar JH (1984) Simple linear correlation. In Kurtz B (ed.): "Biostatistical Analysis 2nd ed.", Prentice Hall, Inc., Englewood Cliffs, New Jersey, pp. 306-326.

135a) Abraha A, Duarte de Freitas DE, Castro MMCA, and Geralds CFGC (1991) Competition between Li^+ and Mg^{2+} for ATP and ADP in aqueous solution: a multinuclear NMR study. J Inorg Biochem 42, 191-198.

135b) Zubay G (1988) Lipids. In Zubay G. (ed.): "Biochemistry 2nd ed.", Macmillan Publishing Co.: New York, pp. 154-174.

136) Pearce JM, Shifman MA, Pappas AA, and Komoroski RA (1991) Analysis of phospholipids in human amniotic fluid by ^{31}P NMR. Magn Reson Med 21, 107-116.

137) Edzes HT, Teerlink T, and Valk J (1991) Phospholipid identification in tissue extracts by two-dimensional ^{31}P-^{1}H NMR spectroscopy with isotropic proton mixing. J Mag Res 95, 387-395.

138) Cowan JA (1991). Metallobiochemistry of magnesium. Coordination complexes with biological substrates: site specificity, kinetics and thermodynamics od binding, and implications for activity. Inorg Chem 30, 2740-2747.

139) Bock JL, Wenz B, and Gupta RK (1987) Studies on the mechanism of decreased NMR-measured free magnesium in stored erythrocytes. Biochim Biophys Acta 928, 8-12.

140) Bock LJ and Yusuf Y (1988) Further studies on alterations in magnesium binding during cold storage of erythrocytes. Biochim Biophys Acta 941, 225-231.

141)   Ramsey TA, Frazer A, and Mendels J (1979) Plasma and erythrocyte cations in affective illness. Neuropsychobiol 5, 1-10.

142)   Riddell RG and Hayer MK (1985) The monensin-mediated transport of sodium ions through phospholipid bilayers studied by ^{23}Na-NMR spectroscopy. Biochim Biophys Acta 817, 313-317.

143)   Riddell FG, Arumugam S and Cox BG (1987) Ion transport through phospholipid bilayers studied by magnetisation transfer; membrane transport of lithium mediated by monensin. J Chem Soc Chem Commun, 1890-1891.

144)   Abraha A, Dorus E and Mota de Freitas D (1991) Nuclear magnetic study of differences between ^{6}Li and ^{7}Li ions in transport across human red blood cell membranes. Lithium 2, 118-121.

145)   Plaush AC and Sharp RR (1976) Ion binding to nucleosides. A ^{35}Cl and ^{7}Li NMR study. J Am Chem Soc 98, 7973-7980.

146)   Hughes MS, Patridge S, Marr G and Birch NJ (1988) Magnesium interactions with lithium and sodium salts of adenosine triphosphate: an investigation by phosphorus-31 nuclear magnetic spectroscopy. Mag Res 1, 35-38.

147)   Woods KL, Walmsley D, Heagerty AM, Turner DL, and Lina LY (1988) ^{31}P NMR measurement of free erythrocyte magnesium concentration in man and its relation to blood pressure. Clin Sci 74, 513-517.

148)   Resnick JM, Gupta RK and Laragh JH (1989) Possible effects of diet and other factors on ^{31}P NMR measurement of intracellular magnesium in hypertension. Clin Sci 76, 565-566.

149)   Rong Q and Mota de Freitas D (1991) Li^{+} binding to RBC membrane in bipolar patients and matched controls: A ^{7}Li NMR relaxation study (in progress).

150)   Ehrlich BE, Diamond JM, and Gosenfield L (1981) Lithium induced changes in sodium-lithium countertransport. Biochem Pharmacol 30, 2539-2543.

Vita

Aida Abraha, the daughter of Mr Abraha Wolde Ghiorgis and Mrs. Abrehet Habtezgi, was born in Addis Ababa, Ethiopia, on the 17th of Dec., 1961.

On October 11, 1980, she came to the USA to pursue undergraduate studies. She received a B.S. in Chemistry (pre-medical) in June, 1985 from Chicago State University.

From Oct. 1985 to Jan. 1987, she worked as a quality control chemist at Soft Sheen Products Inc.

From Jan. 1987 to Dec. 1990, Ms. Abraha was an Illinois Minority Graduate Incentive Program fellow pursuing her doctoral degree at Loyola University of Chicago, under the supervision of Dr. Duarte Mota de Freitas. From Jan. 1990 - May 1990 she received a teaching assistantship from the Loyola graduate school, and from May 1990 - 1991 a research assistantship from a NIMH grant awarded to her supervisor and a University Fellowship that enabled her to conclude her doctoral degree. In Oct. 1991, she received the President's Gold Medallion award for scholarship leadership and service.

Approval Sheet

The dissertation submitted by Aida Abraha has been read and approved by the following committee:

Dr. Duarte Mota de Freitas, Director
Associate Professor, Chemistry, Loyola University

Dr. Patrick M. Henry
Professor, Chemistry, Loyola University

Dr. Bruno Jaselskis
Professor, Chemistry, Loyola University

Dr. Kenneth Olson
Professor, Chemistry, Loyola University

Dr. Nega Beru
Assistant Professor, Biochemistry and Molecular Biology, University of Chicago

The final copies have been examined by the director of the dissertation and the signature which appears below verifies the fact that any necessary changes have been incorporated and that the dissertation is now given final approval by the committee with reference to content and form.

The dissertation is therefore accepted in partial fulfillment of the requirements for the degree of Doctor of Philosophy.

March 9, 1992   _____
Date   Director's Signature